RADAR CROSS SECTION (RCS) OF PERFECTLY CONDUCTING (PEC) THIN WIRES AND ITS APPLICATION TO RADAR COUNTERMEASURE: CHAFF

A THESIS SUBMITTED TO

THE GRADUATE SCHOOL OF ENGINEERING AND SCIENCE

OF BILKENT UNIVERSITY

IN PARTIAL FULFILLMENT OF THE REQUIREMENTS FOR

THE DEGREE OF

MASTER OF SCIENCE

IN

ELECTRICAL AND ELECTRONICS ENGINEERING

By

Rıfat Dalkıran

August, 2015

Radar Cross Section (RCS) of Perfectly Conducting (PEC) Thin Wires
and Its Application to Radar Countermeasure: Chaff
By Rıfat Dalkıran
August, 2015

We certify that we have read this thesis and that in our opinion it is fully adequate, in scope and in quality, as a thesis for the degree of Master of Science.

Prof. Dr. Ayhan Altıntaş(Advisor)

Assoc. Prof. Dr. Vakur B. Ertürk

Assoc. Prof. Dr. Ali Cafer Gürbüz

Approved for the Graduate School of Engineering and Science:

Prof. Dr. Levent Onural
Director of the Graduate School

ABSTRACT

RADAR CROSS SECTION (RCS) OF PERFECTLY CONDUCTING (PEC) THIN WIRES AND ITS APPLICATION TO RADAR COUNTERMEASURE: CHAFF

Rıfat Dalkıran
M.S. in Electrical and Electronics Engineering
Advisor: Prof. Dr. Ayhan Altıntaş
August, 2015

In electronic warfare, active and passive countermeasures are used to jam threat RF radars. While electronic jamming pods are accepted as an active one, chaff is accepted as a passive countermeasure that consists of millions of perfectly conducting thin metallic wires, dipoles. The aim of this thesis is to first implement Van Vleck's Methods A and B [1], Tai's Variational Method [2] and Einarsson's Direct Method [3] to get radar cross section (RCS) of a dipole and then apply the results to calculate RCS of designed chaff cartridges. The ultimate goal is to suggest more effective passive countermeasure system than commercially available ones. In this thesis, performances of these methods are evaluated. According to these evaluations, Van Vleck's Method B and Einarsson's Direct Method are selected for calculating RCS of chaff cartridges. Performance of RR-178 (XN-2) commercial chaff cartridge is compared with three different suggested designs. For each of these designs, 2 to 20 GHz frequency interval is divided into three or six equal sub-frequency intervals and for these intervals particular chaff cartridges with different dipole lengths and numbers are proposed. In terms of total dipole length in the cartridges, instead of 88775 meters dipoles that is used in RR-178 (XN-2), by using chaff cartridges of third proposed design, in average only 25300 meters dipoles are used while providing more flat and equal average RCS value for 2 to 20 GHz frequency interval. Moreover, for the stated frequency interval, if total dipole length for the chaff cartridges of RR-178 (XN-2) and third proposed design keep equal, about 5.2 dB increase in average RCS value is obtained. Analysis of these results shows that designed chaff cartridges are more effective than commercial ones if the designed ones are used together with compatible Radar Warning Receiver (RWR) and Dispensing System.

Keywords: Radar Cross Section (RCS), Dipole, Thin Wire, Chaff, Variational Method, Direct Method, Integral Method, Dispensing System, Radar Warning Receiver (RWR).

ÖZET

MÜKEMMEL İLETKEN İNCE TELLERİN RADAR KESİT ALANI (RKA) VE BUNUN RADAR KARŞI TEDBİRİ OLARAK UYGULAMASI: DİPOL BULUTU

Rıfat Dalkıran
Elektrik ve Elektronik Mühendisliği, Yüksek Lisans
Tez Danışmanı: Prof. Dr. Ayhan Altıntaş
Ağustos, 2015

Elektronik savaşta, aktif ve pasif karşı tedbirler RF tehdit radarlarını karıştırmak için kullanılırlar. Elektronik karıştırma podları aktif olarak kabul edilirken milyonlarca mükemmel iletken metalik ince tellerden oluşan dipol bulutu ise pasif bir karşı tedbir olarak kabul edilir. Bu tezin amacı ilk başta Van Vleck'in Metot A ve B'sini [1], Tai'nin Değişken Metot'unu [2] ve Einarsson'ın Direkt Metot'unu [3] dipollerin radar kesit alanını (RKA) elde etmek için gerçeklemek ve çıkan sonuçları dizayn edilmiş dipol bulutu kartuşlarının RKA'sını hesaplamak amacıyla kullanmaktır. Nihai hedef ise, ticari olarak bulunan sistemlerden daha etkin pasif karşı tedbir sistemi önermektir. Bu tezde belirtilen metotların performansları değerlendirilmiştir. Bu değerlendirmelere göre Van Vleck'in Metot B'si ve Einarsson'ın Direkt Metot'u dipol bulutu kartuşlarının RKA değerlerinin hesaplanması için seçilmiştir. RR-178 (XN-2) ticari dipol bulutu kartuşunun performansı önerilmiş üç farklı dizayn ile karşılaştırılmıştır. Her bir dizayn için, 2-20 GHz frekans aralığı üç veya altı eşit alt-frekans aralıklarına bölünmüş ve her bir aralık için farklı dipol uzunlukları ve sayıları kullanılarak özel dipol bulutu kartuşları önerilmiştir. Kartuşların içindeki toplam dipol uzunlukları açısından, RR-178 (XN-2)'de kullanılan 88775 metre dipol yerine önerilen üçüncü dizayn kullanıldığında ortalamada 25300 metre dipol ile aynı RKA değeri daha düz bir şekilde 2-20 GHz frekans aralığı için sağlanmıştır. Ayrıca aynı frekans aralığı için, eğer RR-178 (XN-2)'de ve önerilen üçüncü dizaynda dipole bulutu kartuşlarının içindeki toplam dipol uzunları eşit tutulursa ortalamada 5.2 dB'lik RKA değerinde artış elde edilmiştir. Bu sonuçların analizi göstermiştir ki dizayn edilmiş dipol bulutu kartuşları uyumlu Radar İkaz Alıcısı (RİA) ve Atım Sistemi ile birlikte kullanılırsa ticari olanlardan daha etkindir.

Anahtar sözcükler: Radar Kesit Alanı (RKA), Dipol, İnce Tel, Dipol Bulutu, Değişken Metot, Direkt Metot, İntegral Metot, Atım Sistemi, Radar İkaz Alıcısı (RİA).

Acknowledgement

I would like to express immeasurable appreciation to my supervisor, Prof. Dr. Ayhan Altıntaş for his guidance, support and immense knowledge. Although his extensive workload, he continually guided and motived me to complete this thesis. I consider myself lucky to be one of his students.

I would like to thank Assoc. Prof. Dr. Vakur B. Ertürk and Assoc. Prof. Dr. Ali Cafer Gürbüz for being members of my thesis committee and reading my thesis.

I especially would like to express my gratitude to Dr. Mehmet Ali Tuğay for sharing his endless knowledge in electronic warfare with me, for leading me to work in electronic warfare field and for his insightful comments about this thesis.

I faithfully appreciate for every piece of knowledge that I learned from my instructors Prof. Dr. Orhan Arıkan, Prof. Dr. Ayhan Altıntaş, Assoc. Prof. Dr. Vakur Ertürk, Dr. Mehmet Ali Tuğay, Prof. Dr. Enis Çetin and Prof. Dr. Ömer Morgül.

I am very grateful to my superior Dr. Yavuz Yapıcı and my colleagues Müge Yılmaz Durmuş and Semih Selçuk Özdemir for their encouragements, comments and guidances.

I would also like to express my sincere gratitude to my dear friends Ece Çetinkaya, Muratcan Alkan, Dide Yiğit, Ozan Duygulu, Nur Timurlenk, Yağmur Yanık, İsmail Emre Ergün, Erkan Yasun, Esra Türkmen, Mustafa Arda Ahi, Ece Cambazoğlu, Burcu Özdemir Kipel and lastly Caner Odabaş for their supports and good friendship.

I thank Bilkent University and for sure its founder İhsan Doğramacı (I pray for him) for the facilities and financial supports that I benefited from.

I would also like to thank The Scientific and Technological Research Council

of Turkey (TÜBİTAK) for supporting me as a scholar (BİDEB 2210 Program) during my graduate study.

I would like to express my endless gratitude to my mother, Güher, my father, Ali and my brother Niyazi for their unrequited loves, helps and encouragements in my whole life. Without them, I could not accomplish any of my successes and could not complete this thesis.

Lastly, I would like to give my whole-hearted appreciation to my beloved, to my darling, to one who gives meaning to my life, to my lovely and beautiful wife, Neşe. Without her support and love, I could not accomplish to write this thesis and life would be much harder than it is.

Contents

List of Figures

List of Tables

Chapter 1

PRACTICAL INTRODUCTION

1.1 What is Dipole / Chaff?

A radar can be deceived by an active or a passive countermeasure. Chaff is the most popular and the most used passive countermeasure against radar.

Chaff consists of conducting thin wires, acting as dipoles, which are designed to generate a radar cross section (RCS) that is very close or greater than the RCS of the target that radar tries to find and track. In most cases, dipole lengths in a chaff cartridge are selected in such a way that their RCS is maximized for the concerned frequency interval by selecting their resonant frequencies accordingly. Not only in resonant frequencies, but also its harmonics, the dipole continues its effectiveness decreasingly [4].

Dipoles are stored in cartridges which are generally in the shape of rectangular prisms. These cartridges are carried in magazines which are placed outside of the aircraft. When the cartridge is dispensed from its magazine, the dipoles with different lengths form a chaff cloud in which they are generally distributed and oriented randomly. Some sample chaff cartridges are given below from related report [5]:

Table 1.1: Chaff Cartridges and Their Content [5]

Type	Designation	Cut No.	Length, Inches	Length, mm	Number, Millions
Cartridge	RR-129T/AL	1	2.00	50.8	0.75
	RR-144/AL	1	0.66	16.764	5.25
Roll	RR-163/AL	1	1.20	30.479	0.079
		2	0.60	15.239	0.5925
	RR-171/AL Roll 1	1	1.99	50.546	0.034
		2	1.12	28.448	0.034
		3	0.82	20.828	0.102
		4	0.71	18.034	0.136
		5	0.61	15.4939	0.136
	RR-171/AL Roll 2	6	1.74	44.196	0.032
		7	1.12	28.448	0.032
		8	0.82	20.828	0.032
		9	0.45	11.43	0.227
		10	0.36	9.1439	0.390
Package	RR-125/AL	1	0.75	19.049	0.36
		2	0.63	16.002	0.72
		3	0.59	14.9859	0.18
		4	0.56	14.224	0.72
		5	0.39	9.9059	0.36
		6	0.36	9.1439	0.72
		7	0.31	7.8739	0.18
	RR-146/AL	1	0.70	17.779	2.25
		2	0.60	15.239	3.00
		3	0.51	12.954	1.50
		4	0.45	11.43	2.25
		5	0.39	9.9059	3.75
	RR-153/AL	1	1.84	46.736	1.50
		2	1.61	40.894	0.54
		3	1.07	27.178	0.75
		4	0.63	16.002	1.50
		5	0.55	13.969	1.50
	RR-153 A/AL	1	1.84	46.736	1.50
		2	1.61	40.894	0.75
		3	1.07	27.178	0.75
		4	0.63	16.002	1.50
		5	0.55	13.969	2.25
	RR-178 (XN-2)	1	1.60	40.640	0.375
		2	1.34	34.036	0.375
		3	0.97	24.638	0.750
		4	0.64	16.256	0.750
		5	0.54	13.716	1.250
		6	0.34	8.636	1.500

1.2 History of Chaff

Combination of different lengths of metal strips was firstly named as "window" by UK, however, the common term nowadays used is "chaff" which was used by the US. It was firstly used on 24^{th} July 1943 [6]. The first chaff cartridge contained 300 mm long and 15 mm wide 1000 metallic strips [7]. Radars that had operated at 570 MHz and 490 MHz became completely ineffective owing to these strips. In 1943, Americans also used the chaff concept with a little bit of difference with today's chaff. First difference was the result of the operating frequencies of the radars. The Japanese radar that was needed to be deceived, was working at the frequency interval of 70 MHz to 200 MHz which are much lower than the frequency that today's radars operate [7]. Therefore, to generate a strong echo signal, they used very long metallic ropes against these radars. The second one was due to lack of dispensing systems. As a result, these ropes were dropped from the aircraft manually.

With increasing radar technology, frequency interval of 2-20 GHz is actively used nowadays [7]. Frequency spectrum from 2 to 6 GHz is generally used by surveillance radars. On the other hand, acquisition, tracking and guidance radars operate at the remaining spectrum up to 20 GHz [7]. The second part of the spectrum - from 6 GHz to 20 GHz - is generally the concerned one in terms of electronic warfare. However, with a simple search on internet, one can easily state that some acquisition, tracking or guidance radars also operate at 2-6 GHz interval. SnowDrift can be a good example to this case. However, a simple survey indicates that tracking radars particularly use the intervals from 8 GHz to 14 GHz like Land Roll, Straight Flush, Gadfly, Gundish, Skyguard, Sentinel, Superfledermaus and so on. Today's dispenser systems and chaff cartridges are generally designed to be effective from 2 to 20 GHz frequency interval for covering all the possible threats as far as is known. Moreover, today's chaff dispensing systems can dispense cartridges by pushing a simple button and the used long ropes are replaced with small strips/wires called dipoles.

1.3 Dipole Materials and Chaff Cartridges

RF resistance is an important criteria while deciding the chaff material [7]. A conductor re-radiates the power received from incident wave with the ratio of $\frac{R_0}{R_0+R_r}$ where R_0 is the radiation resistance of conductor in free space and R_r is the RF resistance [7]. One can easily state by looking at the ratio equation that to get a maximum return, RF resistance value need to be zero. Similar idea can be used for RCS calculation. To increase the scattered power from chaff, the dipoles in the cloud should include conductor that has small RF resistance values. Aluminium, silver, copper and zinc are the today's main materials for dipoles [7].

The properties of materials that are used for manufacturing dipoles are given in Table 1.2 below.

Table 1.2: Dipole Materials and Their Properties [7]

Type	Nominal section dimensions of filaments	Density of material (1)	Normal maximum packing density (2)	Normal maximum bulk density (1)X(2)/ 100	Mean fall rate in still air at sea level	Ratio of number of dipoles per unit volume of payload (silver nylon =1)
	μm	kg/m^3	%	kg/m^3	m/s	
Aluminised glass	25	2550	55	1403	0.30	10.97
Silver coated nylon monofilament	90	1300	65	845	0.60	1.00
2 X 1 aluminium foil	50 X 25	2700	55	1485	0.40 - 0.45	4.31
4 X 1 aluminium foil	100 X 25	2700	55	1485	0.50 - 0.55	2.15
8 X 1/2 V-bend aluminium foil	200 X 12	2700	45	1215	0.50 - 0.55	1.84

Silver Coated Nylons: Nylon filaments are coated with silver (0.5 - 1 μm) which is expensive as everyone knows. The diameter of this type of dipoles cannot be smaller than 90 μm (see Table 1.2) which causes low number of dipoles to fit into a standard chaff cartridge. As number decreases, the RCS decreases, as well. As can be seen in Table 1.2, its bulk density is low and therefore weight of the chaff cartridge is low, as well [7].

Aluminium Foil: As can be understood from its name, the reel of foil is shredded to obtain the filaments [7]. Generally the thickness is determined by the manufacturing process of the foil. On the other hand, the width is determined by the machine that cuts the foils. Some used type names of these aluminium

foils can be seen below:

- Thickness: 25 μm, Width: 50 μm $\rightarrow$ 2 $\times$ 1 Aluminium Foil
- Thickness: 25 μm, Width: 100 μm $\rightarrow$ 4 $\times$ 1 Aluminium Foil
- Thickness: 12.7 μm, Width: 200 μm $\rightarrow$ 8 $\times$ 1/2 V bend Aluminium Foil

After cutting, the filaments are twisted and manufacturing process of the dipoles is completed. Due to twisting, they have special movement in the air [7]. By evaluating Table 1.2, one can easily state that, the speed of these dipoles is lower than the speed of silver coated nylon ones. As speed get lower, time that dipole stay in the air increases. However, one should also be note that low speed also means more time to form an effective cloud.

Aluminium-coated Glass Fibers: As can be seen on table, the diameter of this type of dipole is so small that number of dipoles in a chaff cartridge is maximized. Moreover, due to its low speed, these dipoles stay in the air more than others. Furthermore, compared to others, this type of dipoles are cheap. As a result, as stated by both Butters and Pouliguen, practically used dipoles are mostly aluminum-coated glass fibers and their diameters are about 25 μm [7, 8].

Other Materials: Some other materials can be copper coated polyester filament, zinc coated glass filaments, metal coated carbon or graphite fibers, metal coated silicon carbide or boron [7]. However, they are not used generally because of their cost, manufacturing problems, possible corrosion issues, low melting points of some used materials and so on...

By examining Table 1.2 and knowing possible dipole materials, some important points during manufacturing process of optimized dipoles for maximum RCS can be summarized as:

- Select coating conducting material with small RF resistance,
- Select material so that dipoles are oriented randomly in cloud so as to have equal vertical and horizontal scattering,

- Decrease the diameter of dipole to increase the number of dipoles that can fit into a standard chaff cartridge,
- Select dispensing system and material in a way that the motions of cartridge and dipoles enable to have largest RCS value as soon as and as long as possible,
- Decrease probability of birdnesting by using proper manufacturing techniques,
  Birdnesting is the term used for describing the situation in which dipoles stick to each other and a randomized cloud of dipoles cannot be generated. This situation decreases the radar cross section value that can be achieved.
- Select the coated material such that it does not bend when it is dispensed in the air.

After manufacturing dipoles, they are placed into chaff cartridges. For aircraft, there are two main usages of chaff cartridges: self-protection or corridor laying. For self-protection, dipoles in the practical cartridge are about 100-150 g which changes according to dipole material used and number of dipoles fitted into cartridge [7]. Generally, an aircraft contains one or at most two chaff magazines and each magazine consists of 30 chaff cartridges. This type of usage aims at generating false targets to jam the threat radar. On the other hand, weight of a cartridge can be up to 25 kg for corridor laying application. For this type, an aircraft drops dipoles at a steady rate in order to from a corridor that conceals other aircraft [7].

1.4 Usage Types of Chaff

There are many different situations that a chaff can be used as a countermeasure. Pouligen [8] described all of the usage types as below;

Deception: In this type, target tries to generate many false targets away from the real target by dispensing chaff cartridges so that radar cannot track the real

target and spend its time and energy on generated false target [8].

Distraction: Target deploys a cloud in order to send a false echo signal to the radar before the acquisition phase [8] or as stated in the work of Manji when the missile is fired and in search mode [9]. By doing so, radar system may be deceived so that it thinks the real target is the generated chaff cloud and completes acquisition phase with the false target.

Screening: In this method, a very large and extensive chaff cloud is generated between radar and target. Due to extensive echo return from this cloud, the detection performance and unambiguous range of the radar decreases [8].

Seduction: The aim of this type of usage is to break lock of the radar by creating a great chaff cloud in the resolution cell of the radar [8]. Another explanation of this usage is given by Manji. He states that, when missile is at terminal phase, chaff is dispensed so as to generate a big false target and deceive missile to track the realistic false target [9].

Saturation or confusion: Many false targets are generated near target system by the usage of chaff clouds so that probability of false target rate increases for the radar since it identifies these clouds as false targets on the radar display [8]. Moreover, in the article of Manji, it is given that this method is generally applied when the distance between radar and the target is long [9].

These usage types can be diversified by combining different engagement scenarios.

Chapter 2

THEORETICAL INTRODUCTION

2.1 Dipole Distribution and Orientation Models in a Chaff

In the chaff literature, there is not much information about dipole orientations and distribution in a chaff cloud. Van Vleck [1] and Dedrick [10] proposed that dipoles are distributed in a random fashion in a sphere. Orientation of a dipole is represented with angles γ_i (polar latitude of the wire) and ϕ_i (polar angle) as can be seen in Fig. 2.1. Van Vleck [1] and Dedrick [10] assumed that γ_i can be found by equating an uniform random number between -1 and 1 to $cos(\gamma_i)$. Additionally, they stated that ϕ_i can be found by multiplying second uniform random number with 2π.

For orientation of the chaff dipoles, Zaharis [11] proposed a similar concept as Van Vleck [1] and Dedrick [10] have proposed. He represented the same approach using probability density function. For angle ϕ_i, it is given that:

$$p(\phi_i) = 1/2\pi \tag{2.1}$$

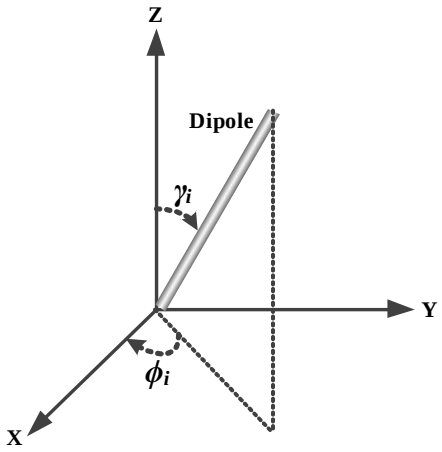

Figure 2.1: Dipole Orientation Geometry

and for γ_i,

$$p(\gamma_i) = \frac{1}{2} sin(\gamma_i) \tag{2.2}$$

Zaharis also stated that, chaff cloud was assumed to have a shape of a sphere while explaining his dipoles distribution model. If the center of the chaff cloud is taken as the reference point on the Cartesian coordinate, the locations of the dipoles are supposed to have a normalized Gaussian probability density function [11]. He represented the position of the i^{th} dipole using x_i, y_i and z_i as the probability density functions:

$$\begin{aligned} p(x_i) &= \frac{1}{\sigma_{x_i}\sqrt{2\pi}} e^{-\frac{{x_i}^2}{2\sigma_{x_i}^2}} \\ p(y_i) &= \frac{1}{\sigma_{y_i}\sqrt{2\pi}} e^{-\frac{{y_i}^2}{2\sigma_{y_i}^2}} \\ p(z_i) &= \frac{1}{\sigma_{z_i}\sqrt{2\pi}} e^{-\frac{{z_i}^2}{2\sigma_{z_i}^2}} \end{aligned} \tag{2.3}$$

Note that, with the change of standard deviations ($\sigma_{x_i}, \sigma_{y_i}$ and σ_{z_i}) different shape of chaff cloud like ellipsoid can be derived. For instance, $\sigma_{x_i} = \sigma_{y_i} = \sigma_{z_i}$ gives a spherical cloud which is the concerned case for this thesis.

On the other hand, Pouliguen [8] proposed different but somewhat complicated

dipole orientations and positioning procedure. He used the work of Vakin and Shustov [12] and stated that dipoles in a chaff cloud are at most likely either vertical or horizontal orientations. In addition to work of [12], he also used his laboratory experiment. The result of this experiment is that dipoles are most likely to have horizontal orientations than vertical ones in chaff cloud [13]. Taking into account the indications of the stated works, he presented a probabilistic approach to the orientation of the dipoles. As before, assume that ϕ_i and γ_i are proposed angles for the orientation of a dipole as can be seen in Fig. 2.1. Then the probability density function of the orientation becomes:

$$p(\phi_i, \gamma) = p(\phi_i)p(\gamma_i) = \frac{p(\gamma_i)}{2\pi} \tag{2.4}$$

Note that, as described above, probability density function of ϕ_i is $\frac{1}{2\pi}$.

With the use of the result of Vakin and Shustov [12], Pouliguen proposed equation for $p(\gamma_i)$ as:

$$p(\gamma_i) = \frac{1}{I}[\frac{K_h}{S_h}e^{-\frac{1}{2}(\frac{\gamma_i - M_h}{S_h})^2} + \frac{K_v}{S_v}e^{-\frac{1}{2}(\frac{\gamma_i - M_v}{S_v})^2}]\sin\gamma_i \tag{2.5}$$

where

$$I = \int_0^{\frac{\pi}{2}} [\frac{K_h}{S_h}e^{-\frac{1}{2}(\frac{\gamma_i - M_h}{S_h})^2} + \frac{K_v}{S_v}e^{-\frac{1}{2}(\frac{\gamma_i - M_v}{S_v})^2}]\sin\gamma_i d\gamma_i \tag{2.6}$$

In these equation subscript h indicates horizontal and v indicates vertical component. The parameter descriptions are as follows [8]:

- K : weighting functions for quantity of dipoles
- S : standard deviation for Gaussian function that is used for angular distribution
- M : mean value of Gaussian function for angular distributions

By using different values of K, S and M, different orientations can be observed. For example, if S_h and S_v are high, than random orientation can be observed with:

$$p(\phi_i, \gamma_i) = \frac{sin\gamma_i}{4\pi} \tag{2.7}$$

As can be noted, this function was also used by Zaharis [11], Van Vleck [1] and Dedrick [10] and this is the case in which all dipoles are oriented randomly.

More than that, Pouliguen [8] also derived a positioning method for dipoles which uses two main assumptions. The first one is that N dipoles exist in chaff cloud and the second one is average distance between dipoles is d.

Then he defines a center point for a cube whose side length is d. N elementary cubes exist totally [8]. Let the center point be (x_c, y_c, z_c) for Cartesian coordinate.

$$\begin{aligned} x_c(p,q,r) &= \frac{d}{2} + (p-1)d \\ y_c(p,q,r) &= \frac{d}{2} + (q-1)d \\ z_c(p,q,r) &= \frac{d}{2} + (r-1)d \end{aligned} \tag{2.8}$$

Where p, q, r are indexes for X, Y, Z reference frames, respectively. The values of p, q, r changes as 1, 2, 3, ... , $N^{1/3}$. The position of the i^{th} dipole is calculated by:

$$\begin{aligned} x_i(p,q,r) &= x_c(p,q,r) + x_{ig} \\ y_i(p,q,r) &= y_c(p,q,r) + y_{ig} \\ z_i(p,q,r) &= z_c(p,q,r) + z_{ig} \end{aligned} \tag{2.9}$$

x_{ig}, y_{ig}, z_{ig} are independent numbers and their values are determined by the Gaussian law [8]. As a result, position of the i^{th} dipole becomes (x_i, y_i, z_i).

Note that, if d is selected as $d > 2\lambda$ (where λ is the wavelength), then no coupling effect is observed [14, 15]. If this effect is included, the interactions between each dipoles need to be considered. However, for almost all the theoretical works, this effect is not included since the equations that need to be solved get complicated and the number of these equations are increased too much.

2.2 Dipole Current and RCS Calculation Methods

In the literature, three main approaches become prominent. The first one is called "Integral Equation Method" and firstly derived by Van Vleck [1] then used by Dike and King [16] and Lindroth [17]. The second one is developed and used by Tai [2] and Hu [18] and named as "Variational Method". The last method has the name "Direct Method" which is investigated by Ufimtsev [19], Fialkovski [20] and Einarsson [21, 3].

For each approach, one method is selected and implemented for this thesis. Van Vleck's, Tai's and Einarsson's methods are the selected ones due to their complete explanations and formulations compared to discussed methods in the above paragraph.

Van Vleck derived two different methods. The first one is called Method A which uses conservation of energy or induced electromotive force to calculate the RCS of dipoles [1]. He equates the real power on the wire surface to the power at far field in order to get the magnitude of the assumed simplified current on the wire. This method is valid when the lengths of the dipoles are not in resonance [1]. Van Vleck's other method is named as Method B which tries to solve antenna problem using first order integral equation that is derived from the works of Hallén [22], Gray [23], King and Middleton [24], chronologically [1]. Then Tai used a different approach based on the variational method which uses infinitely conducting dipoles to offer a solution to problem [2]. Afterwards, Einarsson used a direct method which uses infinite sum of travelling waves to get an exact solution to the RCS of a thin wire [21].

2.3 Assumptions for Theoretical Works

The effectiveness of a chaff cloud depends on many parameters like the cloud shape, atmospheric events and dipole materials [25]. Moreover, properties of dipoles like their technological and aerodynamic characteristics have also an impact on effectiveness [8]. Fall speed of the dipoles and altitude where the chaff is dispensed also have an impact on the performance of the chaff application [4]. In addition to these, lengths of dipoles, number of dipoles dropped at a time, chaff dispensing system characteristics, chaff cartridge properties have influence on the performance of chaff, as well.

There are lots of studies that tried to derive characteristics of chaff cloud and calculate its RCS by considering the above influences. Although, lots of simplified theories exist, none of them can completely describe the properties of chaff [8]. Reaching an exact solution with considering effects like aerodynamics of dipoles, birdnesting, coupling, dispensing system, dipole materials, number of dipoles, length of dipoles, incident wave polarizations, atmospheric events, time dependence of the movement of the dipoles and so on is still a hard problem. Therefore, the proposed simplified solutions to the problem by Van Vleck [1], Tai [2] and Einarsson [3] are still helpful for getting radar cross section of dipoles and average backscattering cross section of a chaff cloud that consists of randomly distributed and oriented dipoles. Using these solutions, one can predict RCS of a chaff cloud with an acceptable error and use it for his/her work with below assumptions:

- Chaff cloud is completely dispersed,
- Dipoles are randomly oriented,
- Dipoles are modelled as "thin" circular cylinders,
  This statement is valid without losing the generality. As stated in the work of F.Bloch and M. Hamermesh [26], circular cylinders have same electrical properties with any arbitrary shape of strips with the conditions that their lengths are same and the diameter of the cylinder is equal to width of the

strip [1].

Moreover, Einarsson also stated that dipoles can be modelled as a finite perfectly conducting thin cylindrical wires. Indeed, the formulas that are available can only model the scattering problem from a thin wire when a plane wave is incident [8].

- " Thin" means that $l/a > 50$ where the diameter is a and length of the dipole is l,
- Screening effect is not concerned,
- No birdnesting is observed,
- Coupling effect is negligible such that $d > 2\lambda$,
- No atmospheric or aerodynamic effects,
- Dipoles are perfectly conducting metallic cylinders,
- Dipole are manufactured perfectly with wanted lengths and numbers,
- No circumferential current on dipoles,
  Circumferential current is not observed when the diameter of the wire is as small as the one fiftieth of wavelength ($\lambda/50$) of the incident wave [5].

By taking into account above assumptions, the theoretical works can be used to decide at least lengths and numbers of dipoles in the chaff cartridge.

2.4 Motivation and Contribution

Although chaff has been used over seventy years, its usage has not been decreased but increased. In 1982, Butters explained why chaff is going to be used in coming years. To summarize the explanations of Butters [7];

- Chaff tactics are continuously improved as new dispensing systems and radar threats are introduced. Although some of the radars have low vulnerability to chaff, mutual improvements still make chaff as an effective countermeasure.

- Operators of the radar systems generally try to track targets automatically. Their effect on the control loop is limited in automatic mode which can be deceived by the chaff such that in the worst case some errors occur in tracking loops or in the best case, the lock may be broken.
- As stated in the first bullet, some improved systems can discriminate between chaff and real target by Doppler processing or by similar processes. However these processes need an extra effort, work and time (especially for old radar systems). As a result, performance of radar system can be degraded by suitable chaff applications compared to no application case.
- Dispensing systems are cheap compared to electronic jamming systems. Since most parts of the dispensing systems are mechanic, their maintenance is easy and mean time before failure (MTBF) value is high. On the other hand, active jamming systems do almost all the work by using electronic equipments whose maintenance are hard and costly. Moreover, the chaff cartridges are also cheap. As a result, chaff systems are good alternative to active jamming systems in terms of cost and maintenance concerns.
- Chaff cartridge can be launched from aircraft or ship to generate false echoes at a great distance. This may help to generate many target in radar display so that operators may not decide which target to track. Conversely, other decoys cannot be launched to a great distance, however, if they can their RCS most of the time will be lower than the chaff. After all, it can be asserted that for long distances, chaff is generally better for generating false targets compared to other countermeasure decoys.

Butters' discussion still remains valid and motivates people to generate more effective chaff cartridges and dipoles with more effective dispensing systems.

In electronic warfare field, some practical observations on both active and passive countermeasures are listed below:

- Dispensing systems are easy to program and use,
- Their cost is very low compared to active jamming systems,

- Chaff application works really fine with a suitable maneuver to deceive the threat radar,
- Chaff is still very effective especially against old radars that do not work on Doppler of the target,
- Chaff decreases the performance of the new radar systems and confuses radar operators,
- Active jamming systems needs to know almost all the receiver parameters of the target radar to be successful, on the other hand, passive jamming systems do not need,
- Preparing an active jamming system to operate needs much more time than a passive system,
- When an active jamming system is prepared for a threat radar, you can use it without any extra work for years,
- During a mission, an active jamming system can be used numerously while the system have power and does not have any failures, however, a passive jamming system can be used until the system has countermeasure ammo,
- Both active and passive jamming system performances depend on many parameters,
- Combination of an active technique with chaff usage is today's one of the most effective jamming technique.

When Butters' explanations and the practical observations are compared, one can easily state that they almost match with each other. Based on these statements, chaff cartridges and Dispensing Systems used in the world are researched with the expectation that new Dispensing Systems and chaff cartridges can be proposed for more effective applications especially when they are used with a Radar Warning System (RWR). *(Main tasks of a RWR are to receive radar signals, to process them to measure the signal parameters, to classify the properties of the radar by using these parameters and to warn the user accordingly.)* Early RWR systems like AN/APR-39A(V)3 [27] is unable to measure the frequency of the received signal. Therefore, old chaff cartridges like RR-153 A/AL (see Table 1.1) were

designed to cover all the possible frequency interval that a radar system can work. Moreover, old dispensing systems were designed to dispense only one type of chaff cartridges due to RCS coverage of these old chaff cartridges *(In this thesis "RCS of chaff cartridge / chaff cartridge RCS" refer to RCS provided by the chaff cloud that is formed by the dipoles after the cartridge is dispensed.)* and lack of received radar signal frequency. With developments on electronic warfare, new RWR systems like SAAB BOW RWR and ESM Systems [28] and Indra ALR-400 RWR [29] can measure the frequency of the received signal, which enable one to dispense a related chaff cartridge that is designed for a narrow frequency interval which also covers the measured frequency. With this design, one can decrease the number of dipoles dispensed, get higher RCS for the concerned frequency, minimize the size of chaff cartridge so that more chaff cartridges can fit into the same magazine.

The main contributions and motivations of this thesis are:

- to implement dipole RCS models which are less complicated compared to exact solutions and take less time to be calculated with an acceptable error,
  Van Vleck's Method A and B [1], Tai's Variational Method [2] and Einarsson's Direct Method [21] are aimed to be described and implemented for this thesis. These methods require less computational work and time compared to exact calculation in exchange of admissible error for the purpose of this thesis.
- to compare these implemented models to decide which model can be used to calculate the RCS of a chaff cloud,
  Tai [2] compared his results with Van Vleck's [1] methods. Moreover, Einarsson [21] separately did a performance comparison of his method with Tai's [2] and Van Vleck's [1] works by using different configuration for each comparison. In this thesis, for the first time, comparison of these three different approaches to the problem is done by using same parameters and conditions.
- to calculate the RCS of early chaff cartridges,
  In the open literature, finding RCS values of chaff cartridges for all the

concerned frequencies is not possible. Even finding the content of a chaff cartridge is a good challenge. In this thesis, some of the found chaff cartridges (see Table 1.1) RCS values are calculated and discussed.

- to describe a procedure for chaff cartridge design,
  A procedure is given in order to get a flat RCS response for a given frequency interval while determining the lengths and numbers of the dipoles automatically.
- to propose more effective chaff cartridges for sub-frequency intervals,
  In this thesis, three different designs of chaff cartridge are suggested by dividing 2 to 20 GHz frequency interval into three or six equal sub-frequency intervals and designing chaff cartridges especially for these sub-frequency intervals to increase the effectiveness. Details are given in Section 8.4, 8.5 and 8.6.
- to introduce operational scenarios which are used to discuss the effectiveness of designed chaff cartridges,
  Three different scenarios are proposed to compare the performance of a commercial chaff cartridge with three different designs.
- to specify the properties of Radar Warning Receiver and Dispensing System that is able to work together with designed chaff cartridges.
  In this thesis, a new practical concept to the chaff countermeasure is discussed and suggested in such a way that chaff usage is optimized and its effectiveness is increased with the help of specified abilities of Radar Warning Receiver and Dispensing System.

2.5 Organization of the Thesis

The thesis is organized as follows. In Chapter 1, practical introduction to the issue is given in order to get familiar with the concepts of dipole and chaff. Next, in Chapter 2, theoretical information is given to introduce the dipole orientation and distribution techniques, the dipole RCS calculation methods and lastly motivation and contribution of this thesis. The following chapter is for giving

basic background knowledge to calculate RCS of a thin wire. For Chapter 4, 5 and 6, Van Vleck's, Tai's and Einarsson's methods for dipole RCS calculation are detailed. Then, in Chapter 7, RCS values of different lengths of dipoles are simulated and evaluated. In Chapter 8, simulations and evaluations about chaff RCS are given. The RCS of different commercial chaff cartridges are calculated. Furthermore, a procedure for designing chaff cartridge for a concerned frequency interval is introduced. Moreover, according to this procedure three different designed chaff cartridge groups are given and their performances are examined. Additionally, three practical scenarios are used to show the performance of the new designs. At the end of this chapter, required properties of Radar Warning Receiver and Dispensing System are described. Finally, in the last chapter, some concluding points are given.

Chapter 3

BACKGROUND

Although, detailed background will be given at Chapter 4, 5 and 6, simple procedure for calculating backscattering cross section of a thin wire will be given here, as well. This procedure is the simplified part of the work [30].

First of all, notations in Table 3.1 are used throughout this chapter.

Table 3.1: Notation for Background Chapter

$2l$	:	Length of the wire
θ	:	Angle of incidence of the wave
$\overline{E}_0$	:	Electric field vector with respect to dipole axis
β	:	$2\pi/\lambda$
λ	:	Wavelength
$\overline{\beta}$	:	Propagation vector
ϕ	:	Angle between $\overline{E}_0$, $\overline{\beta}$ and plane that is normal to wire axis
$\overline{E}^s$	:	Scattered electric field vector
$\overline{A}^s$	:	Scattered vector potential
φ^s	:	Scattered scalar potential
$\overline{E}^i$	:	Incident field
J	:	Current density
I	:	Current on wire
$\overline{E}$	:	Far field scattered field

Assume that a plane wave is incident to a thin wire with an angle θ as in

Fig. 3.1. Then scattered field is given using Maxell's homogenous equations as Eq. (3.1) and Lorentz gauge is given as in Eq. (3.2).

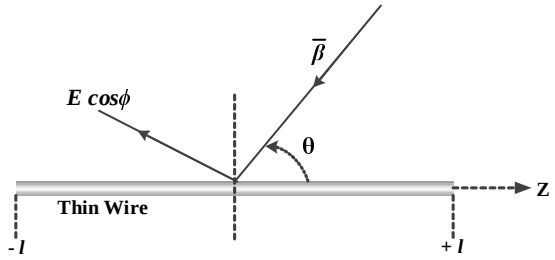

Figure 3.1: Thin Wire Geometry for Background

$$\overline{E}^s = -\overline{\nabla}\varphi^s - \frac{1}{c}\frac{\partial \overline{A}^s}{\partial t} \tag{3.1}$$

$$\overline{\nabla} \cdot \overline{A} + \frac{1}{c}\frac{\partial \varphi}{\partial t} = 0 \tag{3.2}$$

By using Eq. (3.2) in Eq. (3.1), Eq. (3.3) is obtained as:

$$\frac{\partial \overline{E}^s}{\partial t} = c\overline{\nabla}\ \overline{\nabla} \cdot \overline{A}^s - \frac{1}{c}\frac{\partial^2 \overline{A}}{\partial t^2} \tag{3.3}$$

Then if it is assumed that time dependency of the $\overline{E}^s$ only occurs at frequency e^{-iwt}, then Eq. (3.4) is derived,

$$-i\omega\overline{E}^s = c\overline{\nabla\nabla} \cdot \overline{A} + \frac{\omega^2}{c}\overline{A} \tag{3.4}$$

As described in Section 2.3, assume that the wire is a perfect conductor and only tangential component of the incident field contributes to scattered field. Then, it can be obtained that $E_z^s = -E_z^i$ (where subscript z is used for z-component of the field). Using this equality, Eq. (3.4) becomes:

$$\frac{\partial^2 A_z}{\partial^2 z} + \beta^2 A_z = i\beta E_z^i \tag{3.5}$$

The incident field to the wire is given by Eq. (3.6) and the z component of this field without time component is in Eq. (3.7)

$$\overline{E}^i = \overline{E}_0 e^{i\overline{\beta}\cdot\overline{X} - i\omega t} \tag{3.6}$$

$$E_z^i = E_0 \cos\phi \sin\theta e^{i\beta z \cos\theta} \tag{3.7}$$

Now use Eq. (3.7) in Eq. (3.5):

$$\frac{\partial^2 A_z}{\partial^2 z} + \beta^2 A_z = i\beta E_0 \cos\phi \sin\theta e^{i\beta z \cos\theta} \tag{3.8}$$

Two different solutions can be proposed to Eq. (3.8). The homogeneous solution can be seen in Eq. (3.9) and the inhomogeneous one can be seen in Eq. (3.10).

$$A\cos\beta z + B\sin\beta z \tag{3.9}$$

$$iE_0 \cos\phi \sin\theta \int_o^z e^{i\beta\xi\cos\theta} \sin\beta(z-\xi)d\xi = \\ = \frac{iE_0\cos\phi}{\beta\sin\theta}(e^{iqz} - \cos\beta z - i\cos\theta\sin\beta z) \tag{3.10}$$

where $q = \beta\cos\theta$.

Current distribution on the wire generates a vector potential as in Eq. (3.11) by using Maxwell's inhomogeneous equations.

$$\nabla^2\overline{A} - \frac{1}{c^2}\frac{\partial\overline{A}^2}{\partial t^2} = -\frac{4\pi}{c}\overline{J} \tag{3.11}$$

and free space solution of Eq. (3.11) is:

$$\overline{A} = \frac{1}{c}\int \frac{\overline{J}\delta[t' + (|\bar{x} - \bar{x}'|/c)t]}{|\bar{x} - \bar{x}'|}dt'dx'^3 \tag{3.12}$$

To find the vector potential on the surface of the wire, assume that the direction of the current on wire is z and $J = J(\overline{X})e^{-iwt}$. Then

$$A_z(z) = \frac{\pi a^2}{c}\int_{-l}^{l} \frac{Je^{-i\beta r}}{r}dz' \tag{3.13}$$

where

$$r = \sqrt{(z-z')^2 + a^2} \tag{3.14}$$

Moreover, assume that the current density is $J = \frac{I}{\pi a^2}$. Now, Eq. (3.13) can be used in Eq. (3.8) to get Eq. (3.15):

$$\int_{-l}^{l} \frac{I(z')e^{-i\beta r}}{r}dz' = A_1\cos\beta z + B_1\sin\beta z + \frac{i\omega E_0\cos\phi}{\beta^2\sin\theta}e^{iqz} \tag{3.15}$$

The procedure changes after this point since different current equations $I(z)$ can be selected to get a solution of Eq. (3.15). In this thesis, Van Vleck, Tai and Einarsson's current equations are given at Chapter 4, 5 and 6, respectively. To solve Eq. (3.15), one should apply the boundary condition that current becomes zero at the ends of wire. Moreover, for $\theta = 0$, current should also vanish.

When Eq. (3.15) solved by applying boundary conditions, $I(z)$ can be used in Eq. (3.16) to get far field scattered field by using Maxwell's equations:

$$\overline{E}^s = \frac{i}{\beta}\overline{\nabla} \times \overline{\nabla} \times \overline{A} \cong \frac{e^{i\beta r}}{r} \sin\theta' \int_{-l}^{l} I(z')e^{iq'z'}dz' \tag{3.16}$$

Then monostatic RCS of the thin perfectly conducting wire due to incident plane wave is given by

$$\sigma(\theta, \phi) = 4\pi r^2 \frac{|\overline{E}^s|^2}{|E_0|^2} \tag{3.17}$$

Chapter 4

INTEGRAL METHOD

4.1 General Introduction to Van Vleck's Methods

The calculation of radar cross section for a thin perfectly conducting wire starts with calculation of the current on the wire due to radiation from the radar. Two basic methods are mentioned by Van Vleck [1]. The first method is used by Siegel and Labus [31] and named as EMF (Electromotive Force) method. For this method an equation is proposed for the generated current and this equation is evaluated by applying the conservation of energy. Although, the first method gets some important findings, the method does not solve the problem related to antenna theory, receiving antenna [1]. This method is called as "Method A". The second method which is named as "Method B" uses Maxwell equation's and satisfy the boundary condition for the current on the surface of the wire by using successive approximation method. In this perspective, three important statements can be said by concerning discussion at Section 2.3: first, since we assumed at the beginning the wire is a perfect conductor, tangential part of the total electric field become zero at the surface of the thin wire; second, since we assumed that the wire is thin enough, the value of the current for the end of the

wire vanishes and third, incident field and the field due to current induced on the wire is summed to get the total field on the wire. These three statements are the result of the assumption which states that the current on the wire is not placed at the surface but at the center [1]. King and Harrison presented a mathematical expression for combining these three statements [32, 33]:

$$\int_{-l}^{+l} d\xi I(\xi)\frac{e^{-i\beta r}}{\gamma} = \frac{i\omega\cos\phi E_0 e^{iqz}}{\beta^2\sin\theta} + A_1\cos(\beta z) + A_2\sin(\beta z) \tag{4.1}$$

with $r = [(z-\xi)^2 + a^2]^{\frac{1}{2}}$ and $I(\pm l) = 0$

As discussed in the paper of Van Vleck [1], this assumption uses the fact that the exterior potential due to an infinitely long cylindrical charge distribution is equal to potential when these charges are positioned at the center of the cylinder. Therefore, errors due to this assumption is tolerable.

King and Harrison [32] not only proposed the integral equation Eq. (4.1), but also used successive approximation method due to Hallén [22] solving the equation for receiving antenna. However, the method proposed by Hallén [22] fails as l/λ reaches to 1 due to convergence issues. Therefore, higher but complicated approximations need to be used for the method to overcome this failure. Gray [23] introduced different successive approximation procedure that somehow overcame this difficulty while solving Eq. (4.1). More refined form of the procedure is also explained in the article of King and Middleton [24]. Although, the procedure is designed for transmitting antenna, Van Vleck asserted that it is more appropriate for receiving antenna as it will be explained later in this chapter. However, this procedure still has some difficulties when l/λ is very large. Especially, Einarsson paid attention to these difficulties and asserted that Van Vleck's methods fail as the l/λ ratio exceeds two [21]. In addition to criticism of Einarsson, Tavis asserted that Van Vleck's RCS calculation method is problematic especially when the plane wave is incident to the end of the wire [30]. The cause of this inaccurate situation is the simplifications and approximations (particularly Van Vleck used asymptotic values for Cin and Si functions as the input goes to large values) that he did to get an asymptotic expression of backscattering cross section of the thin wire. Although, some problems are inevitable due to approximations, short descriptions of the proposed solutions to the problem are given below:

Method A: Usage of conservation of energy and some guesses on King and Harrison's [32] method for the solution of the considered problem (some corrections are taken from Gray [23] or King and Middleton [24]).

Method B: The integral equation in Eq. (4.1) for receiving antenna is solved by using an estimated solution. The solution uses a similar procedure that is derived from Gray's work [23]. After Van Vleck completed the derivation, King and Middleton investigated similar procedure and published an article using slightly different language [24].

The geometry that Van Vleck used can be seen in Fig. 4.1.

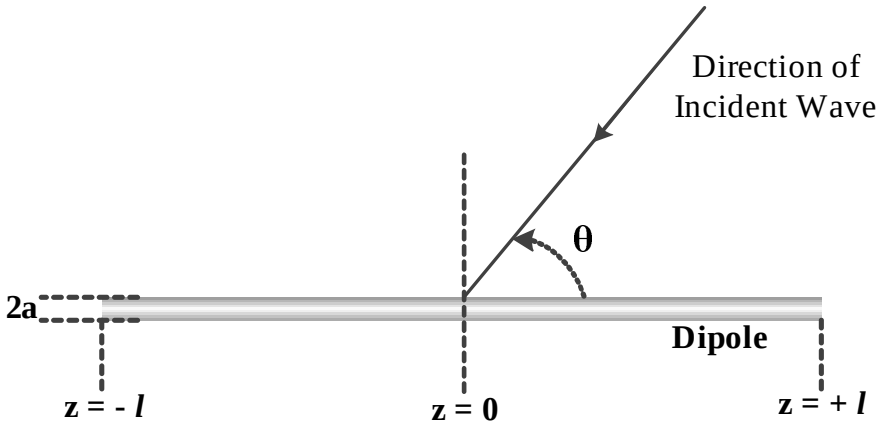

Figure 4.1: Van Vleck's Dipole Geometry

For both methods, with $q = \beta \cos\theta$, the current assumed to be:

$$I(z) = C_1 \cos(qz) + C_2 \cos(\beta z) + C_3 \sin(qz) + C_4 \sin(\beta z) \tag{4.2}$$

For this current equation, below implications can be made with the help of [1]:

- C_i for $i = 1, 2, 3, 4$ depends on $\theta, \phi, l, \lambda, a$ where ϕ is the angle between the plane generated by the wire and the incident electric field and λ is the wavelength of the incident wave,
- $\sin(\beta z)$ and $cos(\beta z)$ are the resonant parts,

- $\sin(qz)$ and $cos(qz)$ are the forced parts,
- C_2 and C_4 are very large when $\beta l/\pi = n/2$ where $n = 0, 1, 2, 3, \ldots$ due to resonance,
- Cosine functions are named as even parts and sine functions are the odd parts,
- For Method A, C_i values are obtained by mainly conservation of energy and an extra assumption that states the solution form is away from resonance,
- For Method B, C values are determined by using integral equation as stated [1],

$$\frac{C_1}{C_2} = -\frac{\cos(\beta l)}{\cos(ql)} \quad ; \quad \frac{C_3}{C_4} = -\frac{\sin(\beta l)}{\sin(ql)} \tag{4.3}$$

To satisfy the boundary condition, the current at the ends of the wire is zero such that $I(\pm l) = 0$, C_i are assumed to be as in Eq. (4.3) for Method A. On the other hand, Method B uses different $\frac{C_1}{C_2}$ and $\frac{C_3}{C_4}$ ratios especially at resonance. At the first impression, change in the $\frac{C_1}{C_2}$ and $\frac{C_3}{C_4}$ ratios implies that $I(\pm l) = 0$ cannot be fulfilled. However, some extra terms added to Eq. (4.2) in order to satisfy the boundary condition. While Van Vleck used these higher order terms to satisfy the boundary condition, he did not use them for calculating radiation; because contributions from ends of the wire is very small to radiation compared the other parts of the wire [1]. On the other hand, when $\sin(\beta l)$ and $cos(\beta l)$ is near zero - at resonance region - these extra terms become again important near the ends of the wire [1]. When Eq. (4.3) is considered at resonance, one of the forced terms become zero for Method A. However, this is not the case experienced since forced terms are not affected by resonance. As a result, Method B uses more refined current expression in fulfilling $I(\pm l) = 0$ compared to Method A which is not able to characterize some details and effects that Method B can characterize [1].

4.2 Details of Method A

When the time dependence ($e^{-i\omega t}$) is omitted from the equation that represents the projection of the incident field on the dipole antenna, the equation becomes $E_0 \sin\theta \cos\phi \; e^{iqz}$ [1]. As stated, the current is selected as described in King and Harrison's article [32].

$$I(z) = -\frac{i\omega E_0}{\beta^2 \sin\theta}\frac{\cos\phi}{\Omega}\left[\frac{\cos(qz)\cos(\beta l) - \cos(\beta z)\cos(ql)}{\cos(\beta l) + (i/\Omega) f(l,q)} + \right. \\ \left. + i\frac{\sin(qz)\sin(\beta l) - \sin(\beta z)\sin(ql)}{\sin(\beta l) + (i/\Omega) g(l,q)}\right] \quad (4.4)$$

$$\Omega = 2[log(2/\gamma\beta\alpha) + Ci(2\beta l)]; \quad \gamma = 1.78; \quad Ci(x) = -\int_z^\infty \frac{\cos t}{t} dt \quad (4.5)$$

The current in Eq. (4.4) can be divided into two parts: even and odd parts. Even part is the first term in the square bracket, and odd part is the remaining term in the square bracket. Only unknown parts in Eq. (4.4) are the functions $f(l,q)$ and $g(l,q)$. The procedure for finding these functions is described below.

$\boldsymbol{E}$, electric and, $\boldsymbol{H}$, the magnetic field on the antenna are generated by the induced current $I(z)$. Moreover, bold parameters represent vector field for this chapter. "Total energy flux radiated from the antenna" is obtained by the law of conservation of energy as in [1]:

$$Re\int_{-l}^{+l} \boldsymbol{E}.\boldsymbol{I}^* dz = \frac{c}{4\pi} Re\int (\boldsymbol{E}\times\boldsymbol{H}^*) R^2 d\omega = \frac{c}{4\pi}\int |\boldsymbol{E}|^2 R^2 d\omega \quad (4.6)$$

While the first integral is calculated over the antenna, the second one is calculated over surface which belong to a sphere with radius R. Moreover, w value is the angular frequency.

For the first integral,

$$\int_{-l}^{l} \boldsymbol{E}.\boldsymbol{I}^{*} dz = \\ -\frac{i\omega E_0^2 \cos^2\phi}{\beta^2 \Omega}\left[\frac{\cos(\beta l\{l+h(2q)\}) - \cos(ql\{h(q+\beta)+h(q-\beta)\})}{\cos(\beta l) - (i/\Omega) f(l,q)} + \right. \\ \left. + \frac{\sin(\beta l\{l-h(2q)\}) - \sin(ql\{h(q-\beta)-h(q+\beta)\})}{\sin(\beta l) - (i/\Omega) g(l,\beta)}\right] \quad (4.7)$$

Similar to Eq. (4.4), for Eq. (4.7) the first term is the even part, the second one is the odd part. Moreover, for this equation we have $h(x) = \sin xl/x$.

At distance R and the angle θ', the current on the antenna generates the electric field:

$$E = \frac{i\beta}{c}\frac{\sin\theta'}{R}\int_{-l}^{+l} I(z) e^{i\beta z\cos\theta'} dz \quad (4.8)$$

And the corresponding flux density is

$$\frac{c}{4\pi}|E|^2 = \frac{c}{4\pi}\frac{\beta^2}{c^2}\frac{\sin^2\theta'}{R^2}\int_{-l}^{+l}\int_{-l}^{+l} I(z) I^{*}(z') e^{i\beta(z-z')\cos\theta'} dz dz' \quad (4.9)$$

Therefore, total flux is:

$$\frac{c}{4\pi}\int_0^{2\pi} d\phi' \int_0^{\pi} \sin\theta' d\theta' |\boldsymbol{E}|^2 R^2 = \\ \frac{1}{\omega}\left\{ \int_{-l}^{+l} \int I^{*}(z') \frac{\sin(\beta(z-z'))}{z-z'}\left[(\beta^2 + \frac{d^2}{dz^2}) I(z)\right] dz dz' - \right. \\ \left. - \int_{-l}^{+l} dz' I^{*}(z') \left(\frac{dI(z)}{dz}\frac{\sin(\beta(z-z'))}{z-z'}\middle| \begin{pmatrix} z=+l \\ z=-l \end{pmatrix}\right)\right\} \quad (4.10)$$

From total flux equation, it can easily be seen that total flux includes an even part which is chosen for $I(z)$ and similarly an odd part which again comes from the current. The integrals due to multiplication of these parts vanishes.

As stated above, Eq. (4.6) is the law of conservation of energy and must be satisfied for the two part described as odd and even. Van Vleck used only the even part in Eq. (4.4) while calculating integrals. When Eq. (4.10) and the even part of the current is used the total flux value is:

$$\frac{1}{\cos^2(\beta l) + \frac{f^2}{\Omega^2}} \frac{1}{\omega}\frac{\omega^2 E_0^2 \cos^2\phi}{\beta^4 \sin^2\theta\ \Omega^2}[\beta\,\gamma(\beta)\cos^2(ql) + K\sigma(q) - L\,\gamma(q) - M\cos^2(\beta l)] \quad (4.11)$$

where

$$K = (\beta^2 - q^2)\{l + h(2q)\}\cos^2(\beta l) + \\ + 2\cos(\beta l)\cos(ql)(q\sin(ql)\cos(\beta l) - \beta\cos(ql)\sin(\beta l)) \quad (4.12)$$

$$L = (\beta^2 - q^2)\cos^2(\beta l)(\cos(2ql)/2q) + \\ + q\cos^2(\beta l)\cos(2ql) + \frac{1}{2}\beta\sin(2ql)\sin(2\beta l) \quad (4.13)$$

$$M = (\beta + q)\sin^2(\beta - q)l + (\beta - q)\sin^2((\beta + q)l), \quad (4.14)$$

$$\sigma(q) = Si(2(\beta + q)l) + Si(2(\beta - q)l) \quad (4.15)$$

$$\gamma(q) = Cin(2(\beta + q)l) - Cin(2(\beta - q)l) \quad (4.16)$$

$$Si(x) = \int_0^x \frac{\sin t}{t} dt \quad (4.17)$$

$$Cin(x) = \int_0^x \frac{1 - \cos t}{t} dt = \log x + 0.577 - Ci(x) \quad (4.18)$$

Now, this equation is equal to even part of the Eq. (4.7). Then $f(l, q)$ is:

$$f(l,q) = \sigma(y)\cos x + A^{-1}\{\gamma(x)\cos^2(xy) - \gamma(y)[\frac{1}{2}y^{-1}(1 + y^2)\cos^2 x\cos(2xy) + \\ + \frac{1}{2}\sin(2x)\sin(2xy)] - \cos^2 x\ [(1 + y)\sin^2(x(1 - y)) + (1 - y)\sin^2(x(1 + y))]\} \quad (4.19)$$

where

$$x = \beta l; \quad y = \cos\theta = q/\beta; \quad \sigma(y) = Si(2x(1 + y)) + Si(2x(1 - y)); \\ \gamma(y) = Cin(2x(1 + y)) - Cin(2x(1 - y)); \quad \gamma(x) = Cin(4x) \quad (4.20)$$

$$A = (1 - y^2)(x + \frac{1}{2}y^{-1}\sin(2xy))\cos x - \\ - \cos(xy)\{(1 + y)\sin(x(1 - y)) + (1 - y)\sin(x(1 + y))\} \quad (4.21)$$

It can be noticed that $g(l, q)$ value can be obtained by using the odd part of

the $I(z)$ and the same procedure. Then $g(l,q)$ becomes:

$$g(l,q) = \sigma(y)\sin x + B^{-1}\{\gamma(x)\sin^2(xy) + \\ + \gamma(y)[\frac{1}{2}y^{-1}(1+y^2)\sin^2 x\cos(2xy) - \frac{1}{2}\sin(2x)\sin(2xy)] - \\ - \sin^2 x\ [(1+y)\sin^2(x(1-y)) + (1-y)\sin^2(x(1+y))]\} \quad (4.22)$$

where

$$B = (1-y^2)(x - \frac{1}{2}y^{-1}\sin(2xy))\sin x - \\ - \sin(\{(1+y)\sin(x(1-y)) - (1-y)\sin(x(1+y))\} \quad (4.23)$$

With the help of found $f(l,q)$ (Eq. (4.19)) and $g(l,q)$ (Eq. (4.22)) values, backscattered electric field in the direction of θ can be found by using Eq. (4.8). When the integral is calculated, the backscattered field is:

$$E = \frac{E_0\cos\phi}{\beta\ \Omega(1-y^2)}\left[\frac{A}{\cos x + if(l,q)/\Omega} - \frac{B}{\sin x + ig(l,q)/\Omega}\right] \quad (4.24)$$

When the backscattered field is found, it is easy to calculate backscattering cross section by using below equation(see also Eq. (3.17)):

$$\sigma = 4\pi R^2\frac{|E|^2}{|E_0|^2} \quad (4.25)$$

When the receiver and the transmitter have the same polarization, Eq. (4.25) need to be multiplied by $\cos^2\phi$ and when their polarizations are crossed the multiplication term becomes $\sin^2\phi$ [1]. For the case that is considered, it is assumed that they have parallel (same) polarization.

The term $|E|^2$ is:

$$|E|^2 = \frac{E_0^2\cos^2\phi}{\beta^2\ \Omega^2\ (1-y^2)^2}\left[\frac{A^2}{\cos^2 x + f(l,q)^2/\Omega^2} + \frac{B^2}{\sin^2 x + g(l,q)^2/\Omega^2} - \right. \\ \left. - \frac{2AB(\sin x\cos x + f(l,q)g(l,q)/\Omega^2)}{(\sin x\cos x + f(l,q)g(l,q)/\Omega^2)^2 + \Omega^{-2}(g(l,q)\cos x - f(l,q)\sin x)^2}\right] \quad (4.26)$$

When Eq. (4.26) is used in Eq. (4.25) with the polarization assumption, backscattered field becomes:

$$\sigma(\theta) = \lambda^2 \cos^4\phi \frac{1}{\pi\Omega^2} \frac{1}{(1-y^2)^2} \left[\frac{A^2}{\cos^2 x + f(l,q)^2/\Omega^2} + \frac{B^2}{\sin^2 x + g(l,q)^2/\Omega^2} - \right.$$
$$\left. - \frac{2AB(\sin x \cos x + f(l,q)g(l,q)/\Omega^2)}{(\sin x \cos x + f(l,q)g(l,q)/\Omega^2)^2 + \Omega^{-2}(g(l,q)\cos x - f(l,q)\sin x)^2} \right] \quad (4.27)$$

The average of $\cos^4\phi$ for all the polarization is 3/8. Moreover, backscattering cross section is divided by the square of the wavelength, it can be obtained the needed equation for the dipole RCS calculation:

$$\frac{\sigma(\theta)}{\lambda^2} = \frac{3}{8\pi\Omega^2} \frac{1}{(1-y^2)^2} \left[\frac{A^2}{\cos^2 x + f(l,q)^2/\Omega^2} + \frac{B^2}{\sin^2 x + g(l,q)^2/\Omega^2} - \right.$$
$$\left. - \frac{2AB(\sin x \cos x + f(l,q)g(l,q)/\Omega^2)}{(\sin x \cos x + f(l,q)g(l,q)/\Omega^2)^2 + \Omega^{-2}(g(l,q)\cos x - f(l,q)\sin x)^2} \right] \quad (4.28)$$

Now, this equation can be used in Eq. (4.29) in order to calculate the average monostatic radar cross section (RCS) - $\bar{\sigma}$ - of chaff whose wires/dipoles are randomly oriented:

$$\bar{\sigma} = \int_0^{\pi/2} \sigma(\theta) \sin\theta \; d\theta \quad (4.29)$$

4.3 Details of Method B

When the time dependence of equation Eq. (4.1) is ignored, the solution of the equation that is interested is represented in Method B as:

$$I(z) = \alpha e^{iqz} + \gamma_1 \cos(\beta z) + i\gamma_2 \sin(\beta z) \quad (4.30)$$

α in Eq. (4.30) is selected in a way that the term related to e^{iqz} in equation Eq. (4.1) is eliminated. Moreover, A_1 and A_2 values in Eq. (4.1) are found by using the boundary condition $I(\pm l) = 0$.

As described in the work of Gray, [23],

$$\int_{-l}^{+l} r^{-1} I(\xi) e^{-i\beta r} d\xi = I(z) \int_{-l}^{+l} r^{-1} \cos(\beta r)\ d\xi + \\ + \int_{-l}^{+l} r^{-1} [I(\xi) - I(z)] \cos(\beta r)\ d\xi - i \int_{-l}^{+l} r^{-1} I(\xi) \sin(\beta r)\ d\xi \quad (4.31)$$

The right side integrals can be grouped into two in terms of Van Vleck's and Gray's approaches to the convergence of these integrals [1, 23]. The second and third terms are evaluated in a way that thickness of the wire is negligible so that the radius (r) of the wire is zero. However, for the first integral this assumption cannot be used since it diverges in this case. Therefore, it is evaluated as the wire has a finite thickness like its radius r. With the help of Gray's [23] procedure and approximations that have been described above, it can be obtained Eq. (4.32) and Eq. (4.34):

$$\int_{-l}^{+l} \frac{\cos(\beta r)}{r} d\xi = Z(z) \quad (4.32)$$

with

$$Z(z) = \log \frac{[(l+z)^2 + a^2]^{\frac{1}{2}} + (l+z)}{[(l-z)^2 + a^2]^{\frac{1}{2}} - (l-z)} - Cin(\beta(l+z)) - Cin(\beta(l-z)) \quad (4.33)$$

$$\int r^{-1} e^{iq\xi} e^{-i\beta r} d\xi = \frac{1}{2} e^{iqz} [2Z(z) + 2Cin(\beta(l-z)) + 2Cin(\beta(l+z)) - \\ - Cin((\beta+q)(l-z)) - Cin((\beta-q)(l+z)) - Cin((\beta-q)(l-z)) - \\ - Cin((\beta+q)(l+z)) - iSi((\beta+q)(l-z)) - iSi((\beta-q)(l+z)) - \\ - iSi((\beta-q)(l-z)) - iSi((\beta+q)(l+z))] + \\ + \frac{1}{2} e^{iqz} [Cin((\beta+q)(l-z)) + Cin((\beta-q)(l+z)) - Cin((\beta+q)(l+z)) - \\ - Cin((\beta-q)(l-z)) + i\{Si((\beta+q)(l-z)) + Si((\beta-q)(l+z)) - \\ - Si((\beta+q)(l+z)) - Si((\beta-q)(l-z))\}] \quad (4.34)$$

In Eq. (4.34), with the change in the value of z, the coefficients of e^{iqz} are slowly varying so that their mean values can be used instead. Note that, especially at the boundaries of the wire, difference between mean and actual value can be

considerably large. However, Van Vleck states that their effect to result is a negligible one [1]. Using mean value, the author ensures that the term in the second square brackets become zero because it is an odd function of z. Moreover,

$$\langle Z(z)\rangle_{Av} = \frac{1}{2}l\int Z(z)dz = 2[\log(2l/a) + \log 2 - Cin(2\beta l) - \\ - (\sin(2\beta l)/2\beta l)] \sim 2[\log(\lambda/\pi a) - 0.577] \quad (4.35)$$

$$\langle Cin(k(l+z))\rangle_{Av} = Cin(2kl) + (\sin(2kl)/2kl) - 1 \sim \log 2kl + 0.577 - 1 \quad (4.36)$$

$$\langle Sin(l+z)\rangle_{Av} = Si(2kl) + (1/2qkl)[\cos(2kl) - 1] \sim \frac{1}{2}\pi \quad (4.37)$$

Van Vleck stated that using asymptotic expansion for Si and Cin functions is legitimate for the wires that are generally at least half wave-length. However, he also emphasized that when the wire length is smaller than half wave-length the asymptotic approximations give much more error than acceptable for cross section. Recall that, there was also problems when the dipole length is greater than 2 times the wavelength. As a result, he preferred to use asymptotic expansion of these function due to two reasons;

- He generally deals with the wires whose length is greater than half wave-length,
- The calculations are much easier with the asymptotic approach.

With the help of asymptotic values of Si and Cin function, Eq. (4.34) becomes Ke^{iqz} where K is given by

$$K = 2\{\log(\lambda/\pi a) - 0.577\} + 2\log(1/\sin\theta) - i\pi \quad (4.38)$$

and α in Eq. (4.30) becomes

$$\alpha = i\omega\cos\phi\ E_0/(K\beta^2\sin\theta) \quad (4.39)$$

When the same approximation is used for Eq. (4.30) to get relation between constants A_1, A_2 and coefficients γ_1, γ_2 it can be stated that

$$\int r^{-1}\cos\beta\ \xi\ e^{-i\beta r}d\xi = L\cos(\beta z); \qquad \int r^{-1}\sin\beta\ \xi\ e^{-i\beta r}d\xi = L\sin(\beta z) \quad (4.40)$$

where

$$L = 2[\log(\lambda/\pi a) - 0.577] + \log(2\beta l) + 0.577 - \log 2 - \frac{i\pi}{2} - 1 \tag{4.41}$$

Thus

$$\gamma_1 = A_1/L; \quad i\gamma_2 = A_2/L \tag{4.42}$$

The simple approach for finding constants A_1 and A_2 is to apply boundary condition to Eq. (4.30). When this equation goes to zero for both $z = +l$ and $z = -l$; γ_1 becomes $-\alpha\frac{\cos ql}{\cos \beta l}$ and γ_2 becomes $-\alpha\frac{\sin ql}{\sin \beta l}$, however at resonance these values give infinite value that is not desired. Instead of this simple approach, second approximation is used to get finite current at resonance. This second approximation is obtained by using the second and third term in Eq. (4.31). Note that, first term is again not used since this term diverges as the radius of the wire gets closer to zero. For a finite value at resonance with a negligible wire radius, remaining terms in Eq. (4.31) should be used. As a result, the boundary condition becomes:

$$\int r^{-1}[I(\xi) - I(\pm l)]\cos(\beta r)\ d\xi - i\int r^{-1} I(\xi)\sin(\beta r)\ d\xi = (i\omega\cos\phi/(\beta^2\sin\theta))\ E_0\ e^{\pm iql} + A_1\cos(\pm\beta l) + A_2\sin(\pm\beta l) \tag{4.43}$$

It can easily be seen that Eq. (4.43) is generated by using Eq. (4.31) in Eq. (4.1) with $z = \pm l$ and assuming that for first integral in right part of Eq. (4.31): $I(\pm l) = 0$.

Note that, in Eq. (4.42) two relations were defined between γ_1 and A_1, γ_2 and A_2. Getting expression for γ_1 and γ_2 is much more straightforward since they are directly used in Eq. (4.30). When Eq. (4.34), Eq. (4.39) and Eq. (4.42) is used with asymptotic expansion of Si and Cin function for large l values, γ_1 and γ_2

can be obtained from below two expressions which are derived from Eq. (4.30);

$$(i\omega\cos\phi E_0/(K\beta^2\sin\theta))\{[\log(1/\sin\theta)-\frac{1}{2}i\pi]\cos(ql)- \\ -\frac{1}{2}i\log[(1+\cos\theta)/(1-\cos\theta)]\sin(ql)\}+ \\ +\gamma_1\{cos(\beta l)(\frac{1}{2}\log(2\beta l)+0.288-\frac{1}{2}\log 2-\frac{1}{4}i\pi)- \\ -\frac{1}{2}i(\log(4\beta l)+0.577)\sin(\beta l)+\frac{1}{4}\pi\sin(\beta l)\}= \\ (i\omega\cos\phi E_0/(\beta^2\sin\theta))\cos(ql)+\gamma_1\ Lcos(\beta l) \quad (4.44)$$

$$(i\omega\cos\phi E_0/(K\beta^2\sin\theta))\{[\log(1/\sin\theta)-i\pi/2]\sin(ql)+ \\ +\frac{1}{2}i\log[(1+\cos\theta)/(1-\cos\theta)]\cos(ql)\}+ \\ +\gamma_2\{\sin(\beta l)(\frac{1}{2}log(2\beta l)+0.288-\frac{1}{2}\log 2-\frac{1}{4}i\pi)+ \\ +\frac{1}{2}i(\log(4\beta l)+0.577)\cos(\beta l)-\frac{1}{4}\pi\cos(\beta l)\} \\ =(i\omega\cos\phi E_0/(\beta^2\sin\theta))\sin(ql)+\gamma_2\ L\sin(\beta l) \quad (4.45)$$

Van Vleck preferred to omit $\log(\frac{1}{\sin\theta})$ and $\frac{\log(1+\cos\theta)}{(1-\cos\theta)}$ terms in Eq. (4.39), Eq. (4.44), Eq. (4.45) because of three reasons [1]:

- He asserts that for $\theta > 30$ most of the scattering comes and the contribution of these terms for this condition are close to zero,
- When these omitted terms are used in equations, angular dependences of the expression may become extremely complicated,
- Lastly, an analytical expression of the radar cross section is hard to obtain without eliminating these terms.

With the last assumption described, the current on PEC wire can be written with the use of Eq. (4.30), Eq. (4.39), Eq. (4.44), Eq. (4.45) as:

$$I(z)=(\frac{i\omega\cos\phi E_0}{\beta^2\sin\theta})[(F'+iF'')e^{iqz}+ \\ +2(G'+G'')\cos(\beta z)\cos(ql)+2i(H'+H'')\sin(\beta z)\sin(ql)] \quad (4.46)$$

$$
\begin{aligned}
F' &= \Omega'/(\Omega'^2 + \pi^2) \\
F'' &= \pi/(\Omega'^2 + \pi^2) \\
\Omega' &= 2\log(\lambda/\pi\alpha) - 1.154 \\
2G' &= \psi(\beta l)[\psi(\beta l)^2 + \Xi(\beta l)^2]^{-1} - \pi\Omega'^{-1}G'' \\
2G'' &= \Xi(\beta l)[\psi(\beta l)^2 + \Xi(\beta l)^2]^{-1} \\
2H' &= \psi(\beta l - \frac{1}{2}\pi)[\psi(\beta l - \frac{1}{2}\pi)^2 + \Xi(\beta l - \frac{1}{2}\pi)^2]^{-1} - \pi\Omega'^{-1}H'' \\
2H'' &= \Xi(\beta l - \frac{1}{2}\pi)[\psi(\beta l - \frac{1}{2}\pi)^2 + \Xi(\beta l - \frac{1}{2}\pi)^2]^{-1} \\
\psi(x) &= -(\Omega' - \Delta)\cos x + \frac{1}{4}\pi \sin x \\
\Xi(x) &= \frac{1}{2}(\log(4\beta l) + 0.577)\sin x - \frac{1}{4}\pi\cos x \\
\Delta &= -\frac{1}{2}\log(\beta l) + 0.712
\end{aligned}
\tag{4.47}
$$

Now, the similar procedure in Method A is used to get the radar cross section of a dipole from current expression in Eq. (4.46). Then we got:

$$
\begin{aligned}
\sigma = \frac{\cos^2\phi\ (4\pi R^2)\ |E|^2}{|E_0|^2} &= 4\pi\cos^4\phi \Big| \int_{-l}^{+l} dz\ e^{iqz}[(F' + iF'')e^{iqz} + \\
&+ 2(G' + iG'')\cos(\beta z)\cos(ql) + 2i(H' + iH'')\sin(\beta z)\sin(ql)]\Big|^2 = \\
&= (4\lambda^2/\pi)\cos^4\phi\{a_1^2(F'^2 + iF''^2) + (a_2 + a_3)^2\cos^2(xy(G'^2 + G''^2)) + \\
&+ (a_2 - a_3)^2\sin^2(xy(H'^2 + H''^2)) + 2(a_2^2 - a_3^2)\sin xy\cos(xy(G'H' + G''H'')) + \\
&+ 2a_1(a_2 + a_3)\cos(xy(F'G' + F''G'')) + 2a_1(a_2 - a_3)\sin(xy(F'H' + F''H''))\}
\end{aligned}
\tag{4.48}
$$

where

$$
\begin{aligned}
x = 2\pi l/\lambda; \quad y = \cos\theta; \quad a_1 = \frac{1}{2}y^{-1}\sin 2xy \\
a_2 = (1+y)^{-1}\sin[x(1+y)]; \quad a_3 = (1-y)^{-1}\sin[x(1-y)]
\end{aligned}
\tag{4.49}
$$

Cross section expression of dipole $\sigma(\theta)$ that is a function of θ can be derived from Eq. (4.48) by averaging the terms related to ϕ.

- For same polarization, the mean of $\cos^4\phi$ needs to be taken as $3/8$,

- For cross polarization, the mean of $\sin^2\phi\cos^2\phi$ needs to be taken as $1/8$

Similar to Method A, for a chaff cloud whose dipoles are randomly oriented average monostatic RCS can be calculated by using cross section expression $\sigma(\theta)$ in Eq. (4.29).

Although, Van Vleck proposed two different methods [1] as explained in this chapter, there are still discussions on their performance as stated at the beginning. However, his methods still hold great validity in spite of these criticisms and it will be showed by simulations, in this thesis.

Chapter 5

VARIATONAL METHOD

Variational method is derived from the work of Schwinger [34] by Tai [2]. As stated by Tai, two main difference exists between variational method and the Van Vleck's methods [2]. The first one is that this method eliminates the dependence on the diameter of the wire. And the second one is related the stationary properties of the variational method. With this property, the function that represent the current distribution can be selected in such way that more accurate backscattering cross section can be calculated.

Before proposing current equation for perfectly conducting thin wire, Tai preferred to derive equation of radar cross section for variational method. He assumed a dipole geometry that can be seen in Fig. 5.1

A simple but known fact in antenna theory is that the current on a wire is the result of an incident plane wave [1, 22]. An approximate form is Eq. (5.1):

$$\frac{d^2 A_z}{dz^2} + k^2 A_z = -j\frac{k^2}{\omega} E_0 \sin\theta \cos\psi e^{jkz\cos\theta} \tag{5.1}$$

with

$$A_z = \frac{\mu}{4\pi}\int_{-l}^{l} I(z')\frac{e^{-jkR}}{R}dz' \tag{5.2}$$

where the notation can be seen Table 5.1

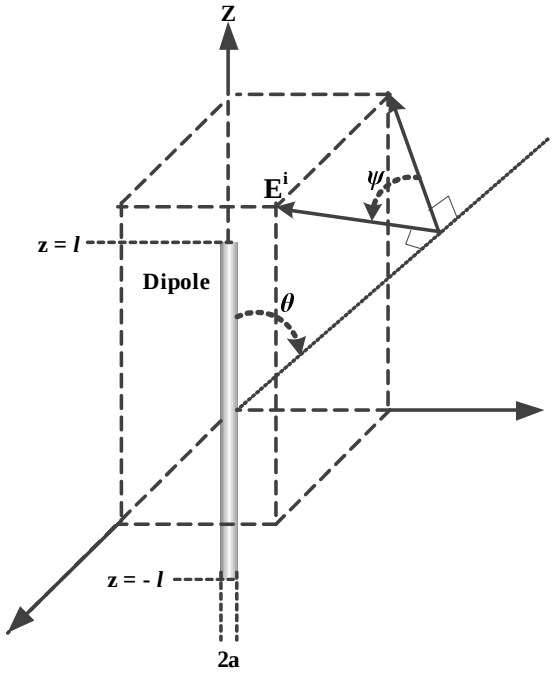

Figure 5.1: Tai's Dipole Geometry

Table 5.1: Notation used for Tai's work

E_0	:	Magnitude of the incident electric field
k	:	$2\pi/\lambda$
λ	:	Wavelenght
$I(z')$	:	At z', the current value
R	:	$\sqrt{[(z-z')^2+a^2]}$
a	:	Radius of the wire
$2l$	:	Length of the wire
θ	:	Angle between the wire and the wave normal
ψ	:	Polarization angle of the wave

When Eq. (5.2) is used in Eq. (5.1), Eq. (5.3) is generated.

$$E_0 \sin\theta \cos\psi e^{jkz\cos\theta} = \frac{j\eta k}{4\pi}\int_{-l}^{l} I(z')\left(1+\frac{\partial^2}{k^2\partial z^2}\right)\frac{e^{-jkR}}{R}dz^2 \qquad (5.3)$$

where $\eta = \sqrt{\frac{\mu}{\epsilon}} = 120\pi$ ohms

This equation and original Hallén's integral equations [22] are same with each other, however, Hallén forms the equation by solving Eq. (5.1) for A_z value and

then substitute the result into right hand side of the Eq. (5.2) [2]. Hallén's result is:

$$\frac{E_0 \cos\psi e^{jkz\cos\theta}}{\sin\theta} + C_1 \sin(kz) + C_2 \cos(kz) = \frac{j\eta k}{4\pi} \int_{-l}^{l} I(z') \frac{e^{-jkR}}{R} dz' \tag{5.4}$$

In variational method, to get the backscattering radar cross section, Eq. (5.3) is multiplied with the current expression $I(z)$ and the result is integrated from $z = -l$ to $z = +l$.

$$4\pi E_0 \cos\psi \sin\theta \int_{-l}^{l} I(z) e^{jkz\cos\theta} dz = j\eta \int_{-l}^{l} \int_{-l}^{l} I(z) I(z') K(z - z') dz dz' \tag{5.5}$$

where

$$K(z - z') = k\left(1 + \frac{\partial^2}{k^2 \partial z^2}\right) \frac{e^{-jkR}}{R} \tag{5.6}$$

From Eq. (5.5), an expression is generated, let's say S, in a way that with variation in current value, it stays stationary. When S value is selected as in Eq. (5.7):

$$S = \frac{\eta k^2 \sin\theta \int_{-l}^{l} I(z) e^{jkz\cos\theta} dz}{4\pi E_0 \cos\psi} \tag{5.7}$$

Then the remaining terms in Eq. (5.5) is Eq. (5.8) and it can be seen that this equation is stationary with the small variation in current:

$$\frac{1}{S} = \frac{j \int_{-l}^{l} \int_{-l}^{l} I(z) I(z') K(z - z') dz dz'}{\left[k \sin\theta \int_{-l}^{l} I(z) e^{jkz\cos\theta} dz\right]^2} \tag{5.8}$$

From definition, backscattering cross section is Eq. (5.9):

$$\sigma(\theta, \psi) = \frac{4\pi R_0^2 |E_\theta \cos\psi|^2}{E_0^2} \tag{5.9}$$

where

$$E_\theta = \frac{j\eta k \sin\theta e^{-jkR_0}}{4\pi R_0} \int_{-l}^{l} I(z) e^{jkz\cos\theta} dz \tag{5.10}$$

which is the electric field at distance R_0 due to the induced current on the wire. Then backscattering cross section turns out to be Eq. (5.11):

$$\sigma(\theta, \psi) = (cos\psi)^2 \frac{|(j\eta k \sin\theta e^{-jkR_0} \int_{-l}^{l} I(z) e^{jkz\cos\theta} dz)|^2}{4\pi E_0^2} \tag{5.11}$$

When Eq. (5.11) is written in terms of S, Eq. (5.12) is derived:

$$\sigma(\theta,\psi) = \frac{4\pi\cos^4\psi}{k^2}|S|^2 \tag{5.12}$$

Similar to work done in Van Vleck [1], to get the backscattering cross section in term of the angle θ only, Eq. (5.12) is averaged over all values of polarization angle ψ. Then, the backscattering formula Eq. (5.13) for variational method.

$$\sigma(\theta) = \frac{1}{\pi}\int_0^\pi \sigma(\theta,\psi)d\psi = \frac{3\pi}{2k^2}|S|^2 = 3\lambda^2|S|^2/8\pi \tag{5.13}$$

Now it is time to calculate the algebraic version of backscattering radar cross section by using variational method. In order to derive this algebraic expression, one needs to propose $I(z)$ and use it to calculate S value.

For variational method, different order of solution can be proposed. As the order increases, not only the accuracy of numerical result increases but also the complexity of the equations increases.

As Tai proposed, for simplicity, zero and first order solution can be used to calculate backscattering cross section. When second or higher order solution is preferred, algebraic expression cannot be easily derived.

Tai introduces a first order solution by selecting current distribution Eq. (5.14) as [2]:

$$I(z) = I_0(f_0(z) + Af_1(z)) \tag{5.14}$$

I_0 and A are arbitrary functions. $f_0(z)$ and $f_1(z)$ are independent trial functions. Value of A is determined by using the stationary characteristics of S^{-1} in terms of $I(z)$. Then it can easily be asserted that $\frac{\partial}{\partial A}(S^{-1}) = 0$ and A value can be found. For zero order solution A value can be selected as 0. Then current distribution become $I(z) = I_0 f_0(z)$. Note that, in terms of $I(z)$, S is homogenous, therefore Eq. (5.13) is independent of I_0.

Now a critical discussion can be made on the boundary condition $I(\pm l) = 0$. Hallén [22] and many authors uses this condition for calculating constants needed for generating current equation on wire. It simply states that current at the end

of the wire is zero. It is acceptable; but may not be used for variational method based on the work of Tai [35]. In this work, it is stated that for transmission antenna $I(\pm l) = 0$ is not satisfied since small value of current exists at the end of the antenna. Because Tai assumes dipoles are cylindrical wire antennas, he states that small current values may exist at the end of wires. Therefore, he asserts that one may prefer not to use $I(\pm l) = 0$ condition and get one more degree of freedom for his/her solution [2].

As described in [1, 22, 32, 36] the most proper function that describes the current distribution on a PEC wire is:

$$I(z) = I_0'[e^{jkz\cos\theta} + \alpha cos(kz) + \beta \sin(kz)] \cdots \tag{5.15}$$

In this equation I_0', α and β are arbitrary constants. If boundary condition that is discussed before is not involved to solution, one can find value of β and α as follows: put Eq. (5.15) in Eq. (5.7) then solve $\frac{\partial}{\partial\alpha}(S^{-1}) = 0$ and $\frac{\partial}{\partial\beta}(S^{-1}) = 0$. When these equations are solved, a second order solution come into existence for solving S by combining Eq. (5.15) and Eq. (5.5). The complexity of this second order solution make deriving algebraic equations harder. Instead of it, for oblique incidence case, Tai prefers to use $I(\pm l) = 0$ boundary condition and get a first order solution which can easily turn expression of S into an algebraic equation. Therefore, $I(\pm l) = 0$ condition is applied on proposed current distribution Eq. (5.15) and get an algebraic version Eq. (5.16) of it with unknown arbitrary constants I_0 and A.

$$\begin{aligned} I(z) = I_0\{&[\cos(kz)\cos(kl\cos\theta) - \cos(kl)\cos(kl\cos\theta)] + \\ &+ A[\sin(kz)\sin(kl\cos\theta) - \sin(kl)\sin(kl\cos\theta)]\} \end{aligned} \tag{5.16}$$

When this current equation is used in Eq. (5.7), the resulting new solution of S become first order as wanted:

$$1/S = (\gamma_c + A^2\gamma_g)/(g_c + A\ g_g)^2 \tag{5.17}$$

The values of g_c, g_g, γ_c and γ_g are the functions that are found by using below procedure:

Eq. (5.16) can be written in the form of a first order solution as described before:

$$I(z) = I_0(f_c(z) + Af_g(z)) \tag{5.18}$$

with

$$\begin{aligned} f_c(z) &= \cos(qkl)\cos(kz) - \cos(qkz)\cos(kl) \\ f_g(z) &= \sin(qkl)\sin(kz) - \sin(qkz)\sin(kl) \\ q &= \cos\theta \end{aligned} \tag{5.19}$$

For the solution of Eq. (5.7) let's define g_c, g_g, γ_c and γ_g as Eq. (5.20), Eq. (5.21), Eq. (5.22), Eq. (5.23), respectively:

$$\begin{aligned} g_c &= k\sin\theta \int_{-l}^{l} f_c(z) e^{jkz\cos\theta} dz \\ &= \frac{4q\ cos^2(qx)\sin x - (1+q^2)\sin(2qx)\cos x - 2q(1-q^2)x\cos x}{2q(1-q^2)^{\frac{1}{2}}} \end{aligned} \tag{5.20}$$

with the abbreviation $x = kl$

$$\begin{aligned} g_g &= k\sin\theta \int_{-l}^{l} f_g(z) e^{jkz\cos\theta} dz \\ &= -j\frac{4qsin^2(qx)\cos x - (1+q^2)\sin(2qx)\sin x + 2q(1-q^2)x\cos x}{2q(1-q^2)^{\frac{1}{2}}} \end{aligned} \tag{5.21}$$

$$\gamma_c = j\int_{-l}^{l}\int_{-l}^{l} f_c(z) f_c(z') K(z-z') dz dz' \tag{5.22}$$

$$\gamma_g = j\int_{-l}^{l}\int_{-l}^{l} f_g(z) f_g(z') K(z-z') dz dz' \tag{5.23}$$

To get an algebraic equation for S, similar to g_c and g_g, algebraic expression for γ_c and γ_g must be derived. Therefore, γ_c and γ_g equations are approximated for the condition that $a \ll l$ which is almost always the case for the dipoles used in

a chaff cloud. Then these equations becomes as in Eq. (5.24) and Eq. (5.25):

$$\begin{aligned}\gamma_c = \cos^2 x[&-1+\cos(2x)\cos(2qx)+q\sin(2x)\sin(2qx)-\\ &-j(\sin(2x)\cos(-q\cos(2x)\sin(2qx))]-\\ &-0.5\left(\frac{1+q^2}{q}\cos^2 x\cos(2qx)+\sin(2x)\sin(2qx)\right)\times\\ &\times[L((1+q)2x)-L((1-q)2x)]+\\ &+j\left\{\cos^2 x\left[\frac{1+q^2}{2q}\sin(2qx)+(1-q^2)x\right]-\sin(2x)\cos^2(qx)\right\}\times\\ &\times[ln4+\Omega-L((1+q)2x)-L((1-q)2x)]\end{aligned} \tag{5.24}$$

$$\begin{aligned}\gamma_g = \sin^2 x[&-1+\cos(2x)\cos(2qx)+q\sin(2x)\sin(2qx)-\\ &-j(\sin(2x)\cos(-q\cos(2x)\sin(2qx))]+\\ &+0.5\left(\frac{1+q^2}{q}\sin^2 x\cos(2qx)-\sin(2x)\sin(2qx)\right)\times\\ &\times[L((1+q)2x)-L((1-q)2x)]+\\ &+j\left\{-\sin^2 x\left[\frac{1+q^2}{2q}\sin(2qx)-(1-q^2)x\right]+\sin(2x)\sin^2(qx)\right\}\times\\ &\times[ln4+\Omega-L((1+q)2x)-L((1-q)2x)]\end{aligned} \tag{5.25}$$

with

$$\begin{aligned}x = kl;\quad \Omega = 2ln\frac{2l}{a}\\ L((1\pm q)2x) = \int_0^{(1\pm q)2x}\frac{1-e^{-ju}}{u}du = \bar{C}i((1\pm q)2x)+jSi((1\pm q)2x).\end{aligned} \tag{5.26}$$

As discussed before, A value can be found by solving $\frac{\partial}{\partial A}(S^{-1})=0$.

$$A = g_g\gamma_c/g_c\gamma_g \tag{5.27}$$

As a result,

$$S = (g_c^2/\gamma_c)+(g_g^2/\gamma_g) \tag{5.28}$$

and using this equation in Eq. (5.13), backscattering cross section is found for variational method as Eq. (5.29):

$$\frac{\sigma(\theta)}{\lambda^2} = \frac{3}{8\pi}\left|\frac{g_c^2}{\gamma_c}+\frac{g_g^2}{\gamma_g}\right|^2 \tag{5.29}$$

where algebraic solutions Eq. (5.20), Eq. (5.21), Eq. (5.24) and Eq. (5.25) can be used for g_c, g_g, γ_c and γ_g in Eq. (5.29), respectively.

Chapter 6

DIRECT METHOD

6.1 General Introduction to Einarsson's Method

As discussed before, integral equation method is derived by Van Vleck and variational method is used by Tai to calculate backscattering cross section of a thin wire [1, 2]. Einarsson introduced a new method called direct method [37] which is inspired from the work of Hallén [38]. In these works, by using infinite sum of travelling waves, exact solution to the scattering from a finite thin-walled tube is derived. Later in 1969, Einarsson applied this work for a perfectly conducting wire and found a closed form for backscattering problem by finding asymptotic equivalent of this infinite sum [3].

Same as Van Vleck's [1] and Tai's [2] work, Einarsson [3] assumed that plane wave that is incident to wire as in Fig. 6.1, is polarized linearly. This assumption does not affect the results since only the parallel part of the field is included in the backscattering calculations.

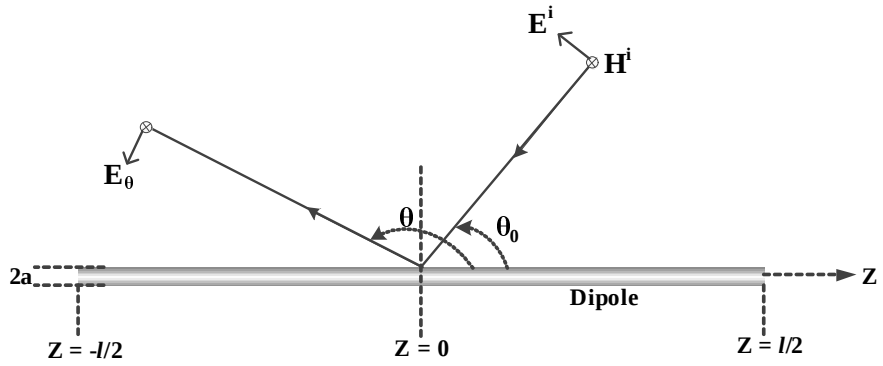

Figure 6.1: Einarsson's Dipole Geometry

In [3], Einarsson used some abbreviations as follows;

$$\begin{aligned} L &= \frac{1}{2}kl = \pi l/\lambda; \\ \gamma &= 0.5772156649\ldots \\ \zeta(3) &= \sum_{n=1}^{\infty} \frac{1}{n^3} = 1.202056903.... \end{aligned} \tag{6.1}$$

where k is the wavenumber and λ is the wavelength.

The incident electric field E_θ^i and the scattering electric field E_θ^s that are drawn in Fig. 6.1 are assumed as Eq. (6.2) and Eq. (6.3), respectively.

$$E_\theta^i = exp\{-ikr(\sin\theta\sin\theta_0 + \cos\theta\cos\theta_0)\} \tag{6.2}$$

$$E_\theta^s(r,\theta,\theta_0) = \frac{e^{ikr}}{kr} S(\theta,\theta_0) \tag{6.3}$$

As Van Vleck [1] and Tai [2] used, similar expression for average backscattering calculation is used by Einarsson except for the fact that he included the polarization effect directly as he assumed that the plane wave is linearly polarized [3]. The used equation is:

$$\bar{\sigma} = \frac{3}{8}\int_0^{\frac{\pi}{2}} \sigma(\theta)\sin\theta d\theta \tag{6.4}$$

As discussed, Tai [2] defined a function and represent backscattering cross section in terms of this function. The function S can be seen in Eq. (5.2). The

corresponding function for direct method is:

$$\frac{1}{S(\theta,\theta_0)} = \\ = \frac{-\int_{-\frac{1}{2}l}^{\frac{1}{2}l}\int_{-\frac{1}{2}l}^{\frac{1}{2}l} I(z,\theta)I(z',\theta_0)K(z-z')dzdz'}{k^2\sin\theta\sin\theta_0\int_{-\frac{1}{2}l}^{\frac{1}{2}l} I(z,\theta_0)exp(-ikz\cos\theta)dz\int_{-\frac{1}{2}l}^{\frac{1}{2}l} I(z,\theta)exp(-ikz\cos\theta_0)dz} \tag{6.5}$$

where $K(z-z')$ is defined as

$$K(z-z') = (k^2 + \frac{\partial^2}{\partial z^2})\frac{e^{ikR}}{kR} \tag{6.6}$$

Note that this function is same with Eq. (5.6) except the negative sign at the exponential term.

In direct method, bistatic cross section is:

$$\frac{\sigma(\theta,\theta_0)}{\lambda^2} = \frac{1}{\pi}|S(\theta,\theta_0)|^2 \tag{6.7}$$

If one wants to calculate monostatic case, he/she can select θ equals to θ_0. For comparing the direct method with others, monostatic case ($\theta = \theta_0$) is considered.

By using the same equation for the current distribution described as Eq. (5.16), for $\theta \neq \pi - \theta_0$, the S function becomes for direct method as:

$$S(\theta,\theta_0) = \frac{2i[F(\theta,\theta_0) + F(\pi-\theta,\pi-\theta_0)]}{[\Omega_0 - 2\log(\frac{1}{2}\sin\theta)][\Omega_0 - 2log(\frac{1}{2}\sin\theta_0)\sin\theta\sin\theta_0]} \tag{6.8}$$

Second order expression for F function is defined as:

$$F(\theta,\theta_0)=\frac{2cos^2\frac{1}{2}\theta\cos^2\frac{1}{2}\theta_0 e^{iL(\cos\theta+\cos\theta_0)}}{(\cos\theta+\cos\theta_0)\Phi(\cos\theta)\Phi(cos\theta_0)}+$$
$$+\frac{2[f(\theta)\sin^2\frac{1}{2}\theta\sin^2\frac{1}{2}\theta_0-f(\pi-\theta_0)\cos^2\frac{1}{2}\theta\cos^2\frac{1}{2}\theta_0]e^{iL(\cos\theta-\cos\theta_0+2)}}{(\cos\theta+\cos\theta_0)\Phi^2(1)\Phi(\cos\theta)\Phi(-cos\theta_0)}+$$
$$+\frac{f(\theta)f(\theta_0)e^{iL(\cos\theta+\cos\theta_0+4)}}{\Phi^4(1)\Phi(\cos\theta)\Phi(cos\theta_0)}\Bigg\{1+\frac{(1+\cos\theta)(1+\cos\theta_0)}{2(\cos\theta+\cos\theta_0)\Omega_0^2}\times$$
$$\times[l_2(4L,4L\cos^2\frac{1}{2}\theta)+l_2(4L,4L\cos^2\frac{1}{2}\theta_0)-T(4L\cos^2\frac{1}{2}\theta)T(4L\cos^2\frac{1}{2}\theta_0)]\Bigg\}+$$
$$+\frac{f(0)h(\theta)e^{iL(\cos\theta+6)}}{\Phi^2(1)[\Phi^4(1)-h^2(0)e^{4iL}]}\left[\frac{f(0)h(\theta_0)e^{iL(\cos\theta_0+2)}}{\Phi^2(1)\Phi(\cos\theta)\Phi(cos\theta_0)}-\frac{h(\pi-\theta_0)e^{-iL\cos\theta_0}}{\Phi(\cos\theta)\Phi(-cos\theta_0)}\right] \tag{6.9}$$

The parameters Ω_0, f, h, T, l_2 and Φ are defined in Eq. (6.12), Eq. (6.14), Eq. (6.15), Eq. (6.19), Eq. (6.23) and Eq. (6.47), respectively.

For $\theta=\pi-\theta_0$, S function is:

$$S(\theta,\pi-\theta)=\frac{2i}{\{\Omega_0-2log(\frac{1}{2}\sin\theta)\}^2\sin^2\theta}\Bigg\{-\cos\theta+\{\Omega_0-2log(\frac{1}{2}\sin\theta)\}\times$$
$$\times\left[1+iL\sin^2\theta-\sin^2\theta\frac{\Phi'(\cos\theta)}{\Phi(\cos\theta)}\right]+G(\theta)+G(\pi-\theta)\Bigg\} \tag{6.10}$$

where

$$G(\theta) = -\frac{e^{2iL(1-cos\theta)}}{\Phi^2(1)\Phi^2(-cos\theta)}\{f(\pi-\theta)+$$
$$+ 2iL\sin^2\theta g^3(2L,\pi-\theta)[l_{01}(4L\sin^2\frac{1}{2}\theta) - T^2(4L\sin^2\frac{1}{2}\theta)]-$$
$$- g^2(2L,\pi-\theta)[\cos^2\frac{1}{2}\theta + iL\sin^2\theta T(4L\sin^2\frac{1}{2}\theta)]\}+$$
$$+ \frac{e^{4iL}}{\Phi^4(1)}[\Omega_0 - 2\log(\frac{1}{2}\sin\theta)]f(\theta)f(\pi-\theta)\times$$
$$\times\{1+\Omega_0^{-2}[\sin^2\frac{1}{2}\theta T(4L\sin^2\frac{1}{2}\theta) + \cos^2\frac{1}{2}\theta T(4L\cos^2\frac{1}{2}\theta)+$$
$$+ iL\sin^2\theta T(4L\sin^2\frac{1}{2}\theta)T(4L\cos^2\frac{1}{2}\theta) - T(4L)]\}-$$
$$- \frac{f(0)h(\pi-\theta)e^{6iL}}{\Phi^2(1)[\Phi^4(1)-h^2(0)e^{4iL}]}\left\{\frac{h(\pi-\theta)}{\Phi^2(-cos\theta)}e^{-2iL\cos\theta}-\right.$$
$$\left.- \frac{h(0)h(\theta)}{\Phi^2(1)}e^{2iL}[\Omega_0 - 2\log(\frac{1}{2}\sin\theta)]\right\} \quad (6.11)$$

with defined parameters

$$\Omega_0 = -2\log ka - 2\gamma + i\pi \quad (6.12)$$

$$g(x,\theta) = [\Omega_0 + l_0(2x) + T(2x\cos^2\frac{1}{2}\theta)]^{-1} \quad (6.13)$$

$$f(\theta) = \left\{\Omega_0 + \frac{l_0(4L) + T(4L\cos^2\frac{1}{2}\theta)}{1+\frac{2l_{01}(4L\cos^2\frac{1}{2}\theta) - T^2(4L\cos^2\frac{1}{2}\theta) - \frac{1}{6}\pi^2}{\Omega_0[l_0(4L)+T(4L\cos^2\frac{1}{2}\theta)]}}\right\}^{-1} \quad (6.14)$$

$$h(\theta) = \left\{\Omega_0 + \right.$$
$$\left. + \frac{l_0(4L) + T(4L\cos^2\frac{1}{2}\theta)}{1+\frac{2l_{01}(4L\cos^2\frac{1}{2}\theta)+l_{01}(4L)+l_2(4L,4L\cos^2\frac{1}{2}\theta) - T^2(4L\cos^2\frac{1}{2}\theta) - T(4L)T(4L\cos^2\frac{1}{2}\theta) - \frac{1}{6}\pi^2}{\Omega_0[l_0(4L)+T(4L\cos^2\frac{1}{2}\theta)]}}\right\}^{-1} \quad (6.15)$$

Values for l_0, T, l_2, l_{01} and $\Phi(\alpha)$ can be calculated by using equations Eq. (6.18), Eq. (6.19), Eq. (6.23), Eq. (6.24) and Eq. (6.47). First four quantities are derived by iterating cosine and sine integrals and taking the amplitude function. The last quantity is the linear split function that is used in Wiener-Hopf technique.

Then monostatic cross section of a thin wire is calculated by selecting $\theta = \theta_0$ for all of the equations that are going to be used and by using Eq. (6.8) in Eq. (6.7). To calculate the average monostatic cross section, he used equation Eq. (6.4) as always.

In Einarsons's Direct Method, the current is defined as Fourier Transform of the equation Eq. (6.8) and the final result of the current is the asymptotic expansion of this Fourier Transform [21].

$$I(z,\theta_0) = \frac{4\pi Y}{ik\sin\theta_0\{\Omega_0 - 2\log(\frac{1}{2}\sin\theta_0)\}}\times \\ \times [e^{-ikz\cos\theta_0} + \psi(L+kz,\theta_0) + \psi(L-kz,\pi-\theta_0)] \quad (6.16)$$

where

$$\psi(x,\theta_0) = -\frac{exp(ix+iL\cos\theta_0)}{\Phi(1)\Phi(\cos\theta_0)}\{g(x,\theta_0) + g^3(x,\theta_0)[l_{11}(2x)+ \\ + 2l_{01}(2x\cos^2\frac{1}{2}\theta_0) - T^2(2x\cos^2\frac{1}{2}\theta_0) - l_2(2x\cos^2\frac{1}{2}\theta_0, 2x) - \frac{1}{6}\pi^2]\}+ \\ + \frac{f(\pi-\theta_0)exp\{ix+iL(2-cos\theta_0)\}}{\Phi^3(1)\Phi(-\cos\theta_0)}\{g(x,0) + g^3(x,0)[l_{11}(2x)+ \\ + l_{01}(2x) - T^2(2x) + T(4L\sin^2\frac{1}{2}\theta_0)(T(2x\cos^2\frac{1}{2}\theta_0) - T(2x))+ \\ + l_2(2x,4L) - l_2(4L\sin^2\frac{1}{2}\theta_0 + 2x\cos^2\frac{1}{2}\theta_0, 2x\cos^2\frac{1}{2}\theta_0)- \\ - l_2(4L\sin^2\frac{1}{2}\theta_0 + 2x\cos^2\frac{1}{2}\theta_0, 4L) + l_2(4L\sin^2\frac{1}{2}\theta_0 + 2x\cos^2\frac{1}{2}\theta_0, 2x) - \frac{1}{6}\pi^2]\}- \\ - \frac{f(0)e^{ix+4iL}}{\Phi(1)[\Phi^4(1) - h^2(0)e^{4iL}]}\left[\frac{h(\theta_0)}{\Phi(\cos\theta_0)}e^{iL\cos\theta_0} - \frac{h(0)h(\pi-\theta_0)}{\Phi^2(1)\Phi(-cos\theta_0)}e^{iL(2-\cos\theta_0)}\right]\times \\ \times \{g(x,0) + g^3(x,0)[l_{11}(2x) + l_{01}(2x) - T^2(2x) + l_2(4L,2x)+ \\ + l_2(2x,4L) - T(4L)T(2x) - \frac{1}{6}\pi^2]\} \quad (6.17)$$

The function g, f and h functions are defined as in equations Eq. (6.13), Eq. (6.14) and Eq. (6.15), respectively. Special functions in Eq. (6.17) can be seen in the special function part.

6.2 Einarsson's Special Functions

To calculate monostatic cross section, the special functions that Einarsson used, are need to be known [3].

Expressions for $l_0(x)$ and $T(x)$ are given as:

$$l_0(x) = \gamma + \log x - \frac{1}{2}i\pi \tag{6.18}$$

$$T(x) = c(x) - is(x) = \int_x^\infty \frac{e^{i(\xi - x)}}{\xi} d\xi = \int_0^\infty \frac{e^{ixu}}{1+u} du = \\ = -e^{-ix}[Ci(x) + iSi(x) - \frac{1}{2}i\pi] \tag{6.19}$$

where cosine and sine integrals are defined as:

$$\begin{aligned} Ci(x) &= -\int_x^\infty \frac{\cos\xi}{\xi} d\xi \\ Si(x) &= -\int_0^x \frac{\sin\xi}{\xi} d\xi \end{aligned} \tag{6.20}$$

A more algebraic version of cosine integral can be written as:

$$Ci(x) = \gamma + \log x - Cin(x) \tag{6.21}$$

$$Cin(x) = \int_0^x \frac{1 - cos\xi}{\xi} d\xi \tag{6.22}$$

As discussed, iterated amplitude functions for these cosine and sine integrals are needed. These functions are:

$$l_2(x,y) = c_2(x,y) - is_2(x,y) = \int_0^\infty \frac{T(y+\tau y)}{1+\tau} e^{ix\tau} d\tau = \\ = \int_0^\infty \frac{\log(1+xu/y)}{1+u} e^{ixu} du \tag{6.23}$$

When $x = y$, the function $l_2(x,y)$ becomes

$$l_{01}(x) = l_2(x,x) = c_{01}(x) - is_{01}(x) = \int_x^\infty \frac{T(\xi)}{\xi} e^{i(\xi - x)} d\xi = \\ = \int_0^\infty \frac{\log(1+u)}{1+u} e^{ixu} du \tag{6.24}$$

and when x = 0,

$$l_{11}(x) = l_2(0,x) = c_{11}(x) - is_{11}(x) = \int_x^\infty \frac{T(\xi)}{\xi} d\xi = \\ = \int_0^\infty \frac{\log(1+u)}{u} e^{ixu} du \quad (6.25)$$

To calculate T function, we need to know $c(x)$ and $s(x)$. From the work of Hastings [39] for $1 \leq x < \infty$:

$$c(x) = x^{-2} \times \\ \times \left[\frac{21.821899 + 352.018498x^2 + 302.757865x^4 + 42.242855x^6 + x^8}{449.690326 + 1114.978885x^2 + 482.485984x^4 + 48.196927x^6 + x^8} \right] + \varepsilon(x), \\ |\varepsilon(x)| < 3 \times 10^{-7} \quad (6.26)$$

$$s(x) = -x^{-1} \times \\ \times \left[\frac{38.102495 + 335.677320x^2 + 265.187033x^4 + 38.027264x^6 + x^8}{157.105423 + 570.236280x^2 + 322.624911x^4 + 40.021433x^6 + x^8} \right] + \varepsilon(x), \\ |\varepsilon(x)| < 5 \times 10^{-7} \quad (6.27)$$

And for $0 < x \leq 1$, [21] :

$$c(x) = f(x)\cos x - g(x)\sin x + \varepsilon_1(x), \qquad |\varepsilon_1(x)| < 3 \times 10^{-9} \quad (6.28)$$

$$s(x) = g(x)\cos x + f(x)\sin x + \varepsilon_2(x), \qquad |\varepsilon_2(x)| < 2 \times 10^{-9} \quad (6.29)$$

where $f(x)$ and $g(x)$ functions that are used in Eq. (6.28) and Eq. (6.29) are

$$f(x) = -\gamma - \log x + 0.25x^2 - 0.010416660x^4 + \\ + 0.000231447x^6 - 0.000003046x^8 \quad (6.30)$$

$$g(x) = -\frac{1}{2}\pi + 0.999999998x - 0.055555480x^3 + 0.001666289x^5 - \\ - 0.000027739x^7 - 0.000003046x^8 \quad (6.31)$$

To calculate $l_{01}(x)$ function, $c_{01}(x)$ and $s_{01}(x)$ are calculated as for $0 < x \leq 2$:

$$c_{01}(x) = f(x)\cos x + g(x)\sin x + \varepsilon_1(x), \qquad |\varepsilon_1(x)| < 8 \times 10^{-10} \quad (6.32)$$

$$s_{01}(x) = f(x)\sin x - g(x)\cos x + \varepsilon_2(x), \qquad |\varepsilon_2(x)| < 6 \times 10^{-10} \tag{6.33}$$

where used $f(x)$ and $g(x)$ functions are defined as:

$$f(x) = \frac{1}{2}(\gamma + \log x)^2 - \frac{1}{24}\pi^2 - x^2(0.125 - 2.60416632 \times 10^{-3}x^2 + \\ + 3.857955 \times 10^{-5}x^4 - 3.87035 \times 10^{-7}x^6 - 2.61455 \times 10^{-9}x^8) \tag{6.34}$$

$$g(x) = -\frac{1}{2}\pi(\gamma + \log x) + x(0.9999999992 - 0.0185185136x^2 + \\ + 3.3332344 \times 10^{-4}x^4 - 4.0422785 \times 10^{-6}x^6 + 3.201246 \times 10^{-8}x^8) \tag{6.35}$$

For $2 < x < \infty$, the corresponding $c_{01}(x)$ and $s_{01}(x)$ functions are:

$$c_{01}(x) = -x^{-2} \times \\ \times \left(\frac{0.005415749x^8 + 0.4371420x^6 + 7.150169x^4 + 20.96173x^2 - 3.85642}{0.005415884x^8 + 0.4965990x^6 + 11.16783x^4 + 70.34218x^2 + 100}\right) + \\ + \varepsilon_1(x), \qquad |\varepsilon_1(x)| < 9 \times 10^{-9} \tag{6.36}$$

$$s_{01}(x) = -x^{-3} \times \\ \times \left(\frac{0.00994286x^8 + 0.846099x^6 + 14.24657x^4 + 43.8841x^2 - 0.542348}{0.003314700x^8 + 0.3369899x^6 + 8.503549x^4 + 60.93657x^2 + 100}\right) + \\ + \varepsilon_2(x), \qquad |\varepsilon_2(x)| < 6 \times 10^{-9} \tag{6.37}$$

To calculate another amplitude function $l_2(x, y)$ of the cosine and sine integral, $c_2(x, y)$ and $s_2(x, y)$ are defined as below.

For $2 \leq x < \infty$ and $1 \leq y \leq x$:

$$c_2(x, y) = f(x, y) + \varepsilon_1(x, y) \tag{6.38}$$

$$s_2(x, y) = g(x, y) + \varepsilon_2(x, y) \tag{6.39}$$

with

$$|\varepsilon_1(x, y)| \leq |\varepsilon_2(x, y)| < 2 \times 10^{-5} \tag{6.40}$$

On the other hand, for the condition $2 \leq x < \infty$ and $0 \leq y < 1$:

$$c_2(x,y) = c(y)c(x-y) - s(y)s(x-y) - f(x,x-y) - \varepsilon_1(x,x-y) \tag{6.41}$$

$$s_2(x,y) = c(y)s(x-y) + s(y)c(x-y) - g(x,x-y) - \varepsilon_2(x,x-y) \tag{6.42}$$

For all the values of $c_2(x,y)$ and $s_2(x,y)$, $f(x,y)$ and $g(x,y)$ that are needed to be used can be seen in equations Eq. (6.43) and Eq. (6.44), respectively.

$$f(x,y) = \frac{1}{2}[c^2(\frac{1}{2}x) - s^2(\frac{1}{2}x)] - c(x)\log\frac{2y}{x} + \frac{A_0}{x^2}\left(2 - \frac{x}{y} + \log\frac{2y}{x}\right) + \\ + \sum_{n=1}^{3}\frac{A_n}{x^2+a_n}\left[\frac{1}{2}\log\frac{y^2+a_n}{\frac{1}{4}x^2+a_n} + \frac{x}{\sqrt{a_n}}arctan\frac{(2y-x)\sqrt{a_n}}{xy+2a_n}\right] \tag{6.43}$$

where the constants are defined as:

$$\begin{aligned} A_0 &= 0.066349174 & a_1 &= 21.85045600 \\ A_1 &= 0.163725227 & a_2 &= 0.770345382 \\ A_2 &= 0.341159970 & a_3 &= 4.557156590 \\ A_3 &= 0.428765629 \end{aligned} \tag{6.44}$$

$g(x,y)$ is:

$$g(x,y) = c(\frac{1}{2}x)s(\frac{1}{2}x) - s(x)\log\frac{2y}{x} - \frac{B_0}{x}\log\frac{2y}{x} - \\ - \sum_{n=1}^{3}\frac{B_n}{x^2+b_n}\left[\frac{1}{2}xlog\frac{y^2+b_n}{\frac{1}{4}x^2+b_n} - \sqrt{b_n}arctan\frac{(2y-x)\sqrt{b_n}}{xy+2b_n}\right] \tag{6.45}$$

with

$$\begin{aligned} B_0 &= 0.282750417 & b_1 &= 17.42007600 \\ B_1 &= 0.052999360 & b_2 &= 0.501312744 \\ B_2 &= 0.422384403 & b_3 &= 3.439665810 \\ B_3 &= 0.241865419 \end{aligned} \tag{6.46}$$

The defined linearised split function is

$$\Phi(\alpha) = exp\{\frac{i}{2\pi}\int_{-\infty}^{\infty}\frac{d\tau}{\tau-\alpha}\log[\Omega_0 + \log\frac{4}{1-\tau^2}]\} \tag{6.47}$$

where the function Ω_0 can be calculated by Eq. (6.12). The function in Eq. (6.47) can be written as:

$$\frac{1}{\Phi(\cos\theta)} \approx \frac{1}{\Phi(1)}\{1-\Omega_0^{-1}\log(\cos^2\frac{1}{2}\theta)+\Omega_0^{-2}Li_2(\sin^2\frac{1}{2}\theta)+ \\ +\Omega_0^{-3}[\log(\cos^2\frac{1}{2}\theta)(Li_2(\cos^2\frac{1}{2}\theta)-\frac{1}{6}\pi^2)+ \\ +2Li_3(\sin^2\frac{1}{2}\theta)-2Li_3(\cos^2\frac{1}{2}\theta)+2\zeta(3)]\} \quad (6.48)$$

when the interval $0 \leq \theta < 0.5\pi$ is considered [38].

When the equation Eq. (6.48) differentiated with respect to $cos\theta$ for the considered interval:

$$\frac{\Phi'(\cos\theta)}{\Phi(\cos\theta)} \approx \Omega_0^{-1}\left\{\frac{1+\pi^2/(3\Omega_0^2)}{1+\cos\theta}-\frac{4\cos\theta}{\sin^2\theta}[\Omega_0^{-1}\log\cos\frac{1}{2}\theta \right. \\ \left. -\Omega_0^{-2}\{Li_2(\sin^2\frac{1}{2}\theta)-2(\log\cos\frac{1}{2}\theta)^2\}]\right\} \quad (6.49)$$

The functions used in these equations are defined as:

Li_2 dilogarithm:

$$Li_2(x) = -\int_0^x \frac{\log(1-\tau)}{\tau}d\tau = \sum_{n=1}^{\infty}\frac{x^n}{n^2}; \qquad |x| \leq 1 \quad (6.50)$$

Li_3 trilogarithm:

$$Li_3(x) = \int_0^x \frac{Li_2(\tau)}{\tau}d\tau = \sum_{n=1}^{\infty}\frac{x^n}{n^3}; \qquad |x| \leq 1 \quad (6.51)$$

When the interval $0.5\pi \leq \theta < \pi$ is concerned, the corresponding equations are:

$$\frac{1}{\Phi(\cos\theta)} = \Phi(-\cos\theta)\{\Omega_0 - 2\log(\frac{1}{2}\sin\theta)\} \quad (6.52)$$

$$\frac{1}{\Phi(0)} = (\Omega_0 + 2\log 2)^{1/2} \quad (6.53)$$

$$\frac{\Phi'(\cos\theta)}{\Phi(\cos\theta)} = \frac{\Phi'(-cos\theta)}{\Phi(-\cos\theta)} - \frac{2\cos\theta}{\sin^2\theta\{\Omega_0 - 2\log(\frac{1}{2}\sin\theta)\}} \quad (6.54)$$

As in the work of Hallén [40], for small values of ka

$$\frac{1}{\Phi^2(1)} \approx \Omega_0 - \frac{1}{6}\pi^2\Omega_0^{-1} - 4\zeta(3)\Omega_0^{-2} \tag{6.55}$$

Chapter 7

SIMULATIONS AND EVALUATIONS FOR DIPOLE RCS

Simulations for dipole RCS with respect to angle θ is given by using Van Vleck's Method A, Van Vleck's Method B, Tai's Variational Method and Einarsson's Direct Method. Note that, dipole geometry can be seen in Fig. 4.1, Fig. 5.1 and Fig. 6.1, θ is the angle between incident plane wave and the plane that is generated by the dipole. Throughout this chapter, it is assumed that the length of the dipole is l and wavelength of the incident field is given by λ. Moreover, the radius of the thin wire is supposed to be a. Six plots are shown below for $\frac{l}{\lambda} = 0.5$, $\frac{l}{\lambda} = 1.25$, $\frac{l}{\lambda} = 1.5$, $\frac{l}{\lambda} = 2$, $\frac{l}{\lambda} = 3.25$, $\frac{l}{\lambda} = 5.75$ with $\frac{l}{a} = 900$ in Fig. 7.1 to Fig. 7.6, respectively.

This chapter is important to understand whether a method can be used to calculate chaff RCS ($\bar{\sigma}$) since Y axis of the plots, $\sigma(\theta)$, is directly used in Eq. (4.29), Eq. (5.13) and Eq. (6.4) to get $\bar{\sigma}$. If a method can predict $\sigma(\theta)$ well, the result of the chaff RCS will be close to experimental results.

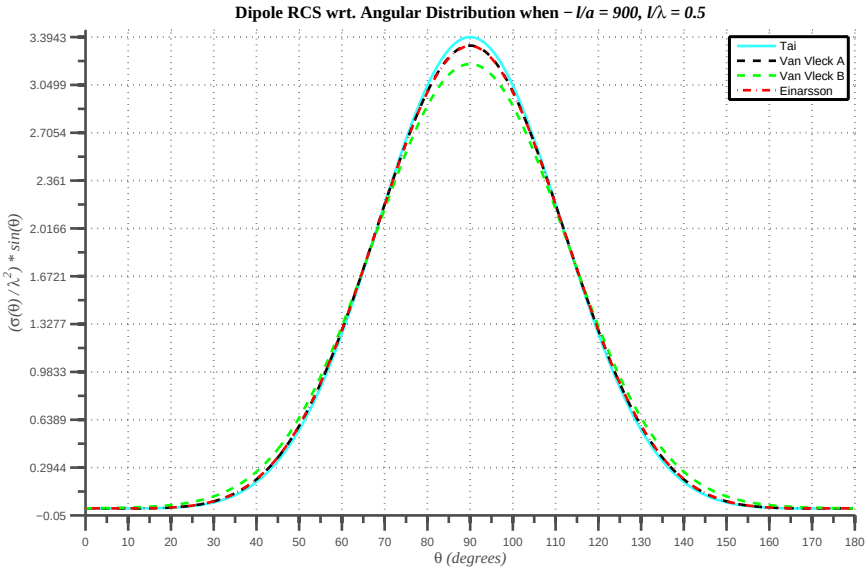

Figure 7.1: Dipole RCS ($(\sigma(\theta)/\lambda^2)sin(\theta)$) vs Angular Distribution (θ(degrees)) for Tai's, Van Vleck's and Einarsson's Methods when $\frac{l}{a} = 900$ and $\frac{l}{\lambda} = 0.5$

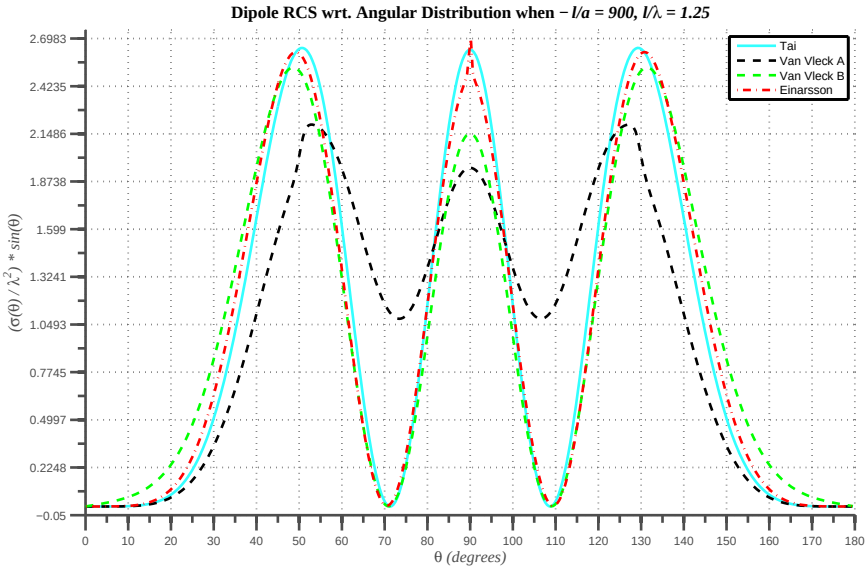

Figure 7.2: Dipole RCS ($(\sigma(\theta)/\lambda^2)sin(\theta)$) vs Angular Distribution (θ(degrees)) for Tai's, Van Vleck's and Einarsson's Methods when $\frac{l}{a} = 900$ and $\frac{l}{\lambda} = 1.25$

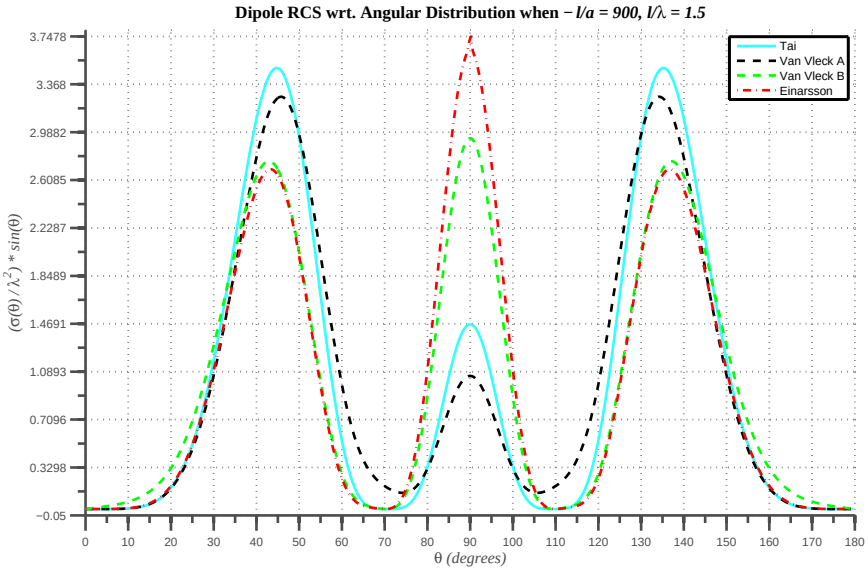

Figure 7.3: Dipole RCS $((\sigma(\theta)/\lambda^2)sin(\theta))$ vs Angular Distribution $(\theta(\text{degrees}))$ for Tai's, Van Vleck's and Einarsson's Methods when $\frac{l}{a} = 900$ and $\frac{l}{\lambda} = 1.5$

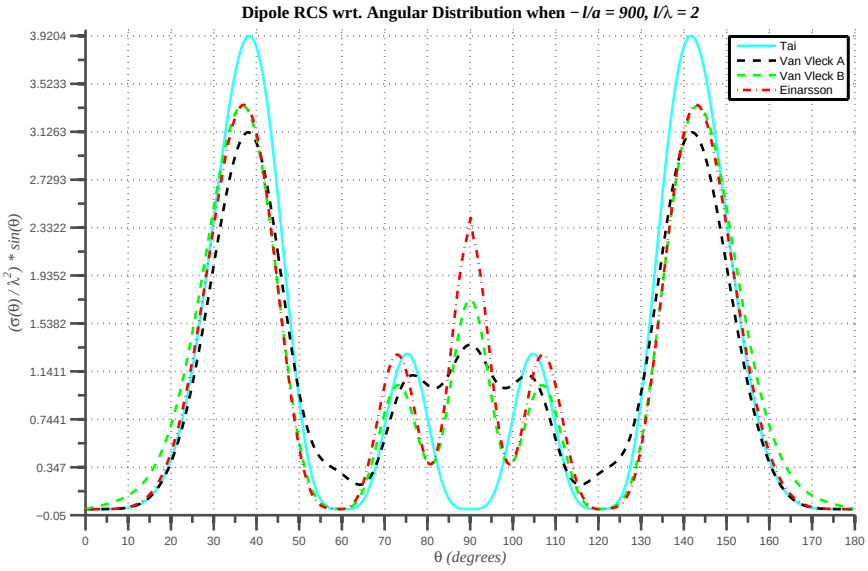

Figure 7.4: Dipole RCS $((\sigma(\theta)/\lambda^2)sin(\theta))$ vs Angular Distribution $(\theta(\text{degrees}))$ for Tai's, Van Vleck's and Einarsson's Methods when $\frac{l}{a} = 900$ and $\frac{l}{\lambda} = 2$

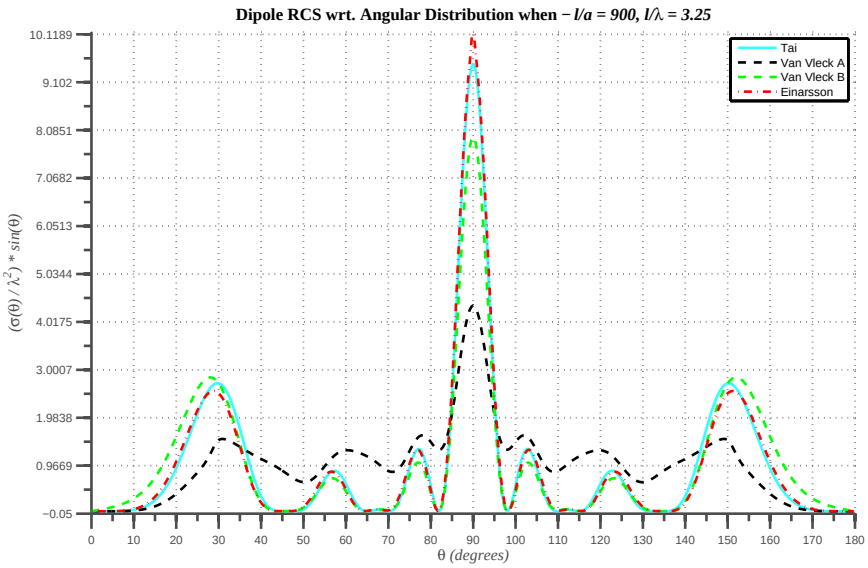

Figure 7.5: Dipole RCS $((\sigma(\theta)/\lambda^2)sin(\theta))$ vs Angular Distribution $(\theta(\text{degrees}))$ for Tai's, Van Vleck's and Einarsson's Methods when $\frac{l}{a} = 900$ and $\frac{l}{\lambda} = 3.25$

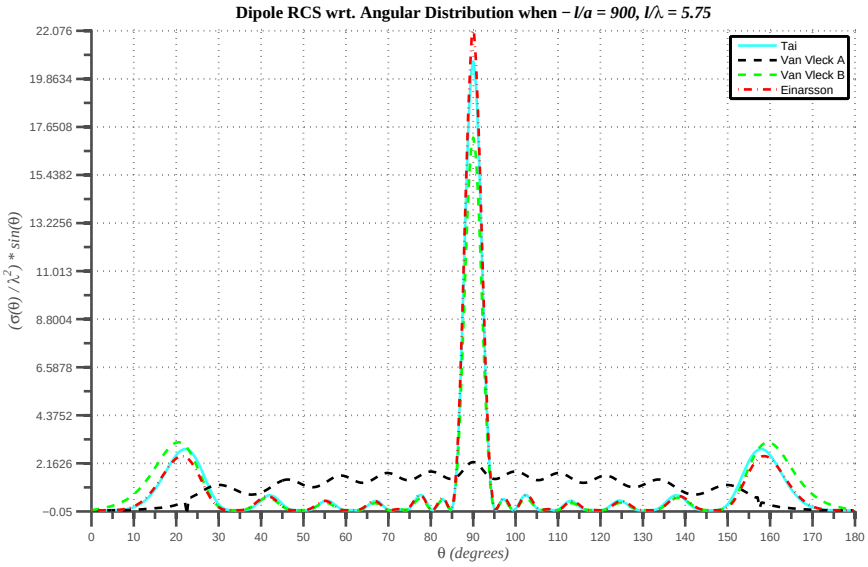

Figure 7.6: Dipole RCS $((\sigma(\theta)/\lambda^2)sin(\theta))$ vs Angular Distribution $(\theta(\text{degrees}))$ for Tai's, Van Vleck's and Einarsson's Methods when $\frac{l}{a} = 900$ and $\frac{l}{\lambda} = 5.75$

Results from these plots are listed below:

- Although, Method A follows the RCS trend that other methods have, it can be seen in the figures that the results have deviations due to two below reasons,
  - Method A does not use the forced oscillations at resonant frequencies and this causes some erroneous calculations especially for broadside response [1],
  - Specifically, Method A fails to predicts the amplitude of the peak values at resonant frequencies since the damping constant that it uses has some errors due to shift in resonance frequencies [1],
- As the length of the dipole increases Method A fails to predict the peak points for angular distribution while other methods predict similar peak locations,
- Particularly, Method B and Direct Method are in quite agreement,
- The difference between Method B and Direct Method generally occurs at $\theta = 90$ except for Fig. 7.1
- Although, Variational Method agrees with Method B and Direct Method, it fails to follow the RCS trend for $\frac{l}{\lambda} = 1.5$ (Fig. 7.3) and $\frac{l}{\lambda} = 2$ (Fig. 7.4) from $\theta = 80$ to $\theta = 100$.

The most significant indication of these simulations is that, Van Vleck's Method B and Tai's Variational Methods generally agree with the work of Einarsson. Although, Einarsson [21] claimed that Tai's [2] and Van Vleck's [1] works fail for longer wires, the simulations refute this claim with the help of Fig. 7.5 and Fig. 7.6. When a comparison is done between the performance of Method B and Variational Method, it can be concluded that Variational Method deviates from Einarsson's dipole RCS plots more than Method B. As a result, since Method B and Direct Method's results match quite well, these two methods will be used for calculation of chaff cartridge RCS in Chapter 8.

Chapter 8

SIMULATIONS AND EVALUATIONS FOR CHAFF RCS

As a result of discussions of previous chapter, Einarsson's Direct Method [21] and Van Vleck's Method B [1] will be used to calculate RCS values of specified chaff cartridges. For this part of the thesis, at first, a comparison will be made between the simulation result of Butters' work [7]. Then, RCS values of package chaffs in Table 1.1 will be calculated using these two methods and the most proper one will be selected for comparison. Then, an explanation of the chaff cartridge design procedure will be given. When the commercial chaff cartridge is selected for following comparison, different chaff cartridge for different frequency intervals will be proposed and compared with the selected one in two cases.

- *Case I*: The total dipole length in the designed cartridge will be the same and/or very close to the total dipole length of the commercial chaff cartridge. In this case, increase in the RCS will be evaluated while keeping dimensions and weights of cartridges equal.
- *Case II*: The average RCS of designed chaff cartridge and the commercial

one will be same for specified frequency interval; but in this case, the main aim is to decrease the total dipole length while getting same average RCS value with the commercial one,

Then, different scenarios will be discussed so as to explain the advantages of the designed chaff cartridges. At last, properties of a Dispensing System and a RWR system will be given in order to be able to use these suggested chaff cartridges.

8.1 Comparison of Butters' Chaff RCS with Simulations

Butters introduced a chaff cartridge that can be seen in Table 8.1. To find RCS of these dipole combinations he used the formula $\sigma = 0.17N\lambda^2$ where N is the number of dipoles and λ is the wavelength [7]. This formula is an rough approximation for chaff RCS calculation. The result for the given cartridge can be seen in Fig. 8.1.

Table 8.1: Chaff Cartridge Content from the Work of Butters [7]

Dipole Length (mm)	Resonant Frequency (GHz)	Number of Dipoles (N)
24.1	6	767000
18	8	1534000
14.4	10	2301000

Using Butters' Table 8.1, Van Vleck's Method B and Einarsson's Direct Method are used to calculate RCS value of the cartridge. The corresponding plots can be seen in Fig. 8.2 and Fig. 8.3, respectively.

By looking at these plots, one can easily state that resonant and harmonic peaks occurs at almost same frequencies compared the Butters' plot. Especially for Van Vleck's and Einarsson's methods, these peaks are at exactly same frequencies. The difference between the Butters' work is the result of his rough approximation. On the other hand, altough amplitude of the peaks are very

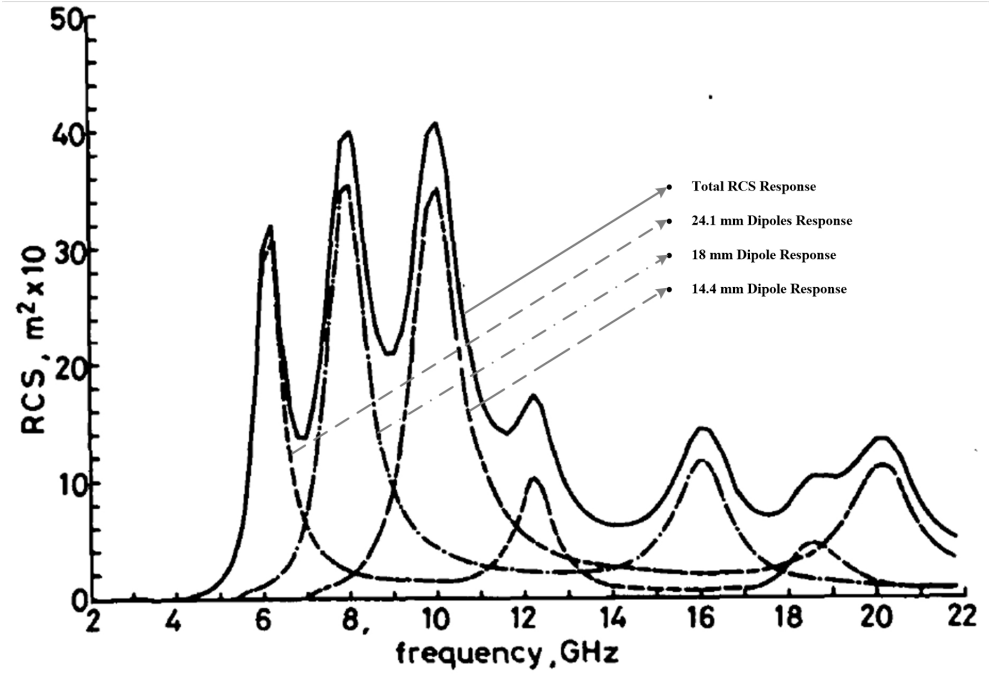

Figure 8.1: Chaff RCS ($m^2 \times 10$) vs Frequency (GHz) From the Work of Butters for Chaff Cartridge as in Table 8.1 [7]

close to each other, they are not same. When the general trend of the plots is concerned, highest RCS value is calculated by Van Vleck's Method B and lowest RCS value is calculated by Einarsson's Direct Method. Average of these two RCS almost gives the RCS value calculated by Butters' formula. One can easily use Van Vleck's or/and Einarsson's method to calculate RCS value of a chaff cartridge since results are close to each other and the trend of the dipole and total RCS plots are very similar to Butters' work.

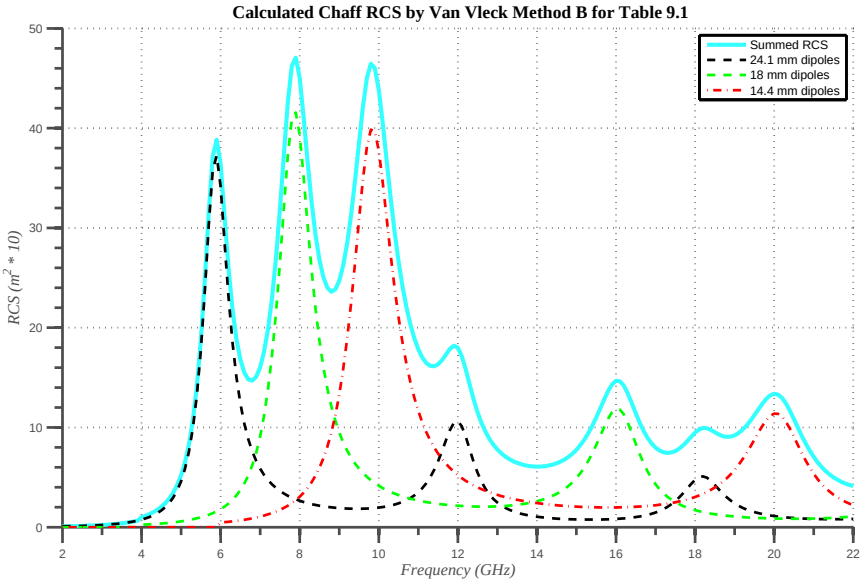

Figure 8.2: Chaff RCS ($m^2 \times 10$) vs Frequency (GHz) - Calculated by Van Vleck's Method B for Table 8.1

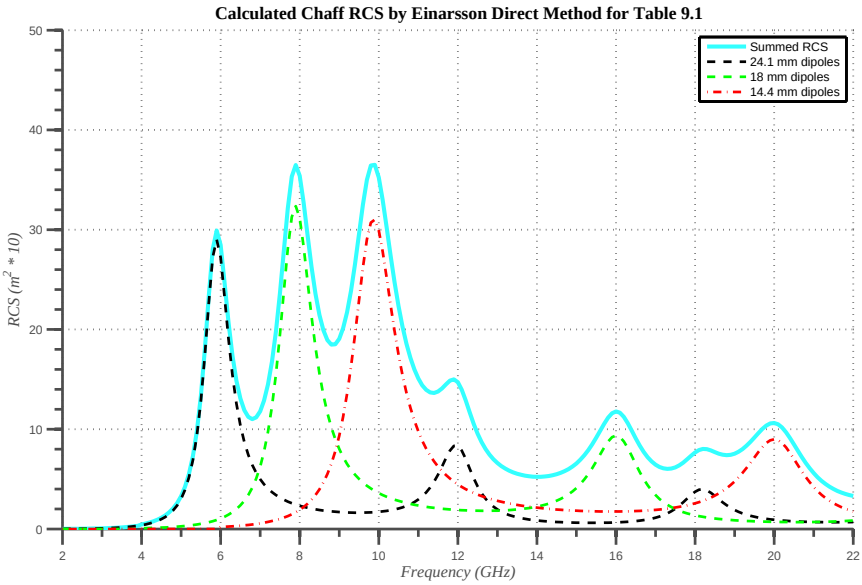

Figure 8.3: Chaff RCS ($m^2 \times 10$) vs Frequency (GHz) - Calculated by Einarsson's Direct Method for Table 8.1

8.2 RCS of Commercial Package Chaff Cartridges

Finding dipole content of a chaff cartridge that is commercial and is used for electronic warfare is almost impossible by only using open sources. However, by extensive search, a report is found. This report [5] was at first declared as confidential; but, in the course of time, the report became non-confidential so that contents of different chaff cartridges is revealed as in Table 1.1. By using Van Vleck's and Einarson's methods, RCS values of package chaff cartridges in the Table 1.1 are calculated and can be seen below. After this point, all the RCS values and y-axis of the RCS plot will be given in decibel (dB) with respect to 1 m^2. For instance, if a chaff cartridge has a RCS value of 1000 m^2 for a frequency, the RCS value will be given as 30 dB (which is equal to $10log(1000)$).

When the RCS trends of the RR-125/AL chaff cartridge plot is concerned, one can easily deduce that the cartridge (RR-125/AL) is designed for 7 to 20 GHz. The first resonant frequency is almost 7.4 GHz and the last one is about 17.9 GHz; but due to harmonics, at 20 GHz, RCS value is above 15 dB. For its designed frequency interval, it provides about 19.72 dB (Van Vleck's Method B) / 18.66 dB (Einarsson's Direct Method) average RCS value. The horizontal dashed lines in Fig. 8.4 and Fig. 8.4 show these average RCS values. Note that, as in the Butters' cartridge, Einarsson's method predicts the average RCS value about 1.06 dB lower than Van Vleck's method. Total length of dipoles in this chaff cartridge is almost 42884 meters.

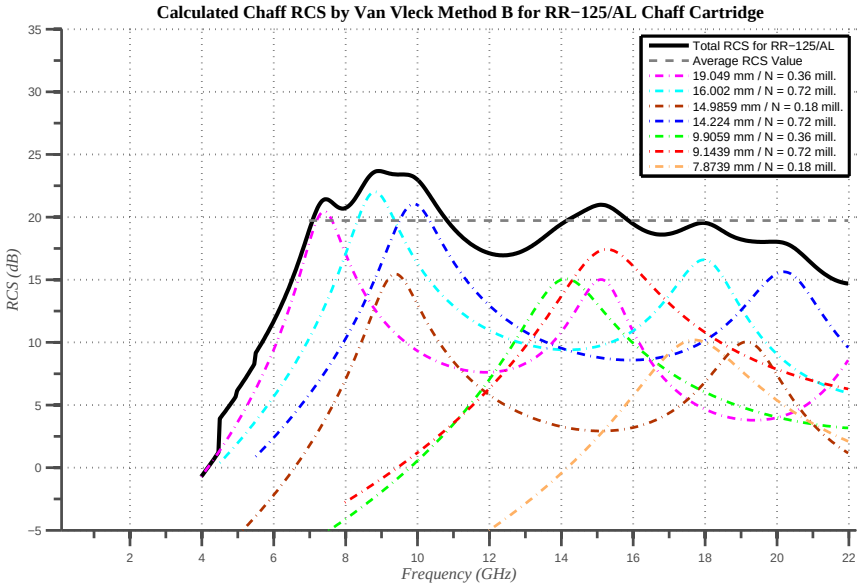

Figure 8.4: RCS (dB) vs Frequency (GHz) for RR-125/AL (Calculated by Van Vleck's Method B)

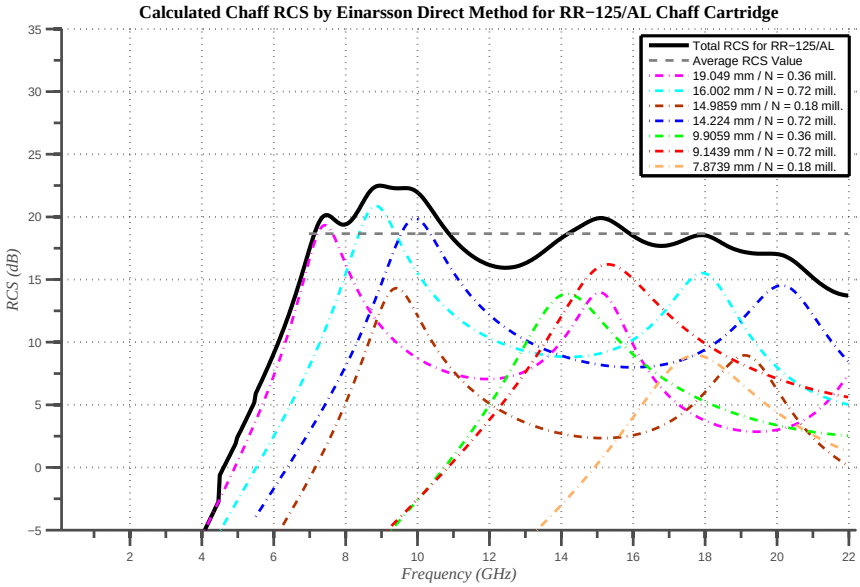

Figure 8.5: RCS (dB) vs Frequency (GHz) for RR-125/AL (Calculated by Einarsson's Direct Method)

Similar to RR-125/AL, RR-146/AL was designed for a specific frequency interval, 8 to 20 GHz as can be seen Fig. 8.6 and Fig. 8.7. The first resonant frequency is almost at 7.9 GHz and the last one is about at 14.2 GHz. It provides about 25.73 dB (Van Vleck's Method B) / 24.7 dB (Einarsson's Direct Method) average RCS value for 8 to 20 GHz. The difference between these two methods becomes 4 dB because dipoles used for RR-146/AL is about 168015 meters which is almost 2 times greater than the total dipole length of RR-125/AL.

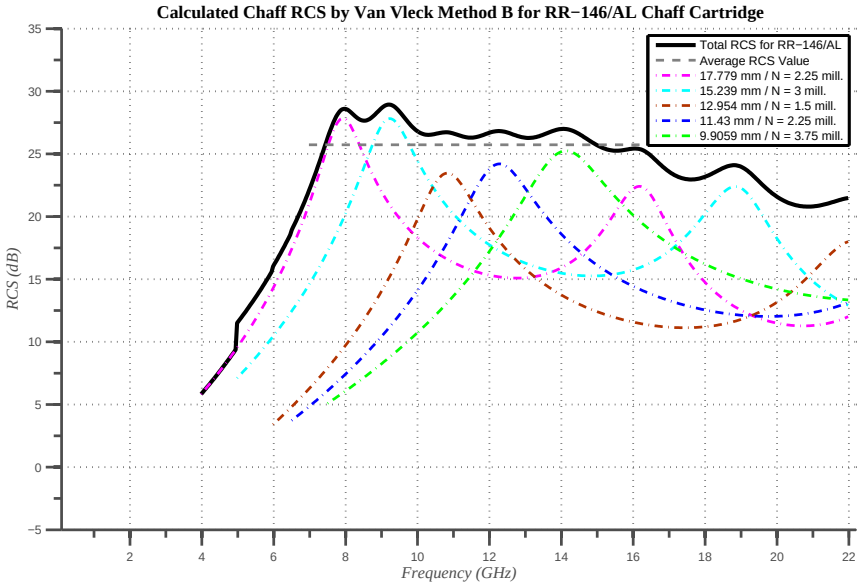

Figure 8.6: RCS (dB) vs Frequency (GHz) for RR-146/AL (Calculated by Van Vleck's Method B)

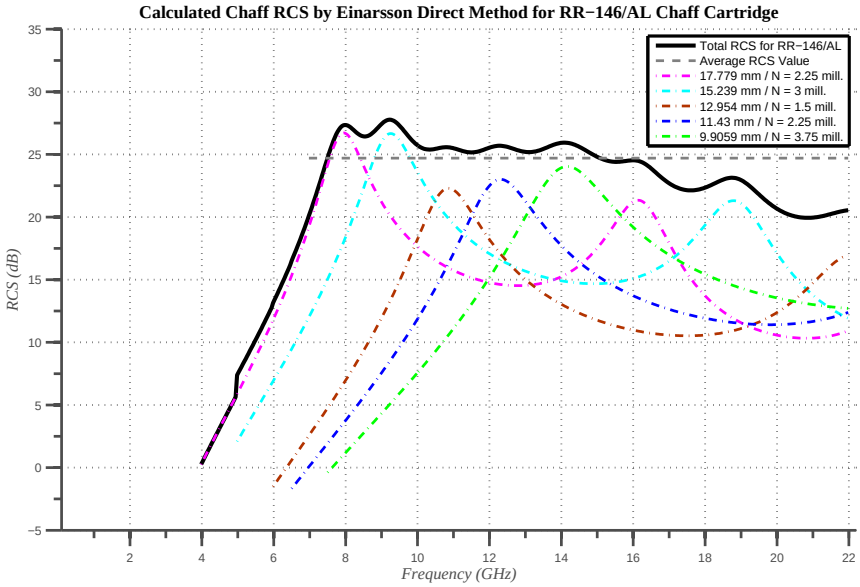

Figure 8.7: RCS (dB) vs Frequency (GHz) for RR-146/AL (Calculated by Einarsson's Direct Method)

When one looks at Fig. 8.8 and Fig. 8.9 calculated for RR-153/AL, it is easy to state that, the cartridge is designed for a longer frequency interval, 3 to 20 GHz. For this cartridge, longest dipole has a resonant frequency of 3 GHz and shortest one has 10 GHz. Again with the contributions of harmonic peaks, it covers up to 20 GHz. For the frequency that is of interest for electronic warfare, 2 to 20 GHz, it supplies 24.1061 dB (Van Vleck's Method B) / 23.1031 dB (Einarsson's Direct Method) average RCS by using 157526 meters of total dipole length. These average RCS values are represented by the horizontal dashed line on the plots.

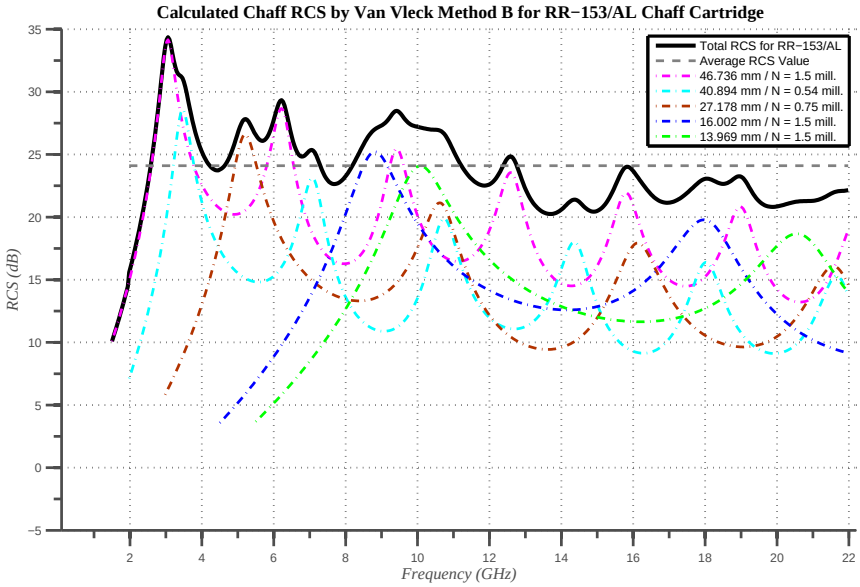

Figure 8.8: RCS (dB) vs Frequency (GHz) for RR-153/AL (Calculated by Van Vleck's Method B)

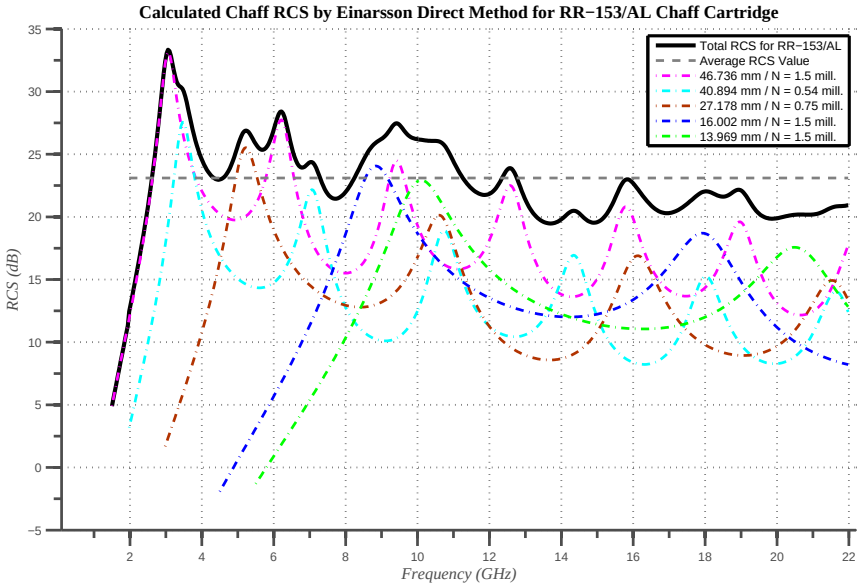

Figure 8.9: RCS (dB) vs Frequency (GHz) for RR-153/AL (Calculated by Einarsson's Direct Method)

For RR-153 A/AL, same dipole lengths are used with different numbers compared to RR-153/AL. Therefore, only RCS value differs. In this case, it provides 24.6041 dB (Van Vleck's Method B) / 23.5999 dB (Einarsson's Direct Method) average RCS by using 176591 meters total dipole length.

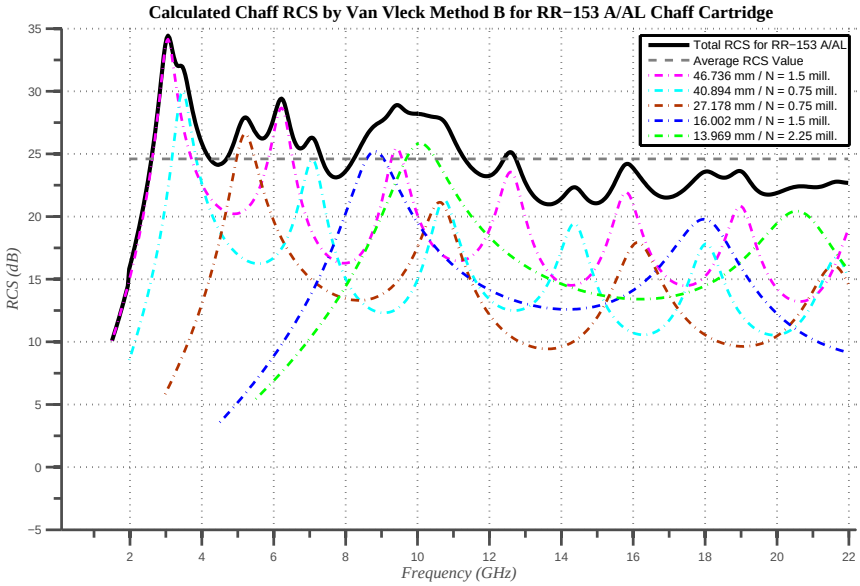

Figure 8.10: RCS (dB) vs Frequency (GHz) for RR-153 A/AL (Calculated by Van Vleck's Method B)

The last package chaff cartridge, RR-178 (XN-2) is designed for 3 to 20 GHz as can be seen in Fig. 8.12 and Fig. 8.13. The first resonant peak is at about 3.5 GHz and the last one is at about 16.5 GHz; but harmonics helps to get a flat RCS value up to 20 GHz. This chaff cartridge enables to get 21.5689 dB (Van Vleck's Method B) / 20.4418 dB (Einarsson's Direct Method) average RCS for concerned frequency interval in this thesis, 2 to 20 GHz. The total dipole length of this cartridge is 88775 meters.

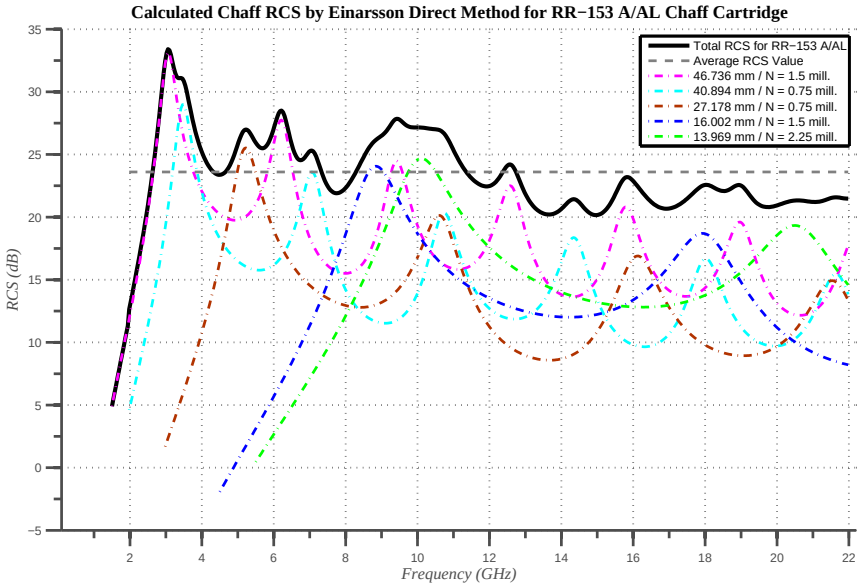

Figure 8.11: RCS (dB) vs Frequency (GHz) for RR-153 A/AL (Calculated by Einarsson's Direct Method)

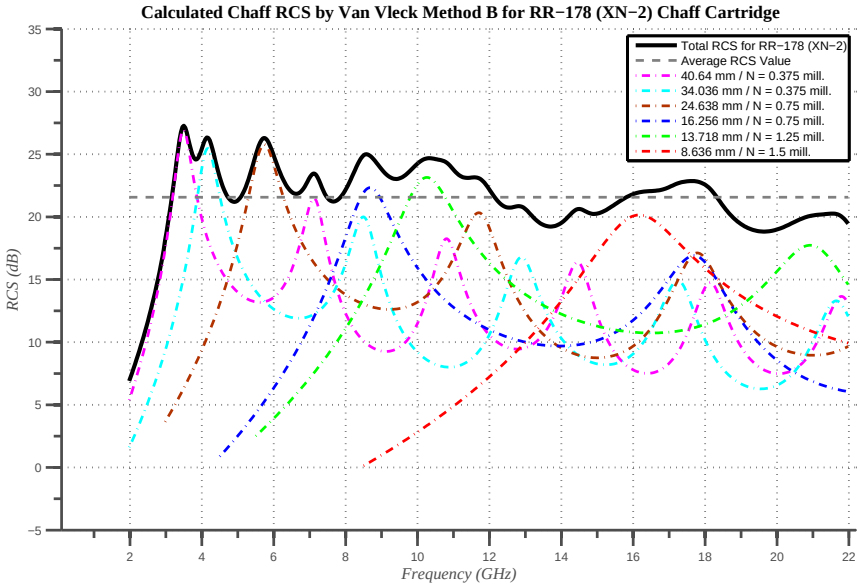

Figure 8.12: RCS (dB) vs Frequency (GHz) for RR-178 (XN-2) (Calculated by Van Vleck's Method B)

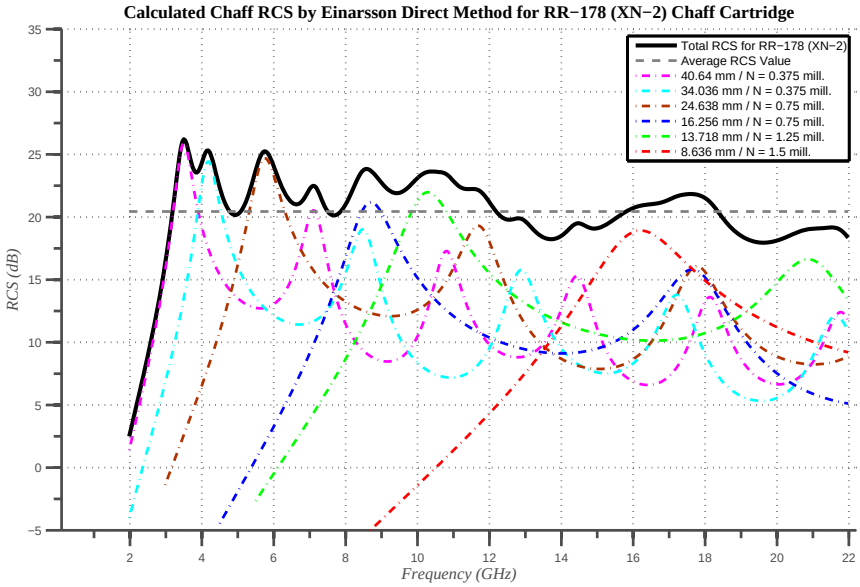

Figure 8.13: RCS (dB) vs Frequency (GHz) for RR-178 (XN-2) (Calculated by Einarsson's Direct Method)

As stated before, the interested frequency interval for this thesis is 2 to 20 GHz. As you can notice RR-153/AL, RR-153 A/AL and RR-178 (XN-2) are almost designed for same frequency interval, 3 to 20 GHz. Total dipole lengths in RR-153/AL, RR-153 A/AL are about 2 times greater than the average total dipole length of RR-178 (XN-2). One can select one of them without a reason to compare the performance of the proposed chaff cartridges in this thesis. RR-178 (XN-2) is preferred to be used since from 2 to 20 GHz, its RCS trend is more flat compared to other two and the total dipole length is lower than the others. Note that, flatness of the RCS values for its designed frequency interval is very significant; because everyone wants to get same/close response for a given frequency interval/value. Moreover, lowering dipole length is an important aim that helps to reduce the dimension of chaff cartridges.

8.3 Procedure for Designing Chaff Cartridge

Related parameters of the design are shown in Fig. 8.14. RCS response of one dipole for different dipole lengths are represented by the solid coloured lines.

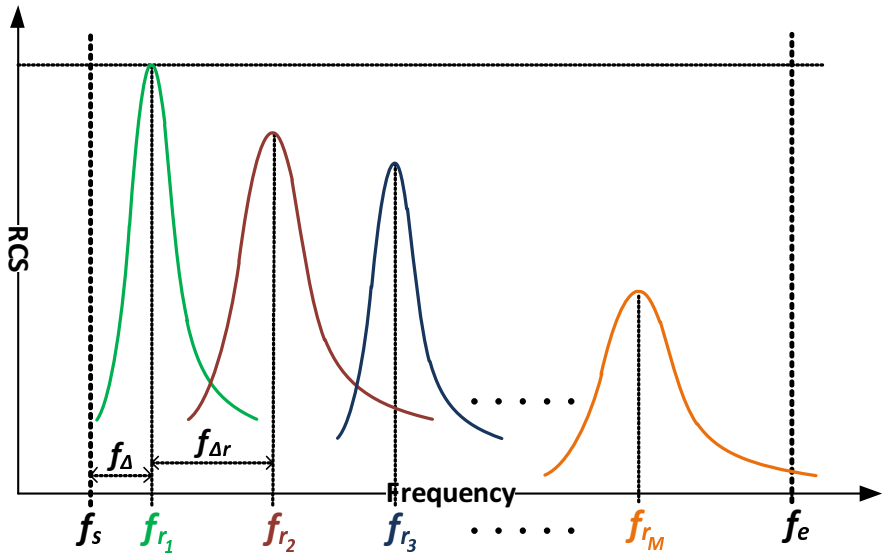

Figure 8.14: Sample Design Plot - RCS vs Frequency

The below procedure is used to design a chaff cartridge for a specified frequency interval.

- Select start and end frequencies (f_s and f_e) of the concerned frequency interval,
- Select safety frequency value (f_Δ) that is used for ensuring that resonant frequencies remain within specified frequency interval,
- Select number of different dipole length (M) that will be used in the cartridge,
- Decide the resonant frequencies (f_{r_i}) by using below formula,
  $f_{r_i} = f_s + f_\Delta + (i-1)f_{\Delta r}$ where $f_{\Delta r} = (f_e - f_s)/M$ and $i = 1, 2, ..., M$
  Note that, the harmonic of the resonant peak is not concerned for the design.

- Decide normalization constants (c_i) which are used to get flat a RCS response for specified frequency interval,

  As it can be noticed by looking at Fig. 8.14, the peak values of the RCS responses for different resonant frequencies are not equal. Each of these responses should be multiplied with a normalization constant so that the peak values become equal and a flat RCS response can be obtained for the designed frequency interval. In order to do that, for all the concerned resonant frequencies (2 to 20 GHz interval with a fine resolution) and for only one dipole, these RCS responses are calculated by both Van Vleck's Method B and Einarsson's Direct Method. For each method, the peak values of these responses are found and their inverses are calculated. These inverse values are the normalization constants (c_i) which equate the peak values of the RCS responses if they are multiplied with the corresponding RCS response. These constants are shown in Fig. 8.15 for different resonant frequencies.

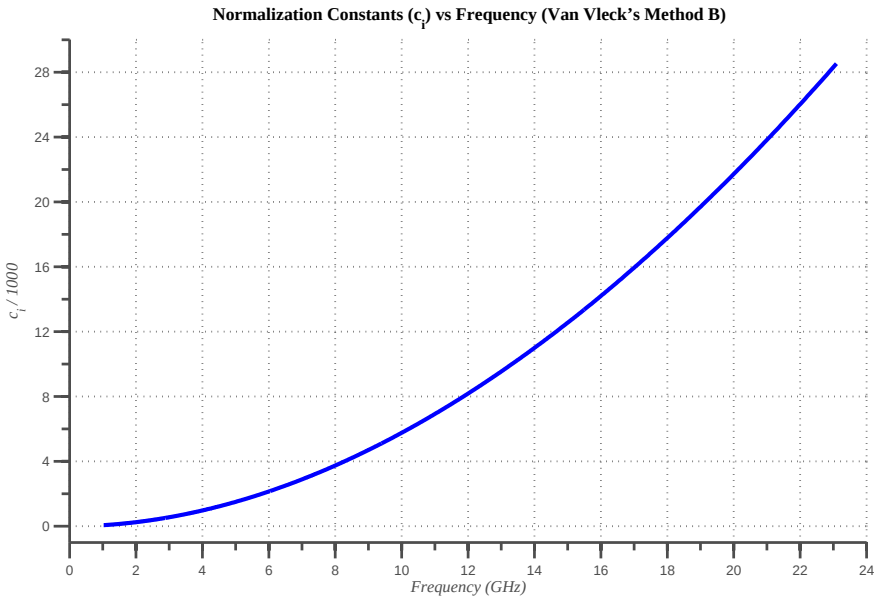

Figure 8.15: Normalization Constants (c_i) vs Frequency (GHz)

- Decide corresponding length of the dipoles (l_i) for each decided resonant frequencies f_{r_i},

  While deciding these lengths, one can easily approximate the value for half

of the resonant wavelength, however, this is not the practical case. As Van Vleck stated, the half of the wavelength is needed to be multiplied by 0.94 to get the practical dipole length for wanted resonant frequency [1]. Therefore, below formula is used:
$l_i = 0.94(\frac{c}{2f_{r_i}}) = 0.47\lambda$ where $i = 1, 2, ..., M$ and c is the speed of light,

For *Case I*:

In this case, the main aim is to equate the total dipole length of the designed chaff cartridge to the total dipole length of the commercial one. To accomplish this aim, below procedure needs to be followed:

- Calculate total dipole length (L_d) of the designed chaff cartridge by using l_i, c_i and formula:
  $L_d = \sum_{i=1}^{M} l_i c_i$.
- Then calculate total dipole length (L_c) of the commercial chaff cartridge by using its dipole lengths and numbers.
- Divide L_c by L_d to get S_I constant.
- Get number of dipole (N_{I_i}) needed for each dipole length (l_i) to equate the total dipole lengths in the considered cartridges by using the formula:
  $N_{I_i} = c_i \times S_I$ where $i = 1, 2, ..., M$
  Note that, N_{I_i} gives the number of dipole for i^{th} dipole length. Moreover, for simulations, N_{I_i} is rounded for hundreds in order to simulate realistic dipole numbers. Therefore, some errors may occur in terms of total dipole length for Case I due to this rounding operation.

For *Case I*:

In this case, the main aim is to equate average RCS value of the designed chaff cartridge to the average RCS value of the commercial one along the designed frequency interval. Below steps needs to be followed so as to reach this aim:

- Calculate average RCS (dB) (σ_d) value for designed chaff cartridge in the interval f_s to f_e by using found l_i and c_i values with the usage of Van Vleck's Method A or Einarsson's Direct Method,

- Calculate average RCS (dB) (σ_c) value for commercial chaff cartridge for the same interval by using its dipole lengths and dipole numbers with the usage of same calculation method,
- Then use below formula to get S_{II} constant.
  $S_{II} = 10^{0.1(\sigma_c - \sigma_d)}$
- Get number of dipole (N_{II_i}) needed for each dipole length (l_i) to equate the average RCS values of the considered cartridges for the designed frequency interval by using the formula:
  $N_{II_i} = c_i \times S_{II}$ where $i = 1, 2, ..., M$
  Note that, N_{II_i} gives the number of dipole for i^{th} dipole length. Moreover, for simulations, N_{II_i} is rounded for hundreds in order to simulate realistic dipole numbers. Therefore, some errors may occur in terms of average RCS values for Case II due to this rounding operation.

8.4 Proposed Chaff Cartridges - Design I

As stated in the introduction part, for electronic warfare environment, especially 2 to 20 GHz frequency interval is significant. For the first case, this frequency interval is divided into three equal sub-intervals: 2 to 8 GHz, 8 to 14 GHz and 14 to 20 GHz. For each interval, six different dipole lengths and corresponding number of dipoles for a flat RCS are suggested. While doing so, the described procedure is used. Moreover, as can be seen in Table 1.1, RR-178 (XN-2) has also six different dipole lengths. The plots for concerned intervals can be seen below for *Case I* and *Case II*.

8.4.1 *Case I*

For 2 to 8 GHz interval and *Case I*, as can be seen in Fig. 8.16 similar flatness is got by using designed chaff cartridge. However, especially between 2 GHz to 3 GHz, higher RCS values is observed compared to RR-178 (XN-2) which

was designed for 3 to 20 GHz as stated before. At the average, the designed cartridge increases average RCS about 3.19 dB (Van Vleck's Method B) / 3.47 dB (Einarsson's Direct Method) while decreasing the length about % 3.4.

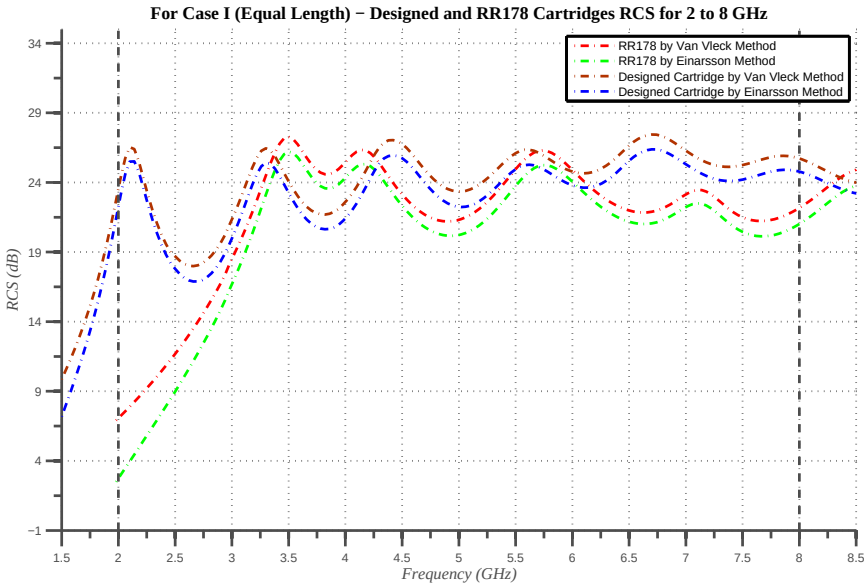

Figure 8.16: Design I: RCS (dB) vs Frequency (GHz) for *Case I* (Equal Total Dipole Length) 2 to 8 GHz

Table 8.2: Design I - Case I: Performance Results for 2 to 8 GHz

Frequency Interval	Calculation Method	Designed Cartridge		Total Length (m)			Average RCS (dB)		
		Dipole Length (mm)	Number	RR-178 (XN-2)	Designed Cartridge	Difference (%)	RR-178 (XN-2)	Designed Cartridge	Difference (dB)
2 to 8 GHz	Van Vleck Method B	67.1429 43.2515 31.9005	128600 274300 446900	88775	85864	3.39	21.1445	24.3405	3.1960
	Einarsson Direct Method	25.2688 20.9199 17.8481	632200 821200 1006000				19.8171	23.2876	3.4705

When Fig. 8.17 is examined, it can be asserted that designed cartridge supplies more flat RCS response for 8 to 14 GHz while getting an increase in average RCS about 2.23 dB (Van Vleck's Method B) / 2.07 dB (Einarsson's Direct Method) compared to RR/178 (XN-2). The lengths of total dipole are very close as can be seen in Table 8.3.

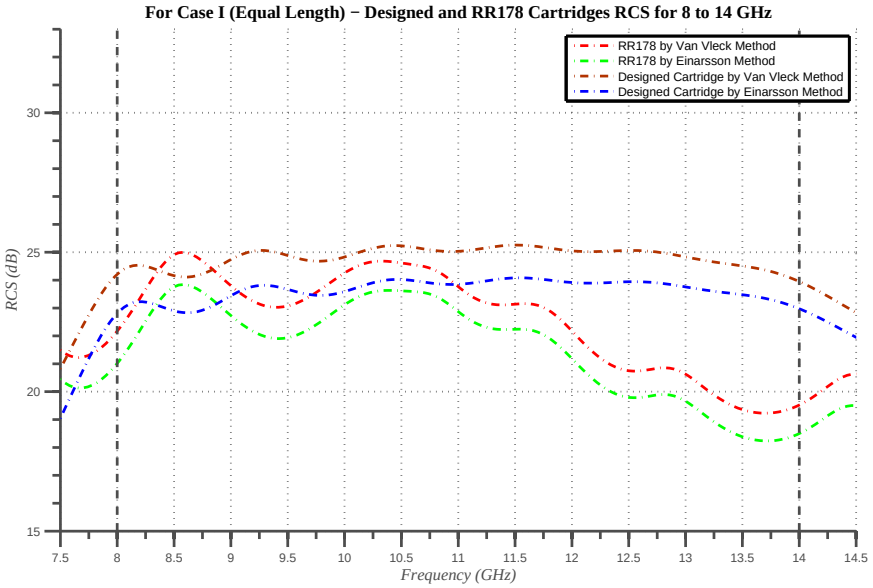

Figure 8.17: Design I: RCS (dB) vs Frequency (GHz) for *Case I* (Equal Total Dipole Length) 8 to 14 GHz

Table 8.3: Design I - Case I: Performance Results for 8 to 14 GHz

Frequency Interval	Calculation Method	Designed Cartridge		Total Length (m)			Average RCS (dB)		
		Dipole Length (mm)	Number	RR-178 (XN-2)	Designed Cartridge	Difference (%)	RR-178 (XN-2)	Designed Cartridge	Difference (dB)
8 to 14 GHz	Van Vleck Method B	17.4074 15.2268 13.5317	843500 983900 1110900	88775	88580	0,22	22.5681	24.7966	2.2285
	Einarsson Direct Method	12.1762 11.0675 10.1439	1225500 1324900 1409500				21.5432	23.617	2.0738

The most flat response is got for 14 to 20 GHz frequency interval by designed chaff cartridge as in Fig. 8.18. By using same total length of dipoles with RR-178 (XN-2), 3.72 dB (Van Vleck's Method B) / 3.51 dB (Einarsson's Direct Method) rise in average RCS is observed. Especially after 18.5 GHz, the difference in RCS is about 5 dB. Detailed results can be seen in Table 8.4.

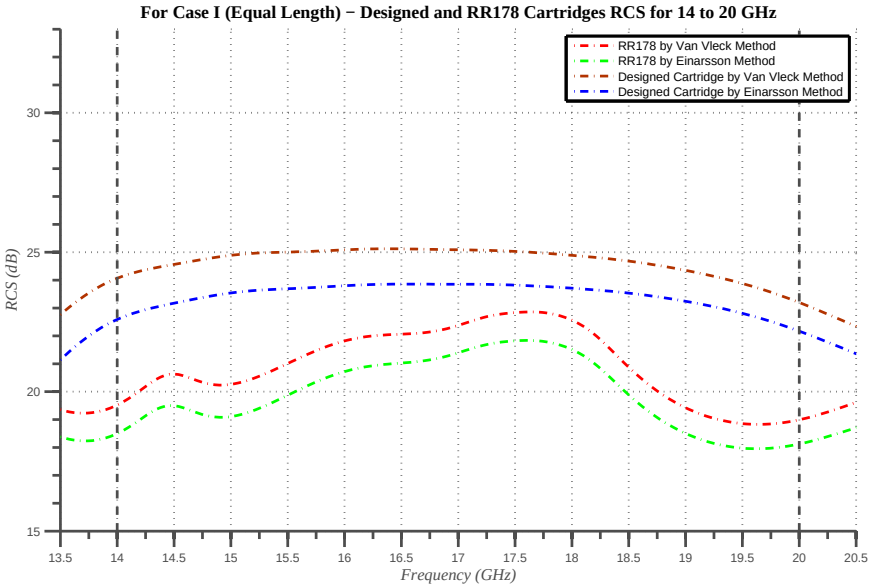

Figure 8.18: Design I: RCS (dB) vs Frequency (GHz) for *Case I* (Equal Total Dipole Length) 14 to 20 GHz

Table 8.4: Design I - Case I: Performance Results for 14 to 20 GHz

Frequency Interval	Calculation Method	Designed Cartridge		Total Length (m)			Average RCS (dB)		
		Dipole Length (mm)	Number	RR-178 (XN-2)	Designed Cartridge	Difference (%)	RR-178 (XN-2)	Designed Cartridge	Difference (dB)
14 to 20 GHz	Van Vleck Method B	10 9.2398 8.5871	1616900 1692700 1751600	88775	88045	0,83	20.944	24.6622	3.7182
	Einarsson Direct Method	8.0205 7.524 7.0854	1796600 1825700 1841600				19.9175	23.4263	3.5088

8.4.2 *Case II*

For this case, used dipole lengths are same; but number of used dipoles to get same average RCS is different for each calculation method.

When the used dipole numbers are analysed in Table 8.5, for the same dipole length the values are very close to each other for both calculation methods. While getting same average RCS value, a decrease of 2.24 times (Van Vleck's Method B) / 2.39 times (Einarsson's Direct Method) is obtained in terms of total dipole length. The response is very similar to *Case I* Fig. 8.16 as can be seen at Fig. 8.19.

Average RCS values are same as it is preferred.

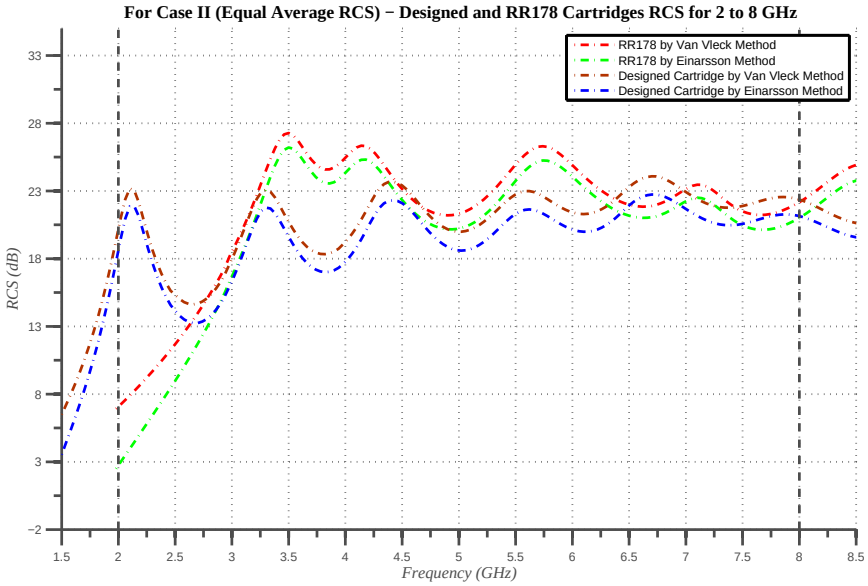

Figure 8.19: Design I: RCS (dB) vs Frequency (GHz) for *Case II* (Equal Average RCS) 2 to 8 GHz

Table 8.5: Design I - Case II: Performance Results for 2 to 8 GHz

Frequency Interval	Calculation Method	Designed Cartridge		Total Length (m)			Average RCS (dB)		
		Dipole Length (mm)	Number	RR-178 (XN-2)	Designed Cartridge	Difference (times)	RR-178 (XN-2)	Designed Cartridge	Difference (%)
2 to 8 GHz	Van Vleck Method B	67.1429	59300	88775	39601	2,242	21.1445	20.9794	0.7808
		43.2515	126500						
		31.9005	206100						
		25.2688	291600						
		20.9199	378800						
		17.8481	464000						
	Einarsson Direct Method	67.1429	55600		37149	2,390	19.8171	19.6487	0.8498
		43.2515	118700						
		31.9005	193400						
		25.2688	273500						
		20.9199	355300						
		17.8481	435300						

Similar to 2 to 8 GHz cartridges, for 8 to 14 GHz same average RCS value is got while decreasing total dipole length in the cartridge 1.67 times (Van Vleck's Method B) / 1.61 times (Einarsson's Direct Method) compared to RR-178 (XN-2). For examining dipole lengths and corresponding dipole numbers, Table 8.6 can be used. For the RCS response, Fig. 8.20 can be analysed.

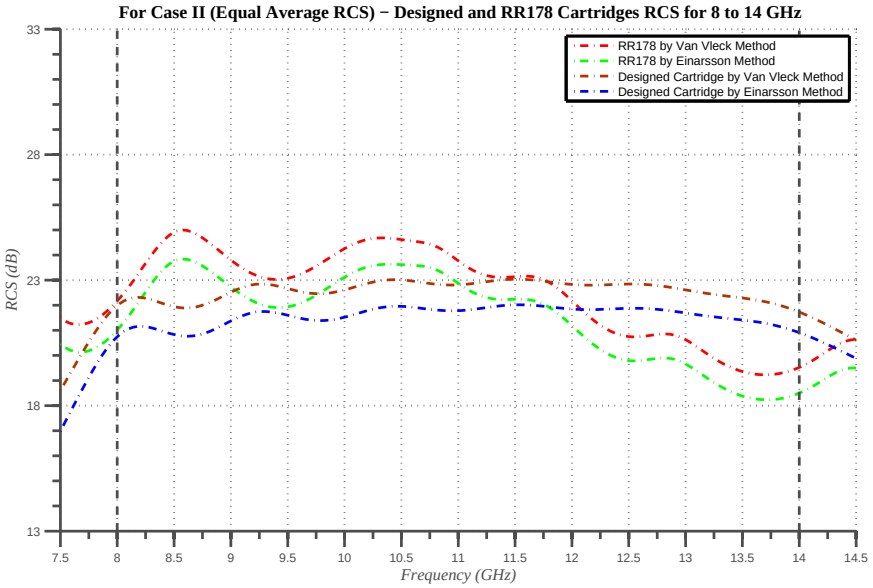

Figure 8.20: Design I: RCS (dB) vs Frequency (GHz) for *Case II* (Equal Average RCS) 8 to 14 GHz

Table 8.6: Design I - Case II: Performance Results for 8 to 14 GHz

Frequency Interval	Calculation Method	Designed Cartridge		Total Length (m)			Average RCS (dB)		
		Dipole Length (mm)	Number	RR-178 (XN-2)	Designed Cartridge	Difference (times)	RR-178 (XN-2)	Designed Cartridge	Difference (%)
8 to 14 GHz	Van Vleck Method B	17.4074	505900	88775	53125	1,671	22.5681	22.5762	-0.0359
		15.2268	590100						
		13.5317	666200						
		12.1762	735000						
		11.0675	794600						
		10.1439	845300						
	Einarsson Direct Method	17.4074	524200		55053	1,613	21.5432	21.5514	-0.0381
		15.2268	611500						
		13.5317	690400						
		12.1762	761700						
		11.0675	823500						
		10.1439	876000						

While getting same average RCS with more flat response as in Fig. 8.21, a decrease of 2.37 times (Van Vleck's Method B) / 2.266 times (Einarsson's Direct Method) is obtained in terms of total dipole length compared to RR-178 (XN-2). Detailed analysis of the comparison can be observed in Table 8.7

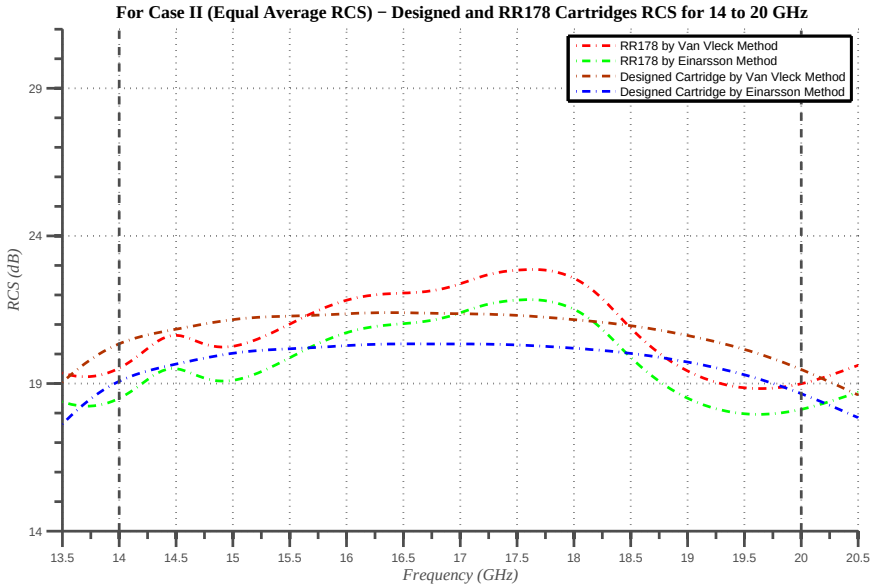

Figure 8.21: Design I: RCS (dB) vs Frequency (GHz) for *Case II* (Equal Average RCS) 14 to 20 GHz

Table 8.7: Design I - Case II: Performance Results for 14 to 20 GHz

Frequency Interval	Calculation Method	Designed Cartridge		Total Length (m)			Average RCS (dB)		
		Dipole Length (mm)	Number	RR-178 (XN-2)	Designed Cartridge	Difference (times)	RR-178 (XN-2)	Designed Cartridge	Difference (%)
14 to 20 GHz	Van Vleck Method B	10	685700	88775	37339	2,378	20.944	20.9368	0.0344
		9.2398	717900						
		8.5871	742800						
		8.0205	761900						
		7.524	774300						
		7.0854	781000						
	Einarsson Direct Method	10	719500		39181	2,266	19.9175	19.91	0.0377
		9.2398	753300						
		8.5871	779500						
		8.0205	799500						
		7.524	812500						
		7.0854	819500						

8.5 Proposed Chaff Cartridges - Design II

For the second proposal, as in the first one the frequency interval is separated into three equal sub-intervals: 2-8 GHz, 8-14 GHz and 14-20 GHz. But for this proposal, 12 different dipole lengths and corresponding number of dipoles for a

flat RCS are suggested for each interval. While doing so, the described procedure is used as before. The plots and comparison tables for concerned intervals can be seen below for *Case I* and *Case II*.

For these cartridges, instead of doing comparison with RR-178 (XN-2) chaff cartridges, the performance of the cartridges will be generally compared with the Design I due to its performance.

8.5.1 *Case I*

Compared to Design I, for 2 to 8 GHz interval, 0.8 dB increase is observed for both calculation methods as can be seen in Table 8.8. The RCS response (see Fig. 8.22) is more flat than both RR-178 (XN-2) and Design I in Fig. 8.16 owing to six more resonant peaks.

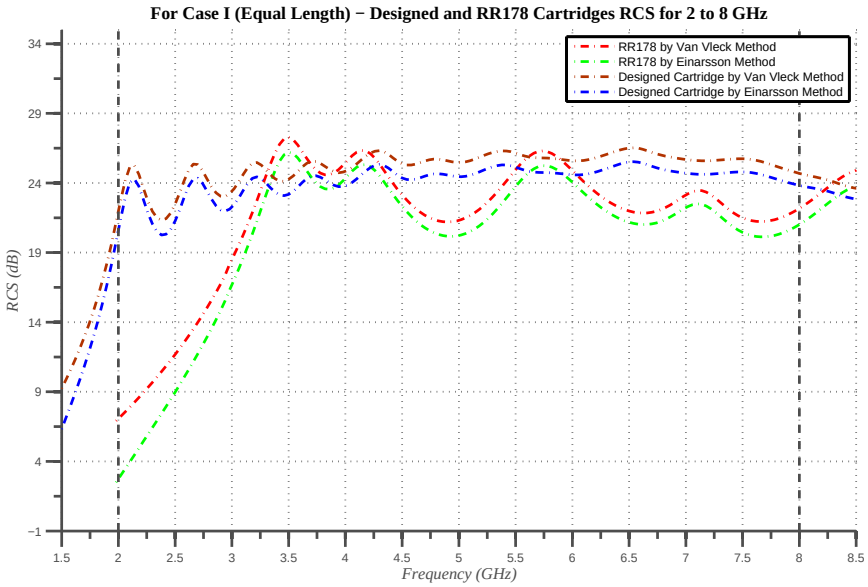

Figure 8.22: Design II: RCS (dB) vs Frequency (GHz) for *Case I* (Equal Total Dipole Length) 2 to 8 GHz

Table 8.8: Design II - Case I: Performance Results for 2 to 8 GHz

Frequency Interval	Calculation Method	Designed Cartridge		Total Length (m)			Average RCS (dB)		
		Dipole Length (mm)	Number	RR-178 (XN-2)	Designed Cartridge	Difference (%)	RR-178 (XN-2)	Designed Cartridge	Difference (dB)
2 to 8 GHz	Van Vleck Method B	66.8246	92300	88775	88112	0,75	21.1445	25.1142	3.9697
		53.4643	128700						
		44.5562	165400						
		38.1926	201000						
		33.4195	234800						
		29.707	265400						
	Einarsson Direct Method	26.7368	293200				19.8171	24.0908	4.2737
		24.3065	317900						
		22.2813	338800						
		20.5676	356100						
		19.0986	369900						
		17.8255	380500						

For 8 to 14 GHz chaff cartridge, increase in average RCS is not as noticeable as for 2 to 8 GHz cartridge. It is 0.14 dB (Van Vleck's Method B) / 0.17 dB (Einarsson's Direct Method) as can be noted by comparing the Average RCS columns of Table 8.9 and Table 8.3. Their flatnesses (Design I and Design II) are very similar as can be seen by comparing Fig. 8.17 and Fig. 8.23.

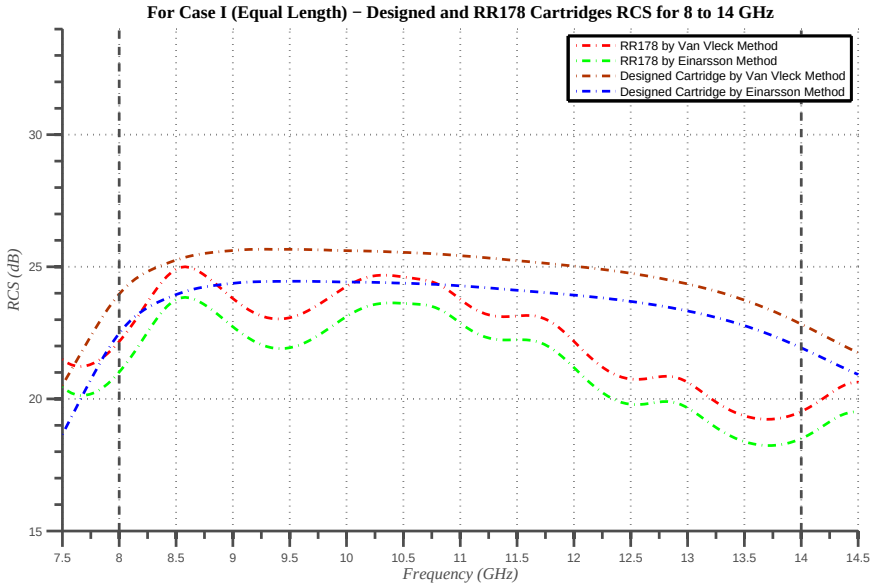

Figure 8.23: Design II: RCS (dB) vs Frequency (GHz) for *Case I* (Equal Total Dipole Length) 8 to 14 GHz

Table 8.9: Design II - Case I: Performance Results for 8 to 14 GHz

Frequency Interval	Calculation Method	Designed Cartridge		Total Length (m)			Average RCS (dB)		
		Dipole Length (mm)	Number	RR-178 (XN-2)	Designed Cartridge	Difference (%)	RR-178 (XN-2)	Designed Cartridge	Difference (dB)
8 to 14 GHz	Van Vleck Method B	17.3859	565500	88775	88464	0,35	22.5681	24.9372	2.3691
		16.3246	574600						
		15.3854	579900						
		14.5484	581000						
		13.7977	579300						
		13.1207	574700						
	Einarsson Direct Method	12.5071	566900				21.5432	23.7918	2.2486
		11.9482	557100						
		11.4372	545300						
		10.9681	531900						
		10.536	517100						
		10.1366	501100						

For 14 to 20 GHz frequency interval, almost same average RCS value is got when Design I and Design II (see Table 8.10) is concerned. Design II response can be seen in Fig. 8.24.

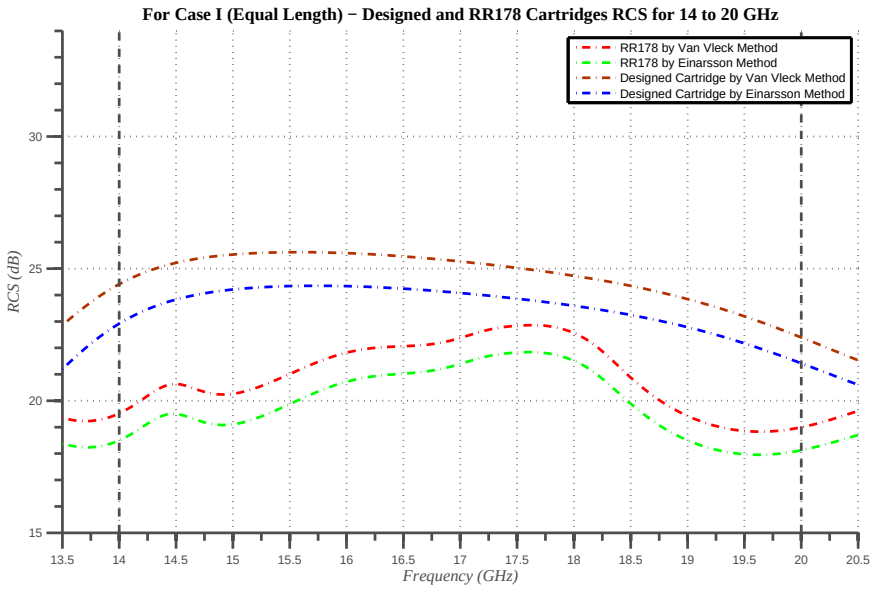

Figure 8.24: Design II: RCS (dB) vs Frequency (GHz) for *Case I* (Equal Total Dipole Length) 14 to 20 GHz

Table 8.10: Design II - Case I: Performance Results for 14 to 20 GHz

Frequency Interval	Calculation Method	Designed Cartridge		Total Length (m)			Average RCS (dB)		
		Dipole Length (mm)	Number	RR-178 (XN-2)	Designed Cartridge	Difference (%)	RR-178 (XN-2)	Designed Cartridge	Difference (dB)
14 to 20 GHz	Van Vleck Method B	9.9929	1072000	88775	87913	0,98	20.944	24.7433	3.7993
		9.6329	1034600						
		9.298	996300						
		8.9856	957200						
		8.6935	917700						
		8.4197	878100						
	Einarsson Direct Method	8.1627	838300				19.9175	23.542	3.6245
		7.9209	799200						
		7.6931	760300						
		7.4779	722200						
		7.2745	685000						
		7.0819	648600						

8.5.2 *Case II*

Like in *Case I*, the result of Design II is compared to Design I instead of RR-178 (XN-2) because Design I has better results than RR-178 (XN-2) as discussed and Design II is expected to get better results than Design I with the help of increase at number of resonant peaks.

Similar to *Case I*, for 2 to 8 GHz, more flat response (see Fig. 8.25) is got than Design I. Moreover, about 5000 meters less dipole is spent in order to get same average RCS value which can be seen in Table 8.11. In this table, dipole lengths and corresponding numbers for both method can be examined. For the same dipole length, very close dipole number is used when two methods are compared.

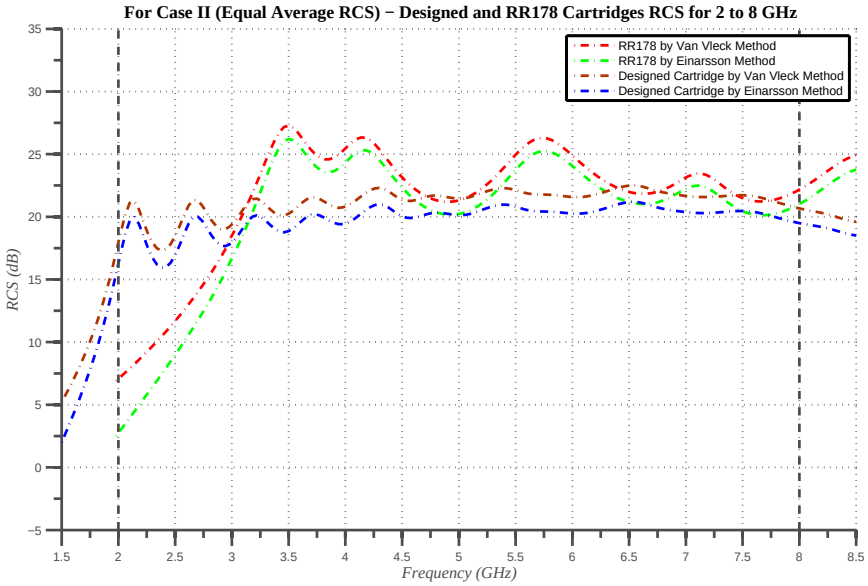

Figure 8.25: Design II: RCS (dB) vs Frequency (GHz) for *Case II* (Equal Average RCS) 2 to 8 GHz

Table 8.11: Design II - Case II: Performance Results for 2 to 8 GHz

Frequency Interval	Calculation Method	Designed Cartridge		Total Length (m)			Average RCS (dB)		
		Dipole Length (mm)	Number	RR-178 (XN-2)	Designed Cartridge	Difference (times)	RR-178 (XN-2)	Designed Cartridge	Difference (%)
2 to 8 GHz	Van Vleck Method B	66.8246	36600	88775	34929	2,542	21.1445	21.0959	0.2298
		53.4643	51000						
		44.5562	65600						
		38.1926	79700						
		33.4195	93100						
		29.707	105200						
		26.7368	116200						
		24.3065	126000						
		22.2813	134300						
		20.5676	141200						
		19.0986	146600						
		17.8255	150800						
	Einarsson Direct Method	66.8246	34100		32537	2,728	19.8171	19.7644	0.2659
		53.4643	47500						
		44.5562	61100						
		38.1926	74200						
		33.4195	86700						
		29.707	98000						
		26.7368	108300						
		24.3065	117400						
		22.2813	125100						
		20.5676	131500						
		19.0986	136600						
		17.8255	140500						

For 8 to 14 GHz interval, only 2000 meters dipole is saved (see Table 8.12) compared to Design I and the flatness of the RCS response is very similar (see Fig. 8.26).

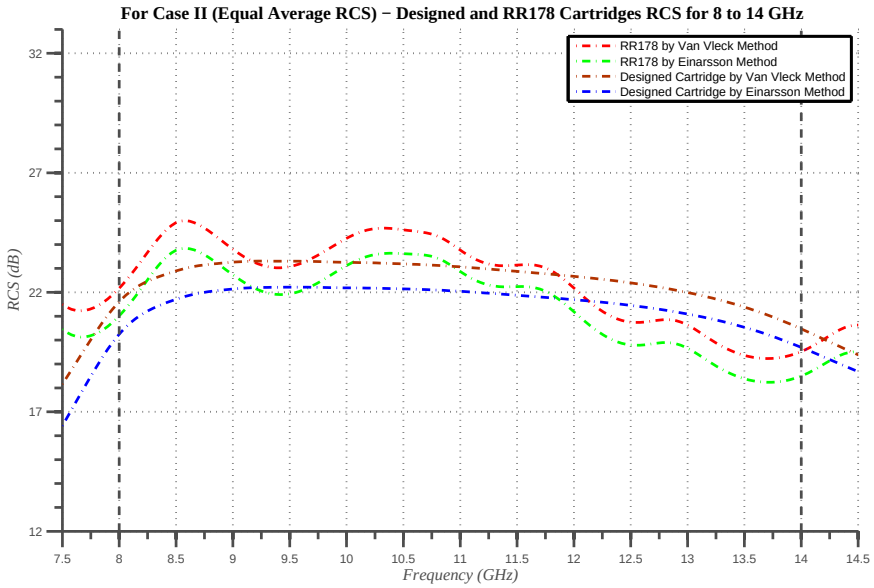

Figure 8.26: Design II: RCS (dB) vs Frequency (GHz) for *Case II* (Equal Average RCS) 8 to 14 GHz

Table 8.12: Design II - Case II: Performance Results for 8 to 14 GHz

Frequency Interval	Calculation Method	Designed Cartridge		Total Length (m)			Average RCS (dB)		
		Dipole Length (mm)	Number	RR-178 (XN-2)	Designed Cartridge	Difference (times)	RR-178 (XN-2)	Designed Cartridge	Difference (%)
8 to 14 GHz	Van Vleck Method B	17.3859	328500	88775	51393	1,727	22.5681	22.5786	-0.0465
		16.3246	333800						
		15.3854	336900						
		14.5484	337600						
		13.7977	336500						
		13.1207	333900						
		12.5071	329300						
		11.9482	323700						
		11.4372	316800						
		10.9681	309000						
		10.536	300400						
		10.1366	291100						
	Einarsson Direct Method	17.3859	337800		52843	1,680	21.5432	21.5541	-0.0506
		16.3246	343200						
		15.3854	346400						
		14.5484	347100						
		13.7977	346000						
		13.1207	343300						
		12.5071	338600						
		11.9482	332800						
		11.4372	325800						
		10.9681	317700						
		10.536	308900						
		10.1366	299300						

When the last dipole design interval is concerned, while obtaining similar average RCS value and RCS response, 1000 meters less dipole is used than Design I.

As a result, for *Case I*, Design II generally accomplishes higher RCS values while keeping total dipole length same. Moreover, for *Case II*, the designed cartridges consume a little bit less dipole length than Design I. Therefore, Design II can be accepted to be more effective and optimized.

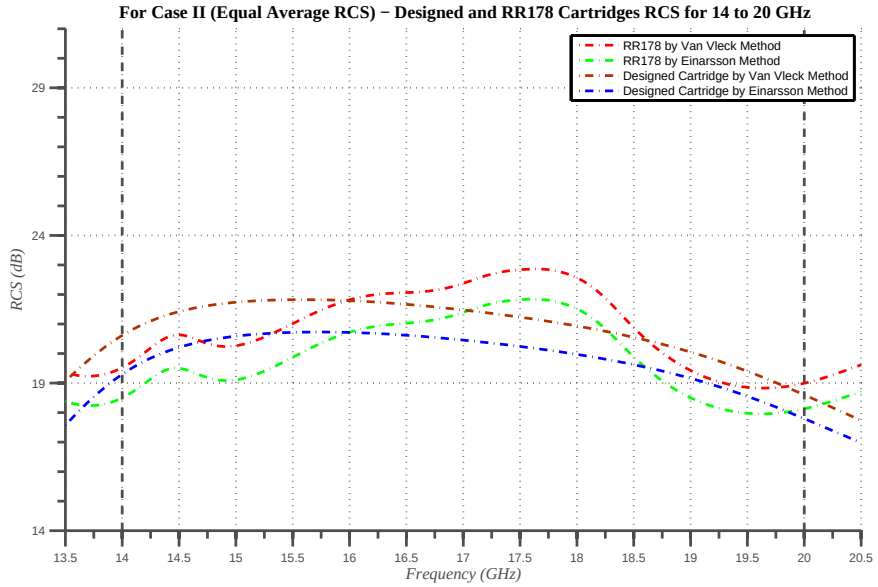

Figure 8.27: Design II: RCS (dB) vs Frequency (GHz) for *Case II* (Equal Average RCS) 14 to 20 GHz

Table 8.13: Design II - Case II: Performance Results for 14 to 20 GHz

Frequency Interval	Calculation Method	Designed Cartridge		Total Length (m)			Average RCS (dB)		
		Dipole Length (mm)	Number	RR-178 (XN-2)	Designed Cartridge	Difference (times)	RR-178 (XN-2)	Designed Cartridge	Difference (%)
14 to 20 GHz	Van Vleck Method B	9.9929	447000	88775	36653	2,422	20.944	20.9439	0.0005
		9.6329	431300						
		9.298	415400						
		8.9856	399100						
		8.6935	382600						
		8.4197	366100						
		8.1627	349500						
		7.9209	333200						
		7.6931	317000						
		7.4779	301100						
		7.2745	285600						
		7.0819	270400						
	Einarsson Direct Method	9.9929	465300		38157	2,327	19.9175	19.9173	0.0010
		9.6329	449000						
		9.298	432400						
		8.9856	415500						
		8.6935	398300						
		8.4197	381100						
		8.1627	363900						
		7.9209	346900						
		7.6931	330000						
		7.4779	313500						
		7.2745	297300						
		7.0819	281500						

8.6 Proposed Chaff Cartridges - Design III

For the third and last proposal, same different dipole lengths is used as in Design I but for six equal sub-intervals: 2-5 GHz, 5-8 GHz, 8-11 GHz, 11-14 GHz, 14-17 GHz and 17-20 GHz. Again, the same procedure is used to decide dipole lengths and numbers for each frequency sub-interval.

Performance comparison tables and related plots can be seen below for each cases and frequency intervals.

For this part, performance comparison will be done with Design II since its performance is higher than both Design I and RR-178 (XN-2).

8.6.1 *Case I*

Although, Design III provides approximately 2 dB higher average RCS value compared to Design II for 2 to 5 GHz, its response is not as flat as Design II (see Fig. 8.28) because Design II chaff cartridges has six more dipole lengths which means six more resonant peaks. Detailed RCS values with dipole lengths can be seen in Table 8.14.

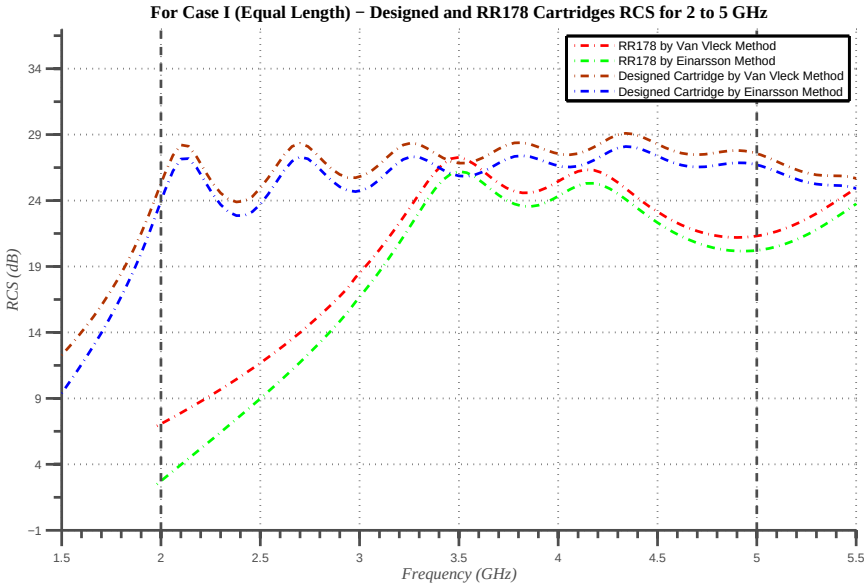

Figure 8.28: Design III: RCS (dB) vs Frequency (GHz) for *Case I* (Equal Total Dipole Length) 2 to 5 GHz

Table 8.14: Design III - Case I: Performance Results for 2 to 5 GHz

Frequency Interval	**Calculation Method**	**Designed Cartridge**		**Total Length (m)**			**Average RCS (dB)**		
		Dipole Length (mm)	**Number**	**RR-178 (XN-2)**	**Designed Cartridge**	**Difference (%)**	**RR-178 (XN-2)**	**Designed Cartridge**	**Difference (dB)**
2 to 5 GHz	Van Vleck Method B	67.1429 53.0075 43.7888	182400 260600 341100	88775	88974	-0,22	19.3516	27.1257	7.7741
	Einarsson Direct Method	37.3016 32.4885 28.7755	420200 494400 564400				17.7151	26.1171	8.4020

For 5 to 8 GHz cartridges, about 1.9 dB increase (for both calculation method) is obtained by using Design III instead of Design II. The flatness of the RCS response is acceptable as can be seen in Fig. 8.29

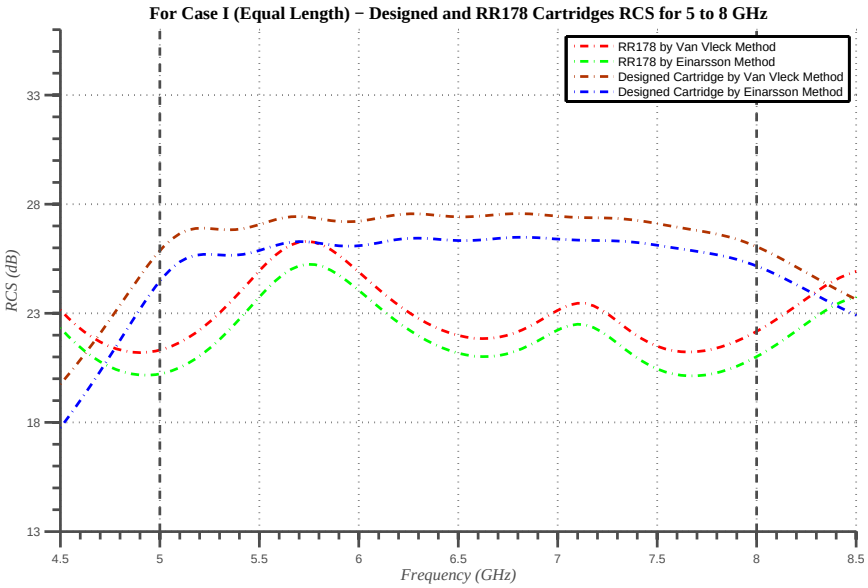

Figure 8.29: Design III: RCS (dB) vs Frequency (GHz) for *Case I* (Equal Total Dipole Length) 5 to 8 GHz

Table 8.15: Design III - Case I: Performance Results for 5 to 8 GHz

Frequency Interval	**Calculation Method**	**Designed Cartridge**		**Total Length (m)**			**Average RCS (dB)**		
		Dipole Length (mm)	**Number**	**RR-178 (XN-2)**	**Designed Cartridge**	**Difference (%)**	**RR-178 (XN-2)**	**Designed Cartridge**	**Difference (dB)**
5 to 8 GHz	Van Vleck Method B	27.6471 24.9117 22.6688	551400 608400 657600	88775	87550	1,40	22.9478	27.0624	4.1146
	Einarsson Direct Method	20.7965 19.2098 17.8481	699200 734000 762100				21.945	25.9632	4.0182

Similar to 2 to 5 GHz case, 2 dB increase in average RCS value is obtained by using Design III cartridges for 8 to 11 GHz frequency interval. The response can be seen in Fig. 8.30, and detailed performance analysis results with dipole lengths and dipole numbers can be seen in Table 8.16.

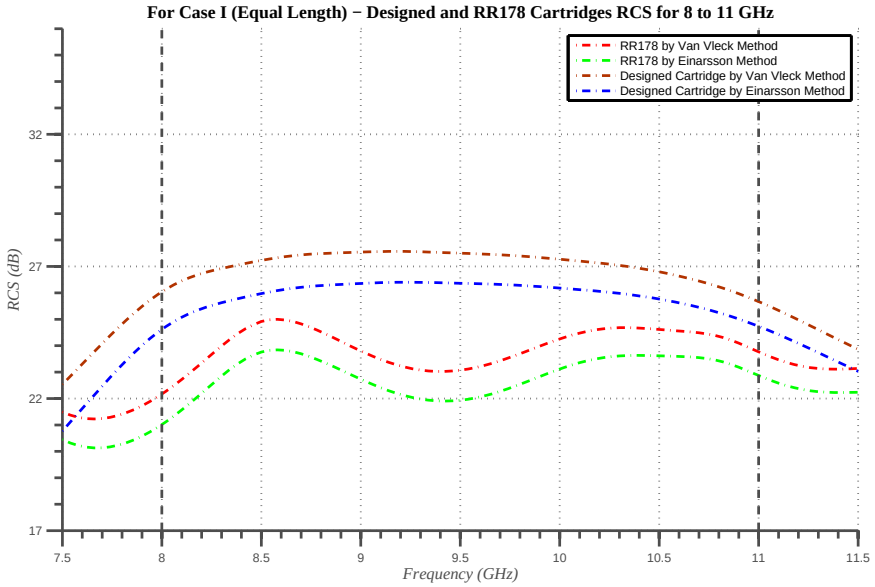

Figure 8.30: Design III: RCS (dB) vs Frequency (GHz) for *Case I* (Equal Total Dipole Length) 8 to 11 GHz

Table 8.16: Design III - Case I: Performance Results for 8 to 11 GHz

Frequency Interval	Calculation Method	Designed Cartridge		Total Length (m)			Average RCS (dB)		
		Dipole Length (mm)	Number	RR-178 (XN-2)	Designed Cartridge	Difference (%)	RR-178 (XN-2)	Designed Cartridge	Difference (dB)
8 to 11 GHz	Van Vleck Method B	17.4074 16.2818 15.2928	958500 982400 997300	88775	89172	-0,45	23.9087	26.9997	3.0910
	Einarsson Direct Method	14.4172 13.6364 12.9358	1006000 1008300 1004000				22.8234	25.8487	3.0253

For both calculation methods, approximately 1.8 dB rise (see Table 8.17) is got in average RCS response for 11 to 14 GHz interval when Design III is preferred to Design II. The RCS response is as good as Design II as can be observed in Fig. 8.31.

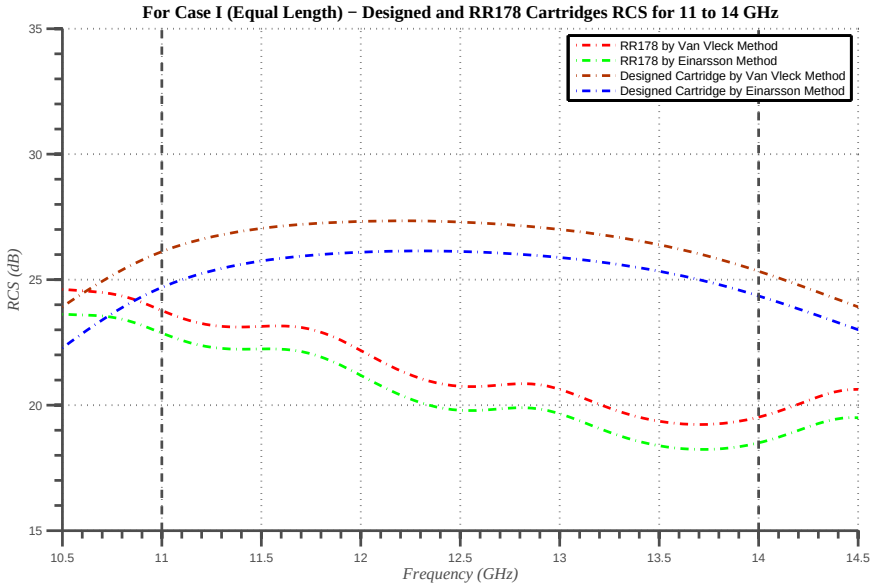

Figure 8.31: Design III: RCS (dB) vs Frequency (GHz) for *Case I* (Equal Total Dipole Length) 11 to 14 GHz

Table 8.17: Design III - Case I: Performance Results for 11 to 14 GHz

Frequency Interval	Calculation Method	Designed Cartridge		Total Length (m)			Average RCS (dB)		
		Dipole Length (mm)	Number	RR-178 (XN-2)	Designed Cartridge	Difference (%)	RR-178 (XN-2)	Designed Cartridge	Difference (dB)
11 to 14 GHz	Van Vleck Method B	12.7027 12.0926 11.5385	1352100 1338200 1317700	88775	88654	0,14	21.3068	26.7603	5.4535
	Einarsson Direct Method	11.0329 10.5697 10.1439	1292900 1263100 1230100				20.35	25.5774	5.2274

Like design for 11 to 14 GHz, close average RCS gain and RCS response is faced for 14 to 17 GHz chaff cartridge design which can be seen in Table 8.18 and Fig. 8.32.

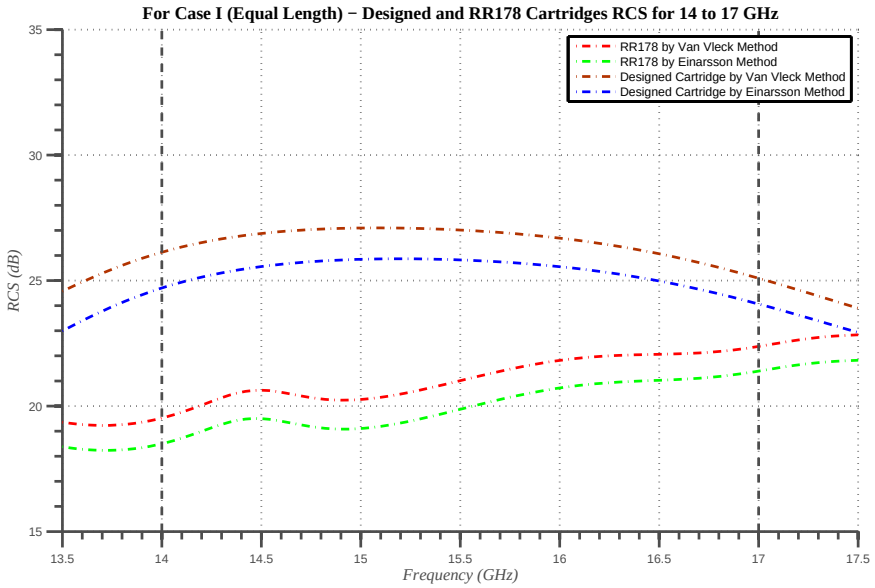

Figure 8.32: Design III: RCS (dB) vs Frequency (GHz) for *Case I* (Equal Total Dipole Length) 14 to 17 GHz

Table 8.18: Design III - Case I: Performance Results for 14 to 17 GHz

Frequency Interval	**Calculation Method**	**Designed Cartridge**		**Total Length (m)**			**Average RCS (dB)**		
		Dipole Length (mm)	**Number**	**RR-178 (XN-2)**	**Designed Cartridge**	**Difference (%)**	**RR-178 (XN-2)**	**Designed Cartridge**	**Difference (dB)**
14 to 17 GHz	Van Vleck Method B	10 9.618 9.2641	1750700 1697000 1640900	88775	88499	0,31	21.0887	26.5278	5.4391
	Einarsson Direct Method	8.9354 8.6291 8.3432	1582200 1522800 1461200				20.0014	25.3236	5.3222

The lowest RCS gain is observed for 17 to 20 GHz chaff cartridge Design III with an increase of 1.5 dB compared to Design II. The response is good enough like in Fig. 8.33.

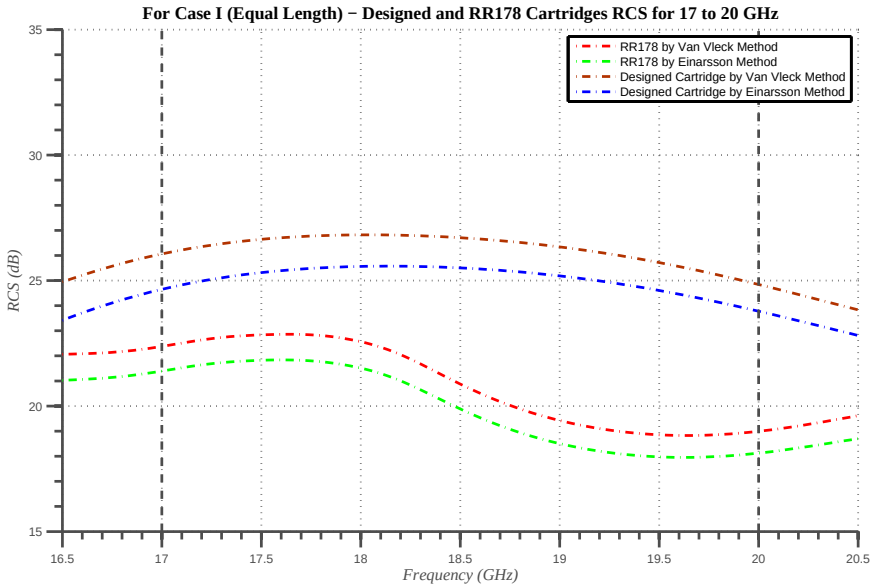

Figure 8.33: Design III: RCS (dB) vs Frequency (GHz) for *Case I* (Equal Total Dipole Length) 17 to 20 GHz

Table 8.19: Design III - Case I: Performance Results for 17 to 20 GHz

Frequency Interval	Calculation Method	Designed Cartridge		Total Length (m)			Average RCS (dB)		
		Dipole Length (mm)	Number	RR-178 (XN-2)	Designed Cartridge	Difference (%)	RR-178 (XN-2)	Designed Cartridge	Difference (dB)
17 to 20 GHz	Van Vleck Method B	8.2456 7.9841 7.7387	2143400 2051400 1959300	88775	88175	0,68	20.8875	26.2538	5.3663
	Einarsson Direct Method	7.508 7.2906 7.0854	1868700 1777800 1689200				19.9246	25.0357	5.1111

8.6.2 *Case II*

There is a huge gain in terms of used total dipole length compared to Design II and RR-178 (XN-2) for 2 to 5 GHz cartridge Design III. For Design II, it is about 2 times and for commercial one it is about 5.99 times (Van Vleck Method

B) / 6.93 times (Einarsson's Direct Method), as can be examined in Table 8.20. Although the RCS response for Design III (see Fig. 8.34) is better than RR-178 (XN-2), flatness of Design II is the best.

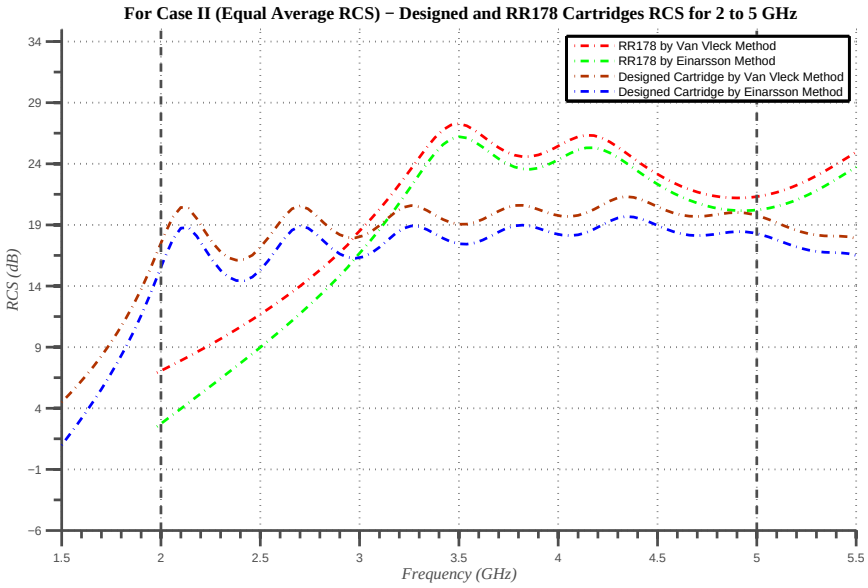

Figure 8.34: Design III: RCS (dB) vs Frequency (GHz) for *Case II* (Equal Average RCS) 2 to 5 GHz

Table 8.20: Design III - Case II: Performance Results for 2 to 5 GHz

Frequency Interval	Calculation Method	Designed Cartridge		Total Length (m)			Average RCS (dB)		
		Dipole Length (mm)	Number	RR-178 (XN-2)	Designed Cartridge	Difference (times)	RR-178 (XN-2)	Designed Cartridge	Difference (%)
2 to 5 GHz	Van Vleck Method B	67.1429	30400	88775	14812	5.993	19.3516	19.3399	0.0605
		53.0075	43400						
		43.7888	56800						
		37.3016	69900						
		32.4885	82300						
		28.7755	93900						
	Einarsson Direct Method	67.1429	26300		12806	6.932	17.7151	17.6999	0.0858
		53.0075	37500						
		43.7888	49100						
		37.3016	60500						
		32.4885	71100						
		28.7755	81200						

For 5 to 8 GHz frequency interval, Design III and Design II provide very similar RCS response while using close total dipole lengths. The results can be seen in Fig. 8.35 and Table 8.21.

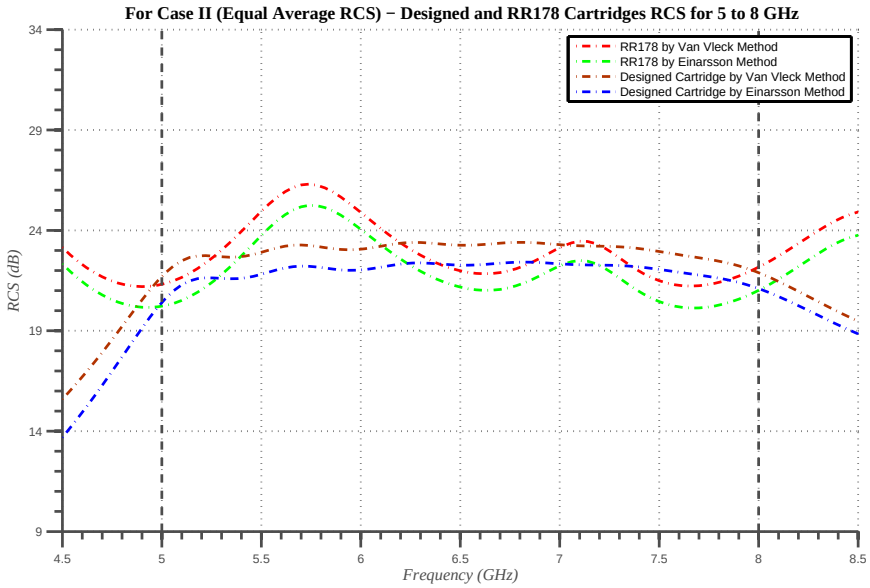

Figure 8.35: Design III: RCS (dB) vs Frequency (GHz) for *Case II* (Equal Average RCS) 5 to 8 GHz

Table 8.21: Design III - Case II: Performance Results for 5 to 8 GHz

Frequency Interval	Calculation Method	Designed Cartridge		Total Length (m)			Average RCS (dB)		
		Dipole Length (mm)	Number	RR-178 (XN-2)	Designed Cartridge	Difference (times)	RR-178 (XN-2)	Designed Cartridge	Difference (%)
5 to 8 GHz	Van Vleck Method B	27.6471 24.9117 22.6688 20.7965 19.2098 17.8481	211500 233400 252200 268200 281500 292300	88775	33580	2,644	22.9478	22.9008	0.2048
	Einarsson Direct Method	27.6471 24.9117 22.6688 20.7965 19.2098 17.8481	216200 238600 257900 274200 287800 298900		34333	2,586	21.945	21.8977	0.2155

Saved dipole length for 8 to 11 GHz cartridges is about 7000 meters for both calculation methods when Design III is used instead of Design II. The RCS response for 8 to 11 GHz with Design III can be seen in Fig. 8.36.

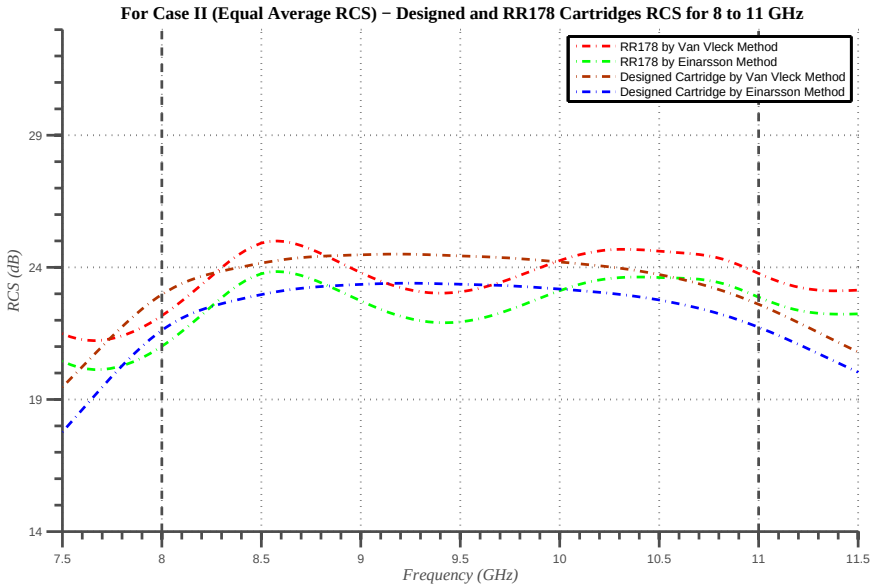

Figure 8.36: Design III: RCS (dB) vs Frequency (GHz) for *Case II* (Equal Average RCS) 8 to 11 GHz

Table 8.22: Design III - Case II: Performance Results for 8 to 11 GHz

Frequency Interval	Calculation Method	Designed Cartridge		Total Length (m)			Average RCS (dB)		
		Dipole Length (mm)	Number	RR-178 (XN-2)	Designed Cartridge	Difference (times)	RR-178 (XN-2)	Designed Cartridge	Difference (%)
8 to 11 GHz	Van Vleck Method B	17.4074	472900	88775	43998	2.018	23.9087	23.9318	-0.0966
		16.2818	484700						
		15.2928	492100						
		14.4172	496400						
		13.6364	497500						
		12.9358	495400						
	Einarsson Direct Method	17.4074	480200		44670	1.987	22.8234	22.8466	-0.1017
		16.2818	492100						
		15.2928	499600						
		14.4172	504000						
		13.6364	505100						
		12.9358	502900						

For 11 to 14 GHz frequency interval, new chaff cartridge for Design III enables to save about 26000 meters more dipole length than Design II, which is a decrease of 3.51 times (Van Vleck's Method B) / 3.34 times (Einarsson's Direct Method) compared to RR-178 (XN-2). The performance comparison table can be in Table 8.23 and the RCS response for the concerned frequency interval is given in Fig. 8.37.

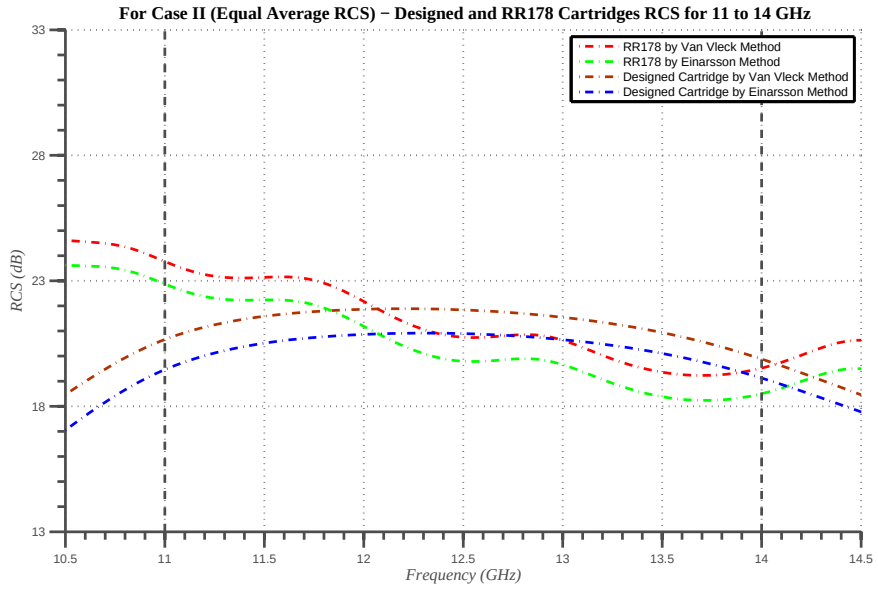

Figure 8.37: Design III: RCS (dB) vs Frequency (GHz) for *Case II* (Equal Average RCS) 11 to 14 GHz

Table 8.23: Design III - Case II: Performance Results for 11 to 14 GHz

Frequency Interval	Calculation Method	Designed Cartridge		Total Length (m)			Average RCS (dB)		
		Dipole Length (mm)	Number	RR-178 (XN-2)	Designed Cartridge	Difference (times)	RR-178 (XN-2)	Designed Cartridge	Difference (%)
11 to 14 GHz	Van Vleck Method B	12.7027	385000	88775	25247	3,516	21.3068	21.3054	0.0066
		12.0926	381100						
		11.5385	375300						
		11.0329	368200						
		10.5697	359700						
		10.1439	350300						
	Einarsson Direct Method	12.7027	405600		26596	3,338	20.35	20.3486	0.0069
		12.0926	401500						
		11.5385	395300						
		11.0329	387900						
		10.5697	378900						
		10.1439	369000						

The decrease in total dipole length when Design III is preferred to Design II, is approximately 11000 meters while getting close average RCS values for interval 14 to 17 GHz. The flatness of the response is acceptable as can be in Fig. 8.38.

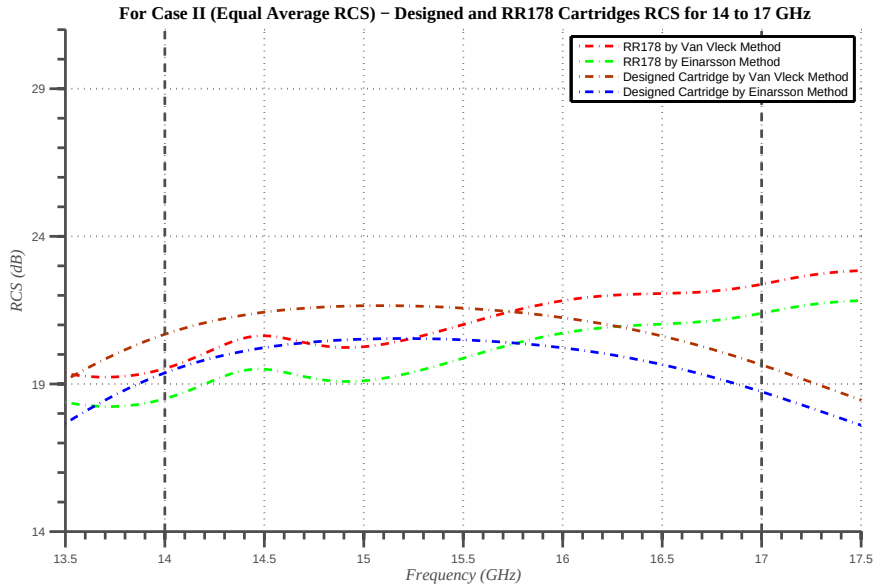

Figure 8.38: Design III: RCS (dB) vs Frequency (GHz) for *Case II* (Equal Average RCS) 14 to 17 GHz

Table 8.24: Design III - Case II: Performance Results for 14 to 17 GHz

Frequency Interval	Calculation Method	Designed Cartridge		Total Length (m)			Average RCS (dB)		
		Dipole Length (mm)	Number	RR-178 (XN-2)	Designed Cartridge	Difference (times)	RR-178 (XN-2)	Designed Cartridge	Difference (%)
14 to 17 GHz	Van Vleck Method B	10	499500	88775	25250	3,516	21.0887	21.0811	0.0360
		9.618	484200						
		9.2641	468200						
		8.9354	451400						
		8.6291	434500						
		8.3432	416900						
	Einarsson Direct Method	10	513100		25938	3,423	20.0014	19.9935	0.0395
		9.618	497400						
		9.2641	480900						
		8.9354	463700						
		8.6291	446300						
		8.3432	428300						

Similar to 14 to 17 GHz frequency interval, decrease in total dipole length is about 11000 meters for 17 to 20 GHz. The comparison results can be seen Table 8.25 and the corresponding RCS trend can be seen in Fig. 8.39.

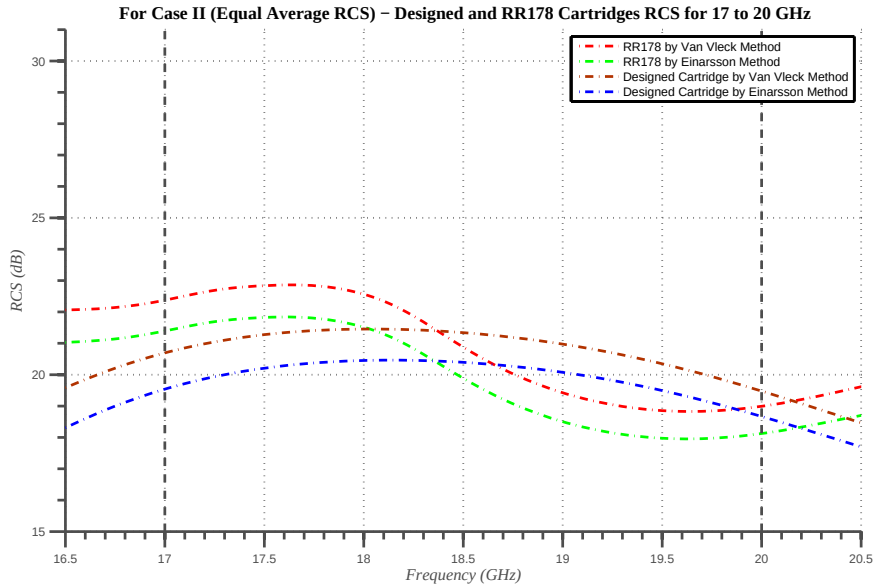

Figure 8.39: Design III: RCS (dB) vs Frequency (GHz) for *Case II* (Equal Average RCS) 17 to 20 GHz

Table 8.25: Design III - Case II: Performance Results for 17 to 20 GHz

Frequency Interval	Calculation Method	Designed Cartridge		Total Length (m)			Average RCS (dB)		
		Dipole Length (mm)	Number	RR-178 (XN-2)	Designed Cartridge	Difference (times)	RR-178 (XN-2)	Designed Cartridge	Difference (%)
17 to 20 GHz	Van Vleck Method B	8.2456	622900	88775	25624	3,465	20.8875	20.8869	0.0029
		7.9841	596200						
		7.7387	569400						
		7.508	543000						
		7.2906	516600						
		7.0854	490900						
	Einarsson Direct Method	8.2456	660600		27175	3,267	19.9246	19.9241	0.0025
		7.9841	632300						
		7.7387	603900						
		7.508	575900						
		7.2906	547900						
		7.0854	520600						

As stated before, performance of Design II is higher than the performances of both Design I and RR-178 (XN-2) for both cases. On the other hand, Design III is more effective than Design II while providing average mean RCS values by continuing same total dipole length as discussed in *Case I*. Furthermore, for *Case*

II, Design III provides same average RCS although it uses less total dipole length compared to Design II. In conclusion, the most effective and optimized design can be accepted as Design III.

8.7 Operational Scenarios

In this part, three different scenarios will be handled in such a way that performance and effectiveness of the designed chaff cartridges can be evaluated. Only Van Vleck's Method B is used for RCS calculation since it is faster than Einarsson's Direct Method and the used method does not affect the comparison results dramatically.

8.7.1 Scenario I

In this scenario, assume that chaff cartridges are designed for *Case II*, and loaded to four helicopters. Note that for *Case II*, designed cartridges provide same average RCS value compared to RR-178 (XN-2) for a concerned interval. Each of these helicopters are loaded with cartridges of Design I, Design II, Design III and RR-178 (XN-2). The helicopters go to a mission where different radars operate. Operating frequencies of these radars are assumed to be 3.7 GHz, 7.9 GHz, 10.6 GHz, 12.9 GHz, 16.2 GHz, 18.1 GHz which somewhat cover 2 to 20 GHz interval. Then for each radar, each of four helicopters only dispense one chaff cartridge that is the most effective one for the concerned radar frequency. For instance, helicopter that is loaded with Design I and Design II dispense a chaff cartridge that is designed for 2 to 8 GHz cartridge for a target that operates at 7.9 GHz. On the other hand, the helicopter that is loaded with Design III dispenses a 5 to 8 GHz cartridge for the same frequency. As can be predicted, RR-178 (XN-2) cartridges are same for all frequencies, therefore, the corresponding helicopter dispenses always the same cartridge. When all of these helicopters complete the mission, each one dispenses six chaff cartridges and below Table 8.26 is generated.

Table 8.26: Scenario I: Results

Threat Frequency (GHz)	Commercial Cartridge Total Dipole Length (m)	Design I			Design II			Design III		
		Frequency Interval (GHz)	Total Dipole Length (m)	Gain (m)	Frequency Interval (GHz)	Total Dipole Length (m)	Gain (m)	Frequency Interval (GHz)	Total Dipole Length (m)	Gain (m)
3.7	88775	2 to 8	39601	49174	2 to 8	34929	53846	2 to 5	14812	73963
7.9	88775	2 to 8	39601	49174	2 to 8	34929	53846	5 to 8	33580	55195
10.6	88775	8 to 14	53125	35650	8 to 14	51393	37382	8 to 11	43998	44777
12.9	88775	8 to 14	53125	35650	8 to 14	51393	37382	11 to 14	25247	63528
16.2	88775	14 to 20	37339	51436	14 to 20	36653	52122	14 to 17	25250	63525
18.1	88775	14 to 20	37339	51436	14 to 20	36653	52122	17 to 20	25624	63151
Total (m)	532650	-	260130	272520	-	245950	286700	-	168511	364139
Average (m)	88775	-	43355	45420	-	40992	47783	-	28085	60690

In this table one can easily follow how much dipole length is gained for each radar frequency by using designed chaff cartridges. Furthermore, total dipole lengths of the dispensed chaff cartridges and their names can be seen on the table for concerned operating frequency.

If the helicopter is loaded by RR-178 (XN-2), the six dispensed chaff cartridges spends totally 532650 meters aluminium glass dipoles. On the other hand, the spent dipole lengths become 260130 meters, 245950 meters and 168511 meters for Design I, Design II and Design III, respectively. Especially by using Design III, 364139 meters of total dipole length is preserved while getting same average RCS value compared to RR-178 (XN-2) chaff cartridges. Close values are reached for Design I and Design II designs, as well.

When we look at the average total dipole length for these six chaff cartridges, it can be noticed that Design III has the lowest value with 28085 meters which is 3.16 times smaller than the total dipole length of RR-178 (XN-2). One can easily conclude that, the cartridge volume of RR-178 (XN-2) can be minimized at least three times with use of Design III. This volume reduction can enable helicopter to carry 3 times more chaff cartridges.

Note that, helicopters that are loaded by designed chaff cartridges must have an RWR System that can find the operating frequency of the radar and transmit this information to Dispensing System which should be able to dispense the most effective chaff cartridge by evaluating the frequency of the radar. On the other hand, the helicopter that has RR-178 (XN-2) cartridges should have RWR system that can warn the pilot or Dispensing System so that they can trigger to dispense

any of the chaff cartridges.

8.7.2 Scenario II

This scenario is same with Scenario I with an exception. In the first scenario, chaff cartridges are designed for *Case II*, for this scenario, they are designed for *Case I* in which same total dipole length is used for each cartridge, therefore, an increase in provided RCS value for concerned frequency interval is observed for designed cartridges. The results can be seen in Table 8.27.

Table 8.27: Scenario II: Results

Threat Frequency (GHz)	Commercial Cartridge Provided RCS (dB)	Design I			Design II			Design III		
		Frequency Interval (GHz)	Provided RCS (dB)	Gain (dB)	Frequency Interval (GHz)	Provided RCS (dB)	Gain (dB)	Frequency Interval (GHz)	Provided RCS (dB)	Gain (dB)
3.7	25.32	2 to 8	21.99	-3.33	2 to 8	25.56	0.24	2 to 5	27.92	2.60
7.9	21.72	2 to 8	25.90	4.18	2 to 8	24.93	3.21	5 to 8	26.39	4.67
10.6	24.54	8 to 14	25.18	0.64	8 to 14	25.52	0.98	8 to 11	26.60	2.06
12.9	20.81	8 to 14	24.91	4.10	8 to 14	24.44	3.63	11 to 14	27.08	6.27
16.2	21.99	14 to 20	25.12	3.13	14 to 20	25.55	3.56	14 to 17	26.46	4.47
18.1	22.35	14 to 20	24.85	2.50	14 to 20	24.66	2.31	17 to 20	26.82	4.47
Total (dB)	136.73	-	147.95	11.22	-	150.66	13.93	-	161.27	24.54
Average (dB)	22.79	-	24.66	1.87	-	25.11	2.32	-	26.88	4.09

In this table, one can observe the provided RCS value (dB) for specified frequencies by using each design. Moreover, increase or decrease in RCS value compared to the RCS of RR-178 (XN-2) cartridge can be observed. In addition to that, for six chaff cartridges, average provided RCS and total provided RCS can be reached from the table.

By examining this table, it can be asserted that Design III performance is higher compared to RR-178 (XN-2), Design I and Design II. Smallest total RCS value is provided by RR-178 (XN-2) cartridges. Design III supplies 4.09 dB higher RCS than RR-178 (XN-2) cartridges in average. This value means that instead of dispensing two RR-178 (XN-2) cartridges, one Design III cartridge can be enough to get higher RCS value for specified frequency interval.

Again note that, requirements of designed chaff cartridges and RR-178 (XN-2) cartridge for RWR and Dispensing Systems are same as in Scenario I.

8.7.3 Scenario III

This scenario is different than the other two scenarios. For this scenario, assume that cartridges are designed according to Design III and *Case II*. A helicopter is loaded with all types of cartridges and during a mission only 2 to 5 GHz and 5 to 8 GHz cartridges left and the other ones were consumed. Suddenly, RWR system gives a warning about a threat radar that operates between 11 to 14 GHz. In this case, the Dispensing System should have the ability to calculate and decide how many of remaining cartridges should be dispensed to get same average RCS value that can be provided by 11 to 14 GHz cartridge. To do that, the system should know the response of the cartridges for all frequencies. For this case, if Dispensing System dispenses two 2 to 5 GHz and two 5 to 8 GHz cartridges, Fig. 8.40 can be got.

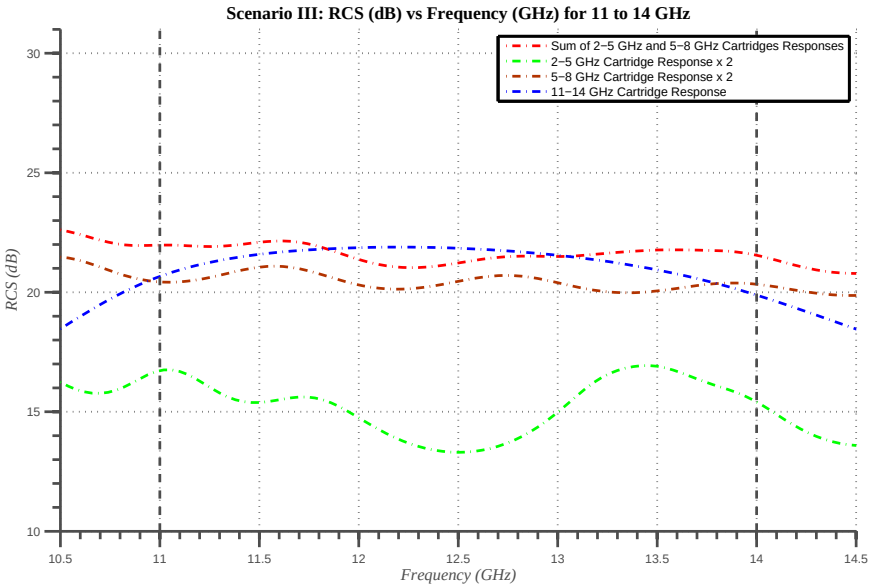

Figure 8.40: Scenario III: RCS (dB) vs Frequency (GHz) for 11 to 14 GHz

In this figure, one can notice that a flat response for RCS between 11 to 14 GHz is obtained by sum of the responses of two different cartridges. Average total RCS for this dispensing regime is 21.64 dB and total dipole length dispensed is 96786 meters. If a 11 to 14 GHz cartridge was dispensed, 21.31 dB average RCS

value would be obtained by dispensing 25247 meters dipoles. If it is compared with RR-178 (XN-2) cartridges, 88775 meters dipoles should be dispensed to get the same average RCS response. With these result, compared to RR-178 (XN-2), this dispensing regime is effective with an % 9 increase of used dipole length. However, if it is compared with dispensing a 11 to 14 GHz cartridge, to get the same average RCS value, 4 times higher total dipole length should be spent.

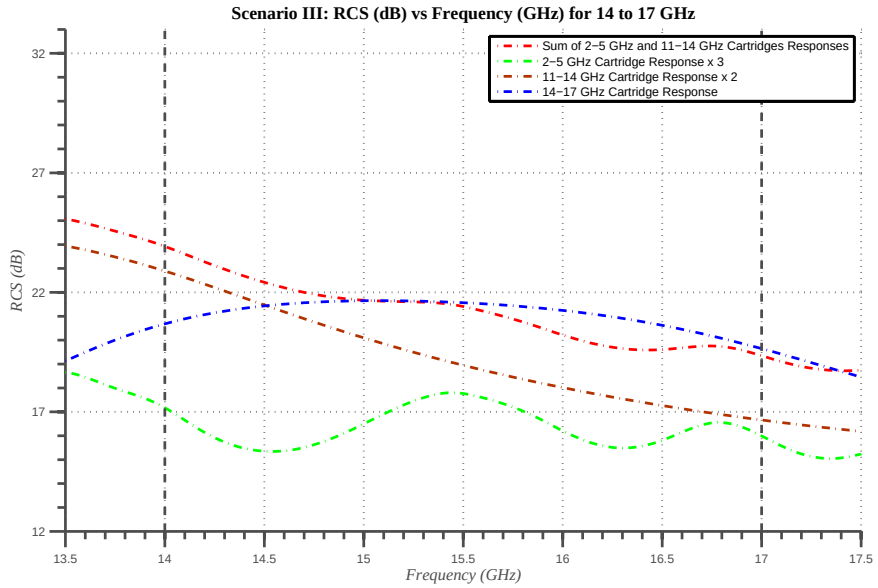

Figure 8.41: Scenario III: RCS (dB) vs Frequency (GHz) for 14 to 17 GHz

This scenario can be applied to other situations. For example, if helicopter does not have any cartridge of 14 to 17 GHz, the Dispensing System can decide to dispense two 11 to 14 GHz and three 2 to 5 GHz cartridges to get the similar average RCS response for concerned frequency interval as in Fig. 8.41. Average RCS that is got owing to this regime is 21.22 dB for frequency interval 14 to 17 GHz. If the specified cartridge was used, the average RCS would be 0.14 dB lower than the average RCS that is provided by this dispensing regime. Since the total dipole length dispense by this regime is 94930 meters, same discussion in first situation can be done in terms of total dipole length spent.

As a result, the Dispensing System must be capable of deciding different dispensing regimes by concerning threat frequency and remaining chaff cartridges.

These regimes should provide similar RCS response as above situations even if some of the cartridge types are consumed.

8.8 RWR and Dispensing System Properties

At the end of Section 8.6 and Section 8.7, it can be concluded that using Design III is more effective than RR-178 (XN-2) and other designs that I proposed. However, as stated before, loading helicopter or aircraft with these cartridges is not enough, RWR and Dispensing Systems should have some extra capabilities so as to use them as effective as possible. The aircraft / helicopter / ship should have below properties to use Design III effectively:

- RWR System should be able to measure the frequency of the received signal,
- RWR System should be able to transmit this frequency information to the Dispensing System,
- Dispensing System should be able to recognize the loaded chaff cartridges in terms of their designed frequency interval,
- Dispensing System should be able to manually or automatically dispense chaff cartridges according the received frequency information from RWR System,
- All frequency response of the chaff cartridges should be uploaded to Dispensing System,
- Dispensing System should be able to process these uploaded RCS responses to decide a chaff regime as described in Scenario III when a chaff cartridge is finished,
- Chaff Magazines should be designed to be loaded with smaller cartridges, *As stated in Scenario I, the volume of the cartridges can be reduced at least three times, therefore, if today's maganizes are loaded with 30 cartridges, new designed one should be able to be loaded with 90 smaller cartridges.*

- The dimensions of the Design III cartridges should be optimized in such a way that for all specified frequency intervals chaff cartridges can provide enough RCS while having same cartridge size,
- By using Mission Data File (MDF) of RWR System, numbers of loaded chaff cartridges should be optimized for the mission,
  In MDF, the frequencies of the threat system is generally written. By looking at these frequencies, number of different chaff cartridges should be optimized. For example, if the mission does not include any threat radar that operates between 5 to 8 GHz, the chaff cartridge that is designed for this frequency interval may not be loaded. For another case, if threats are predominantly operating between 9 to 13 GHz for a specific mission, increasing numbers of 8 to 11 GHz and 11 to 14 GHz chaff cartridges can be a good idea.

Chapter 9

CONCLUSION

For perfectly conducting thin wires, different methods are implemented to calculate backscattering cross section. These are Van Vleck's Method A, Van Vleck's Method B [1], Tai's Variational Method [2] and Einarsson's Direct Method [3]. According to comparison of these methods for different wire lengths, it is asserted that results of Van Vleck's Method A deviate from the results of other three methods much more than expected. Moreover, as θ goes from 80 to 100 degrees, Tai's Variational Method fails to follow the RCS trend that remaining two methods give. Therefore, Van Vleck's Method B and Einarsson's Direct Method are preferred for simulation about chaff RCS calculation. Although, in some literature [3, 30], it is stated that Van Vleck's and Tai's methods do not give correct results when the wire length is greater than two wavelengths, the simulations prove the opposite for particularly Van Vleck's Method B [1] and Tai's Direct Method [2].

In addition to dipole RCS evaluations, chaff RCS simulations are employed in this thesis. RCS response of Butters' chaff cartridge is calculated by selected two methods and the results are as in Butters' work with small amplitude deviations.

As known, finding the lengths and number of the dipoles of commercial chaff cartridges is not easy by only using open sources. Only some of them are found and their RCS values are calculated for concerned frequency interval, 2 to 20

GHz. By evaluating these RCS plots, RR-178 (XN-2) cartridge is selected due to its relatively flat RCS response so as to compare its performance and effectiveness with the designed chaff cartridges.

For content of chaff cartridges, three different designs are proposed and two cases are handled for each designs. For the first case, the total dipole length in the cartridges is kept same and increase in RCS value is evaluated. For the second case, average RCS value for a concerned sub-frequency interval is kept equal and decrease in total dipole length is discussed. For the first and second designs, 2 to 20 GHz frequency interval is divided into three equal sub-frequency intervals. The difference between these designs are the number of used dipole lengths. For the first one, six different dipole lengths and for the second one, twelve different dipole lengths are used. For the last design, the number of different dipole lengths is same with the first design; but six sub-frequency intervals are used instead of three. To propose chaff cartridges for these designs, a procedure is described in such a way that one can get dipole lengths and numbers for concerned frequency interval.

The best results among these three designs are observed in Design III when its compared with the RR-178 (XN-2) commercial chaff cartridge. For *Case I*, from 2 to 20 GHz frequency interval, 5.2 dB average RCS gain is observed while keeping total dipole length in the cartridges equal with RR-178 (XN-2) chaff cartridge. For *Case II* and for the same interval, instead of 88775 meters dipole that is used by RR-178 (XN-2) chaff cartridge, 25300 meters dipole is used in Design III while getting equal average RCS value .

After the most effective design is decided, three different practical scenarios are described so as to demonstrate the effectiveness and performance of the proposed designs. For the first two scenearios, specific six radar frequencies are concerned for comparison purpose. By using Design III in the first scenario, it is concluded that the volume of the designed cartridges can be reduced to one third of the RR-178 (XN-2) chaff cartridges if one wants to provide same average RCS values. According to second scenario, by using Design III, in average 4 dB increase in RCS value is got when the cartridge size is not changed compared to commercial

one. Moreover, for the last scenario, the ability that Dispensing System should have to cover up the possible system deficiency is described. The system should be able to determine a dispensing regime by using available cartridges to provide similar RCS response if one of the cartridge type is completely consumed.

To use these cartridges efficiently, it is asserted that the most important property is to have a RWR system that can measure the frequency of the received signal and transmit this information to Dispensing System. This system should be able to dispense designed chaff cartridges according to received frequency information so that an increase in RCS value or a reduction in total dipole length is obtained compared to commercial systems.

As a future work, different commercial chaff cartridges can be used while comparing the performance of the designed ones. Moreover, different chaff cartridge designs can be proposed and more effective designs can be published, if found. According to indications, it is expected to get more effective chaff cartridges as the sub-frequency intervals get smaller and the number of different dipole lengths in each interval gets higher. Additionally, a MATLAB GUI can be implement so that users can decide the parameters and the RCS value for decided parameters can be plotted interactively. Furthermore, if possible, the designed chaff cartridges can be manufactured and their RCS measurements can be done by using special RCS measurement systems in order to understand the feasibility of the designs and to compare the theoretical work with real-life.

Bibliography

[1] J. H. V. Vleck, F. Bloch, and M. Hammermesh, "Theory of Radar Reflections from Wires and Thin Metallic Strips," *Journal of Applied Physics*, vol. 18, pp. 274–94, 1946.

[2] C. T. Tai, "Electromagnetic Backscattering from Cylindrical Wires," *Journal of Applied Physics*, vol. 23, pp. 909–916, 1952.

[3] O. Einarsson, *Electromagnetic and Acoustic Scattering by Simple Shapes*, ch. The Wire, pp. 472–502. Hemisphere Publishing Company, 1969.

[4] D. D. Ducata, G. Foglia, D. Pistoia, and A. Sindico, "A Comprehensive Model for Chaff Characterization," in *European Radar Conference, 2009. EuRAD 2009*, (Rome), pp. 485 – 488, IEEE, IEEE, Sept 2009.

[5] E. F. Knott, D. J. Lewinski, and S. D. Hunt, "Chaff Theoretical/Analytical Characterization and Validation Program," report, Georgia Institude Of Technology, Atlanda, Georgia, September 1981. Also DTIC Document ADA105893.

[6] R. V. Jones, *Most Secret War*. London: Hamish Hamilton, 1978.

[7] B. C. F. Butters, "Chaff," *IEE Proceedings of Communications, Radar and Signal Processing*, vol. 129, pp. 197–201, June 1982.

[8] P. Pouliguen, "Complete Modelling of Electromagnetic Scattering by a Cloud of Dipoles," *Annals of Telecommunications*, vol. 48, pp. 305–318, 1993.

[9] N. Manji, A. Kitsikis, A. Louie, and S. Kashyap, "A Tool for Studying Monostatic and Bistatic Chaff Cloud Radar Cross Section For Naval Electronic Warfare Simulations," vol. 34, (Ottawa, Ontario, Canada), pp. 158 – 168, Society for Modeling and Simulation International in Simulation Series, 2002.

[10] K. G. Dedrick, A. R. Hessing, and G. L. Johnson., "Bistatic Radar Scattering by Randomly Oriented Wires," *IEEE Transactions on Antennas and Propagation*, vol. 26, pp. 420 – 426, May 1978.

[11] Z. Zaharis and J. Sahalos, "On the Electromagnetic Scattering of a Chaff Cloud," *Electrical Engineering - Springer*, vol. 85, pp. 129–135, July 2003.

[12] S. A. Vakin and L. N. Shustov, *Principles of Jamming and Electronic Reconnaissance*, vol. I. Air Force Systems Commend Foreign Technology Division, May 1969. Also DTIC Document AD692642.

[13] P. Pouliguen, "Etude des proprits lectromagntiques de quelques cibles radar diffuses artificielles," *Thse de troisime cycle de l'Universit de Rennes*, October 1990.

[14] R. Wickliff and R. Garbacz, "The Average Backscattering Cross Section of Clouds of Randomized Resonant Dipoles," *IEEE Transactions on Antennas and Propagation*, vol. 22, pp. 503–505, May 1974.

[15] T.J.Garbacz, V. Cable, R. Wickliff, R. Caldecott, J. Buk, D. Lam, K. Demarest, and A. Yee, "Advanced Radar Reflector Studies," Report AFAL-TR-75-219, Electroscience Laboratory, Ohio State University, Columbus, Dec 1975. Also DTIC Document ADB013005.

[16] D. D. King and S. H. Dike, "The Absorption Gain and Backscattering Cross Section of the Cylindrical Antenna," *Proceedings of the IRE*, vol. 40, pp. 853–860, 1952.

[17] K. Lindroth, "Reflection of Electromagnetic Waves from Thin Metal Strips," *Trans. Royal Inst. Tech. Stockholm*, vol. 91, 1955.

[18] Y. Y. Hu, "Backscattering Cross Section of a Center-loaded Cylindrical Antenna," *IRE Transactions on Antennas and Propagation*, vol. AP-6, pp. 140–148, 1958.

[19] P. Y. Ufimtsev, "Diffraction of Plane Electromagnetic Waves by a Thin Cylindrical Conductor," *Radio Eng. Electron Phys.*, vol. 7, pp. 241 – 249, 1962.

[20] A. T. Fialkovskii, "Scattering of Plane Electromagnetic by a Thin Cylindrical Conductor of Finite Length," *Soviet Phys. - Tech. Phys.*, vol. 11, pp. 1300–1304, 1967.

[21] O. Einarsson, "Electromagnetic scattering by a thin finite wire," *Acta polytechnica Scandinavica - Electrical engineering series*, vol. 23, 1969.

[22] E. Hallén, "Theoretical Investigations into the Transmitting and Receiving Qualities of Antennas," *Nova Acta Regiae Soc. Sci. (Upsula)*, vol. 11, p. 3, Nov 1938.

[23] M. C. Gray, "A Modification of Hallén's Solution of the Antenna Problem," *Journal of Applied Physics*, vol. 15, no. 61, 1944.

[24] R. King and D. Middleton, "The Cylindrical Antenna: Current and Impedance," *Quarterly of Applied Mathematics*, vol. 3, pp. 302–335, 1946.

[25] P. Z. Peebles, "Bistatic Radar Cross Sections of Chaff," *IEEE Transactions on Aerospace and Electronic Systems*, vol. AES-20, pp. 128 – 140, March 1984.

[26] F. Bloch and M. Hamermesh Report 411-TM125, Radio Research Laboratory.

[27] fas.org Military Analysis Network, "AN/APR-39 Radar Warning Receiver," Reached on 08.07.2015. Available online at `http://fas.org/man/dod-101/sys/ac/equip/an-apr-39.htm`.

[28] SAAB, "BOW Advance Radar Warning System," Reached on 08.07.2015. Available online at `http://saab.com/globalassets/`

commercial/air/electronic-warfare/radar-warning-receivers/bow/bow-product-sheet.pdf.

[29] Indra, "ALR-400 Radar Warning Receiver," Reached on 08.07.2015. Available online at http://www.indracompany.com/sites/default/files/ALR-400%20RADAR%20WARNING%20RECEIVER.pdf.

[30] M. T. Tavis, "Van Vleck Revisited - The RCS (Radar Cross Section) of Thin Wires," tech. report, Aerospace Corporation, July 1973. Also DTIC Document AD0768336.

[31] E. Siegel and J. Labus, "Scheinwiderstand von Antennen," *Z. Hochfrequenztechnik und Elektroakustik*, vol. 43, pp. 166–172, 1934.

[32] R. King and C. W. Harrison, "The Receiving Antenna," *PROC. l.R.E.*, vol. 32, pp. 18–32, January 1944.

[33] R. King and C. Harrison, "Distribution of Current along a Symmetrical Center-driven Antenna," *Proceedings of the Institute of Radio Engineers*, vol. 31, p. 548, October 1943.

[34] J. Schwinger, "A Variational Principle for Scattering Problems," *Physical Review*, vol. 72, p. 742, 1947.

[35] C. T. Tai, "A Study of the E.M.F. Method," *Journal of Applied Physics*, vol. 20, no. 7, pp. 717–723, 1949.

[36] R. King, "Graphical Representation of the Characteristics of Cylindrical Antennas," Technical Report 20, Cruft Lab., Harvard University, Cambridge, Massachusetts, 1947.

[37] O. Einarsson, *The Current Distribution on Cylindrical Antennas of Arbitrary Length*, vol. 216. Stockholm: Trans. Roy. Inst. Technology, 1963.

[38] E. Hallén, *Exact Solution of the Antenna Equation*, vol. 183. Stockholm: Trans. Roy. Inst. Technology, 1961.

[39] C. Hastings, *Approximations for Digital Computers*. Princeton, New Jersey: Princeton University Press, 1955.

[40] E. Hallén, "Exact Treatment of Antenna Current Wave Reflection at the End of a Tube-shaped Cylindrical Antenna," *IRE Transactions on Antennas and Propagation*, vol. 4, pp. 479 – 491, July 1956.